



Politecnico di Bari

Repository Istituzionale dei Prodotti della Ricerca del Politecnico di Bari

Smart control systems for rural energy communities

This is a PhD Thesis

Original Citation:

Smart control systems for rural energy communities / Askari Noghani, Saba. - ELETTRONICO. - (2026).

Availability:

This version is available at <http://hdl.handle.net/11589/295820> since: 2026-01-18

Published version

DOI:

Publisher: Politecnico di Bari

Terms of use:

(Article begins on next page)

22 April 2026



Italian National Ph.D. Program in Autonomous Systems

ACADEMIC DISCIPLINE: SYSTEMS AND CONTROL ENGINEERING (IINF-04/A)

Final Dissertation

Smart Control Systems for Rural Energy Communities

by

Saba Askari Noghani

Hosting University and Administrative Headquarters:

Politecnico di Bari – Department of Electrical and Information Engineering

Referees:

Dr. Vijay Pratap Paidi

Dr. Chen-Wei Yang

Supervisors:

Prof. Mariagrazia Dotoli

Prof. Raffaele Carli

Dr. Paolo Scarabaggio

Coordinator of Ph.D. Program

Prof. Mariagrazia Dotoli

LIBERATORIA PER L'ARCHIVIAZIONE DELLA TESI DI DOTTORATO

Al Magnifico Rettore
del Politecnico di Bari

La sottoscritta Saba Askari Noghani nata a Tehran (Iran) il 25 Settembre 1992 residente a Giovinazzo in via Papa Giovanni XXIII n. 71/2, e-mail s.askarinoghani@phd.poliba.it, iscritta al 3° anno di Corso di Dottorato di Ricerca in Autonomous Systems (DAUSY) ciclo 38° ed essendo stata ammessa a sostenere l'esame finale con la prevista discussione della tesi dal titolo:

Smart Control Systems for Rural Energy Communities

DICHIARA

- 1) di essere consapevole che, ai sensi del D.P.R. n. 445 del 28.12.2000, le dichiarazioni mendaci, la falsità negli atti e l'uso di atti falsi sono puniti ai sensi del codice penale e delle Leggi speciali in materia, e che nel caso ricorressero dette ipotesi, decade fin dall'inizio e senza necessità di nessuna formalità dai benefici conseguenti al provvedimento emanato sulla base di tali dichiarazioni;
- 2) di essere iscritta al Corso di Dottorato di ricerca Autonomous Systems (DAUSY) ciclo 38°, corso attivato ai sensi del "Regolamento dei Corsi di Dottorato di ricerca del Politecnico di Bari", emanato con D.R. n.286 del 01.07.2013;
- 3) di essere pienamente a conoscenza delle disposizioni contenute nel predetto Regolamento in merito alla procedura di deposito, pubblicazione e autoarchiviazione della tesi di dottorato nell'Archivio Istituzionale ad accesso aperto alla letteratura scientifica;
- 4) di essere consapevole che attraverso l'autoarchiviazione delle tesi nell'Archivio Istituzionale ad accesso aperto alla letteratura scientifica del Politecnico di Bari (IRIS-POLIBA), l'Ateneo archiverà e renderà consultabile in rete (nel rispetto della Policy di Ateneo di cui al D.R. 642 del 13.11.2015) il testo completo della tesi di dottorato, fatta salva la possibilità di sottoscrizione di apposite licenze per le relative condizioni di utilizzo (di cui al sito <http://www.creativecommons.it/Licenze>), e fatte salve, altresì, le eventuali esigenze di "embargo", legate a strette considerazioni sulla tutelabilità e sfruttamento industriale/commerciale dei contenuti della tesi, da rappresentarsi mediante compilazione e sottoscrizione del modulo in calce (Richiesta di embargo);
- 5) che la tesi da depositare in IRIS-POLIBA, in formato digitale (PDF/A) sarà del tutto identica a quelle **consegnate**/inviolate/inviarsi ai componenti della commissione per l'esame finale e a qualsiasi altra copia depositata presso gli Uffici del Politecnico di Bari in forma cartacea o digitale, ovvero a quella da discutere in sede di esame finale, a quella da depositare, a cura dell'Ateneo, presso le Biblioteche Nazionali Centrali di Roma e Firenze e presso tutti gli Uffici competenti per legge al momento del deposito stesso, e che di conseguenza va esclusa qualsiasi responsabilità del Politecnico di Bari per quanto riguarda eventuali errori, imprecisioni o omissioni nei contenuti della tesi;
- 6) che il contenuto e l'organizzazione della tesi è opera originale realizzata dal sottoscritto e non compromette in alcun modo i diritti di terzi, ivi compresi quelli relativi alla sicurezza dei dati personali; che pertanto il Politecnico di Bari ed i suoi funzionari sono in ogni caso esenti da responsabilità di qualsivoglia natura: civile, amministrativa e penale e saranno dal sottoscritto tenuti indenni da qualsiasi richiesta o rivendicazione da parte di terzi;
- 7) che il contenuto della tesi non infrange in alcun modo il diritto d'Autore né gli obblighi connessi alla salvaguardia di diritti morali od economici di altri autori o di altri aventi diritto, sia per testi, immagini, foto, tabelle, o altre parti di cui la tesi è composta.

Saba Askari Noghani



Bari, 16 Gennaio 2026

La sottoscritta, con l'autoarchiviazione della propria tesi di dottorato nell'Archivio Istituzionale ad accesso aperto del Politecnico di Bari (POLIBA-IRIS), pur mantenendo su di essa tutti i diritti d'autore, morali ed economici, ai sensi della normativa vigente (Legge 633/1941 e ss.mm.ii.),

CONCEDE

- al Politecnico di Bari il permesso di trasferire l'opera su qualsiasi supporto e di convertirla in qualsiasi formato al fine di una corretta conservazione nel tempo. Il Politecnico di Bari garantisce che non verrà effettuata alcuna modifica al contenuto e alla struttura dell'opera.
- al Politecnico di Bari la possibilità di riprodurre l'opera in più di una copia per fini di sicurezza, back-up e conservazione.

Saba Askari Noghani



Bari, 16 Gennaio 2026



Saba Askari Noghani

Smart Control Systems for Rural Energy Communities

Thesis submitted for the degree of Philosophiae Doctor

National Ph.D. Program in Autonomous Systems
Politecnico di Bari

Tutors

Prof. Engr. *Mariagrazia Dotoli*

Prof. Engr. *Raffaele Carli*

Dr. Engr. *Paolo Scarabaggio*



2026



Ministero
dell'Università
e della Ricerca



Italia
domani
PIANO NAZIONALE
DI RIPRESA E RESILIENZA



Politecnico
di Bari

The doctoral scholarship was funded by the Italian National Recovery and Resilience Plan (NRRP)–funded by the European Union Next-GenerationEU– Mission 4 Component 1 Investment 4.1 - Decree no. 351 of April 9, 2022 of Italian Ministry of University and Research (MUR) (project code: D93C22000850005) within the Italian National Ph.D. Program in Autonomous Systems (DAuSy).

Dissertation submitted for the degree of *Philosophiae Doctor*
Italian National Ph.D. Program in Autonomous Systems

Cycle:

38th

Administrative Headquarters:

Politecnico di Bari

Hosting University:

Politecnico di Bari

Title:

Smart Control Systems for Rural Energy Communities

Ph.D Candidate:

Saba Askari Noghani, Politecnico di Bari (Bari, Italy)

Tutors:

Prof. Engr. Mariagrazia Dotoli, Politecnico di Bari (Bari, Italy)

Prof. Engr. Raffaele Carli, Politecnico di Bari, (Bari, Italy)

Dr. Engr. Paolo Scarabaggio, Politecnico di Bari, (Bari, Italy)

Coordinator:

Prof. Engr. Mariagrazia Dotoli, Politecnico di Bari (Bari, Italy)

External Reviewers:

Dr. PAIDI Vijay Pratap, Dalarna University (Borlänge, Sweden)

Dr. YANG Chen-Wei, Luleå University of Technology (Luleå, Sweden)

Last version:

Nov 10, 2025

All rights reserved. No part of this publication may be reproduced or transmitted, in any form or by any means, without permission.

Abstract

The transition to sustainable energy systems is a critical challenge for modern society. It is particularly important in rural areas where energy poverty, land-use conflicts, and the integration of renewable energy sources (RESs) present unique obstacles. Traditional centralized energy infrastructures struggle to accommodate the variability of RESs, the electrification of transport, agriculture, and the increasing autonomy of energy users. These challenges are more critical when considering the need to balance food and energy production, ensure grid stability, and engage consumers in active energy management. Motivated by these issues, this thesis explores innovative control frameworks and data-driven methodologies to enable the reliable, efficient, and sustainable operation of future rural energy communities.

The first part of this thesis focuses on increasing the RESs penetration through development of novel frameworks into smart energy systems, with a particular emphasis on dynamic agrivoltaic (AV) systems and smart parking infrastructures compatible with solar-powered electric vehicles (SPEVs). A geometric and optimization-based approach is proposed for dual-axis AV systems, enabling adjustment of solar panel orientation to maximize energy capture while respecting agricultural constraints such as crop shading and daily light requirements. Afterward, we introduced a convex model predictive control (MPC) framework for managing energy flows in parking lots compatible with both conventional electric vehicles (EVs) and SPEVs. The proposed MPC ensures operational safety, prevents simultaneous charging and discharging, and maintains feasibility even under uncertain vehicle behaviors and solar radiation, and the models are validated by real-world data.

The second part of this thesis, addresses the coordination of decentralized and self-interested agents in smart control energy communities (SCECs) and energy communities (ECs). Here, a novel game-theoretic, learning-based control framework is developed, where the behavior of individual prosumers is modeled using neural networks. This approach enables distributed energy management by approximating each user's optimal response strategy and seeking equilibrium through a distributed algorithm. The effectiveness of the proposed method is demonstrated through numerical simulations, showing its potential to enhance flexibility, scalability, and user autonomy in energy communities.

*The children of Adam are limbs of one another,
Created from the same essence and origin.
If one limb is afflicted with pain,
The others cannot remain at ease.
You who are indifferent to the suffering of others,
Deserve not to be called a human being.*

Saadi Shirazi

Contents

Preface	viii
List of Papers Written by the Author	viii
1 Introduction	1
1.1 Future Trends and Challenges for the Rural Energy Communities	1
1.2 Emerging Renewable Energy Technologies and the Evolving Complexity of Future Power Grids	3
1.3 Learning-Based and Game-Theoretic Control for Smart Control Energy Communities	4
1.4 Positioning of the Thesis with Respect to Related Literature and Scientific Contributions	5
Part 1	
2 Optimal Shadow-Aware Dynamic Solar Panel Orientation in Dual-Axis Agro-Voltaic Systems for Smart Energy-Agriculture Integration	10
2.1 Introduction	10
2.2 Geometric Modeling of Solar Panel Shadowing on Farmland	12
2.3 Shadow-aware Dynamic Optimization of Solar Panel Orientation	14
2.4 Numerical Experiments and Performance Evaluation	16
2.5 Conclusions	19
3 Predictive Energy Scheduling of Smart Parking Infrastructure with Solar-powered Electric Vehicles	22
3.1 Introduction	22
3.2 Related Works	23
3.3 The Smart Parking Infrastructure Model	25
3.4 Predictive Control of the Parking Facility	27
3.5 Numerical Experiments	29
3.6 Conclusions	38
Part 2	
4 Noncooperative Control of Energy Communities through Learning-based Response Dynamics	43
4.1 Introduction	43
4.2 Related Works	44
4.3 The Energy Community Model	45
4.4 The Learning-Based Game Model	47
4.5 Numerical Experiments	49
4.6 Conclusions	51
5 Summery & Conclusions	54

List of Figures

2.1	Schematic representation of the proposed dynamic AV system: the farmland is divided into rectangular cells, each hosting an individual dual-axis solar tracking unit.	12
2.2	(a) Panel top view with corners' coordinates expressed in the local frame centered at the panel midpoint, where the x- and y-axes are aligned with the panel's width and length, respectively. (b) View of the panel and its shadow projected along the Sun's direction onto the ground within the corresponding cell area: the coordinates of panel corners and their shadow projections are expressed in the global frame, where the X- and Y-axes aligned with East and North, respectively.	14
2.3	Solar path (a) and solar elevation profile (b) over the test date (June 21, 2024), as observed from the scenario location (Bari, Italy).	17
2.4	Panel azimuth (top) and tilt (bottom) angles as a function of time. Pointwise constrained results shown in color, unconstrained in dashed gray.	19
2.5	Effect of alignment target on overall radiation across the entire area . . .	19
2.6	Comparison of constrained (a, c) and unconstrained (b, d) optimization results at 09:00 and 12:00. Shadow overshoot in the unconstrained cases emphasizes the need for spatial constraints.	20
3.1	Schematic of the smart parking infrastructure supporting both EVs and SPEVs. Pink arrows indicate data flow, while purple arrows denote power flow.	25
3.2	Scenario 1. Simulation results of configuration PL1: (a) grid power exchange g , PV power generation R , and curtailed PV power v ; (b) charging and discharging profiles of vehicles at CP #3; (c) SoC profiles for vehicles at CP #3.	30
3.3	Scenario 1. Simulation results of configuration PL2: (a) grid power consumption g , PV power generation R , and curtailed PV power v ; (b) Charging and discharging profiles of vehicles at CP #3; (c) SoC profiles for vehicles at CP #3; (d) PV generation and curtailed power from SPEVs at CP #3.	31
3.4	Scenario 1. Difference in power exchanged with the main grid between configurations PL1 (roofed parking lot) and PL2 (unroofed parking). . .	32
3.5	Scenario 2. Simulation results for two prediction horizons ($H = 6$ and $H = 24$). (a) SoC profiles for vehicles at CP #5 and (b) power exchanged with the main grid over the simulation period.	32
3.6	Scenario 2. Cumulative energy exchanged with the main grid under different prediction horizons.	33
3.7	Simulation results of the unroofed V2G parking lot incompatible with SPEVs (PL 2) under scenario # 2: (a) Power profile obtained through the MPC implementation, (b) ESS charging and discharging behavior of vehicle connected to charging pile # 2, (c) ESS state of charge related to SPEV in charging pile # 2, (d) P_{PDC} , PV power profile and the related curtailed power of SPEV in charging pile # 2.	34
3.8	Simulation results of integrated V2G system for EVs and SPEVs (PL 3) under scenario # 2: P_{PDC} , PV power profile, and the related curtailed power of SPEV in charging pile # 2.	35

3.9	Overview of Lonsdale Street, Melbourne, Australia: aerial perspective from Google Earth, providing a broader context of the street within the cityscape.	35
3.10	Scenario 3. (a) On-street parking occupancy; (b) Solar radiation measurements on a 15-minute interval scale; (c) Energy prices.	36
3.11	Scenario 3. Power exchanged with the main grid for (a) 0% SPEV and (b) 100% SPEV integration.	37
3.12	Scenario 3. Charging and discharging profiles for CP #3 with (a) 0% SPEV and (b) 100% SPEV integration.	37
3.13	Scenario 3. Cumulative energy exchanged with the main grid as a function of the percentage of SPEVs.	38
3.14	Scenario 3. Cumulative energy exchanged with the main grid under different prediction errors.	38
4.1	Scheme of the proposed energy community with a specific focus on a single prosumer $n \in \mathcal{N}$	46
4.2	Learning process: MSE evolution over epochs.	49
4.3	Equilibrium among the prosumers through the proposed algorithm in Scenario 1: (a) EC Manager power convergence (b) convergence of the price.	50
4.4	Equilibrium among the prosumers through the proposed algorithm in Scenario 2; (a) EC Manager power convergence, (b) convergence of the price.	52

List of Tables

2.1	Definition of Geometric Quantities	13
3.1	Comparative Review of EV Charging Control Literature	25
3.2	Pricing scheme for Scenario 1 and 2.	30

Preface

This thesis is submitted in partial fulfillment of the requirements for the degree of *Philosophiae Doctor* in Autonomous Systems at the *Politecnico di Bari*.

This work was supported by the Italian National Recovery and Resilience Plan (NRRP)–funded by the European Union Next-GenerationEU– Mission 4 Component 1 Investment 4.1 - Decree no. 351 of April 9, 2022 of Italian Ministry of University and Research (MUR) (project code: D93C22000850005) within the Italian National Ph.D. Program in Autonomous Systems (DAuSy).

The research presented in this dissertation was conducted at the Decision and Control Laboratory of Politecnico di Bari under the supervision of Professors Mariagrazia Dotoli and Raffaele Carli, between November 2022 and October 2025.

This work is to the best of my knowledge original, except where acknowledgments and references are made to previous work. All of this thesis has been published during these three years in different scientific publications where I am the first author. The papers are preceded by an introductory chapter (Chapter 1), that relates them to each other and provides background information and motivation for the work. A version of Chapters 3 have been presented in peer-reviewed international journals while Chapters 2 and 4 have been published in top peer-reviewed international conferences in the field of control and automation. A concluding chapter (Chapter 5) summarizes the main outcomes and findings for future developments.

Professors Mariagrazia Dotoli and Raffaele Carli were involved in the early stages of concept formation, as well as data collection, numerical implementation, analysis of experiments, and composition of the above-mentioned manuscripts. Data collection, numerical implementation, analysis of experiments, and preparation of the original version of Chapter 3 and 4 was done primarily by Saba Askari Noghani while Dr. Paolo Scarabaggio contributed in the concept formation and during the manuscript composition.

Chapters 2 were part of international research collaborations with Professor Joerg Raisch at Technical University of Berlin. He was involved in the early stages of concept formation, numerical implementation, analysis of experiments, and composition of the above-mentioned manuscripts in the collaboration with D&C lab.

List of Papers Written by the Author of this Thesis and other Coauthors

1. **S.A. Noghani**, N. Mignoni, R. Carli, M. Dotoli, J. Raisch. Optimal Shadow-aware Dynamic Solar Panel Orientation in Dual-axis Agro-voltaic Systems for Smart Energy-agriculture Integration In IEEE International Conference on Systems, Man, and Cybernetics (SMC) 2025 Oct 5-8 Vienna.
2. **S.A. Noghani**, P. Scarabaggio, R. Carli, M. Dotoli. Solar-powered electric vehicles into V2G-capable smart parking infrastructure for enhanced energy efficiency. In 2024 10th International Conference on Control, Decision and Information Technologies (CoDIT) 2024 Jul 1 (pp. 575-580). IEEE.
3. **S.A. Noghani**, P. Scarabaggio, R. Carli, M. Dotoli. Predictive energy scheduling of smart parking infrastructure with solar-powered electric vehicles. IFAC Journal of Systems and Control. 2025 Jul 17:100322.
4. **S.A. Noghani**, P. Scarabaggio, R. Carli, M. Dotoli. Noncooperative Control of Energy Communities through Learning-based Response Dynamics. In 2024 IEEE 20th International Conference on Automation Science and Engineering (CASE) 2024 Aug 28 (pp. 2732-2737). IEEE.

Acknowledgements

Undertaking this Ph.D. in Italy as an international student has truly been a life-changing experience. It has shaped me into a different person, an individual who no longer fears challenges but embraces them with confidence.

I would like to express my gratitude to Prof. Mariagrazia Dotoli, my primary supervisor, for her support and guidance throughout my doctoral journey. She has always responded to my requests positively, and her mentorship has been instrumental in my professional growth. My sincere thanks also go to Prof. Raffaele Carli and Dr. Paolo Scarabaggio for their invaluable supervision. They consistently offered valuable suggestions on the next steps, and even when things did not go as planned, they always managed the situation.

It has been a privilege to collaborate with Prof. Joerg Raisch. His thoughtful suggestions have enriched my research and broadened my scientific perspective in ways that I will carry with me beyond this work. I am equally grateful to the entire D&C Lab research group for their collaboration, encouragement, and friendship.

On a personal note, I owe everything to my family. My parents always believed in me and gave me the strength to reach this point. And to my kind husband, I am forever grateful for your patience, encouragement, and countless acts of support that kept me going even in the most difficult times. Without my husband, this journey would have been far more daunting, and I feel truly lucky to have Ali in my life.

Acronyms

AEMO – Australian Energy Market Operator
AI - Artificial Intelligence
AV – Agrivoltaic (Agro-voltaic)
BRTDP – Bounded Real-Time Dynamic Programming
CP – Charging Pile
CS – Charging Station
DLI – Daily Light Integral
DNN – Deep Neural Network
EC – Energy Community
EM – Energy Manager
ESS – Energy Storage System
EV – Electric Vehicle
EVCS – Electric Vehicle Charging Station
GHI – Global Horizontal Irradiance
LSTM – Long Short-Term Memory
MDP – Markov Decision Process
ML – Machine Learning
MPC – Model Predictive Control
MSE – Mean Squared Error
NE - Nash Equilibrium
NIMBY – Not In My Backyard
NN - Neural Network
PHEV – Plug-in Hybrid Electric Vehicle
PV – Photovoltaic
RES – Renewable Energy Source
SCEC – Smart Control Energy Community
SLSQP – Sequential Least Squares Programming
SoC – State of Charge
SPEV – Solar-Powered Electric Vehicle
V2G – Vehicle-to-Grid

Chapter 1

Introduction

The global energy landscape faces significant challenges in achieving a sustainable future. Residential energy consumption alone contributes to 27% of global energy consumption and 17% of CO₂ emissions [1]. The power generation sector is a major source of environmental pollution and carbon emissions [2]. To reduce climate change, nations are committed to limiting the global average temperature increase to well below 2°C [2]. This highlights the urgent need to move away from traditional and fossil-fuel-dependent energy systems [3], [4]. In response, a global shift towards renewable energy sources (RES) has been started, which is driven by the expansion of distributed energy resources [1]. Europe, in particular, is actively pursuing clean energy transitions, with RES being central to decarbonization strategies [1], [5]. Smart grid technologies have a key role in this transformation. These intelligent electricity networks integrate sensors, smart meters, and communication systems to optimize energy use and enhance grid efficiency and resilience [3], [5]. Smart grids facilitate a bidirectional flow of energy and information, enabling consumers to become active "prosumers" who both produce and consume electricity [3], [5], [6]. Advanced smart grids further aim to interconnect the prosumers and incorporate advanced computing and artificial intelligence for predictive analytics and real-time decision-making [5].

The need for clean, decentralized, and community-driven energy solutions gave rise to Energy Communities (ECs), collaborative models where citizens, businesses, and local authorities jointly produce, manage, and consume energy [7], [8]. ECs offer multiple benefits. They increase local empowerment, enhance social cohesion, and contribute to sustainable development by reducing CO₂ emissions [6], [7]. Economically, ECs can lead to cost savings on energy bills, create local jobs, and improve grid efficiency by reducing transmission losses [7], [8]. Rural areas play a unique and crucial role in the energy transition. Often characterized by lower population density and reliance on agriculture, they possess significant untapped potential for renewable energy generation, especially from solar, wind, and biomass resources [7], [9]. However, implementing ECs, particularly in rural settings, presents challenges. The irregular behavior of renewable sources like wind and solar creates grid balancing issues [10]. High capital costs for energy storage solutions, such as battery energy storage systems, can be a financial barrier [6], [8]. A lack of proper data on consumption and generation also complicates effective management [8]. To overcome these obstacles and ensure the reliable, efficient, and sustainable operation of rural energy communities, smart control methods are essential.

1.1 Future Trends and Challenges for the Rural Energy Communities

From the points discussed above, we can see some clear trends in the rural energy communities. These trends are mostly driven by the need to find better and more reliable ways to build strong and eco-friendly power systems and management systems. However, while these changes bring new ideas, they also create some tough problems that the power industry needs to solve to build a better future. In this part, we look at some of the main trends and challenges the industry faces as it works toward stronger and greener energy systems.

1.1.1 Demand Pressures on Energy Infrastructure Due to Sector Electrification

Future demand pressures on energy infrastructure are significantly increasing due to the widespread electrification of various sectors [5], [6]. The residential sector demand is projected to rise significantly with the adoption of electric vehicles (EVs) and heat pumps

[1], [6], [11]. Furthermore, the agricultural sector is increasingly electrifying its operations to reduce greenhouse gas emissions, shifting from fossil fuels to clean electricity [9]. We should note that the rural energy systems were often designed for lower, centralized demand. These energy systems are facing aging (with almost 40% of the EU grid being over 40 years old) [5], and this can lead to issues such as local grid congestion [6]. To efficiently balance this growing supply and demand, smart control methods and digital technologies are becoming crucial [5], [10]. Machine learning (ML) and model predictive control (MPC) methods, for instance, enhance demand forecasting and energy supply prediction, helping to avoid mismatches and optimize resource use [10]. Load shifting, through coordinated control of devices like energy storage systems and electric EVs, can reduce peak loads by as much as 30% [12]. Specific examples include smart charging strategies for EVs, which optimize energy use and mitigate the intermittent nature of renewable energy sources [10], [13]. Additionally, integrating distributed energy generation from agricultural lands supports aligning local energy needs [7], helping a more flexible and resilient energy system [10], [14].

1.1.2 Land-Use Competition and Spatial Constraints

Rural landscapes are traditionally utilized for diverse purposes like farming, and housing. This causes significant land-use competition when accommodating large-scale energy infrastructure such as solar farms or wind turbines. The RES often demands substantial land areas that makes potential conflicts between energy projects and landowners. This can manifest as NIMBYISM (Not In My Backyard), where local public acceptance issues lead to project delays and opposition against necessary grid reinforcements or new installations due to concerns like noise or visual pollution [15]. To solve these spatial problems, smart energy systems and innovative frameworks are crucial. Repurposing existing spaces like parking facilities and agricultural lands with Photovoltaic (PV) panels allows for energy generation without requiring new land. Furthermore, smart control methods could enable more efficient grid management and load shifting [16].

1.1.3 Low Consumer Engagement, Untransparent Demand Response, and Unpredictable Behaviors

Low consumer engagement, particularly in rural areas, stems from a lack of active involvement in energy management and limited awareness of consumption patterns. This happens often due to difficulties in accessing clear data from utilities, and even leads to customer suspicion and resistance to participation. Moreover, unpredictable user behaviors, including temporal and temperature habits, as well as the complex nature of RES, significantly prevent energy balancing and effective demand-side management. To address these challenges, smart control solutions are crucial. Game-theoretic control enabled in smart grids and advanced metering infrastructure can directly manage and interact with prosumers to optimize energy use and reduce peak loads without inconveniencing users [17]. ML and particularly deep neural networks (DNNs) can characterize and predict user energy consumption behaviors, including preferred operation times and forecast energy needs, leading to personalized home energy management systems (HEMS). Additionally, game-theoretic control and novel price mechanisms can encourage greater consumer participation and promote desired energy behaviors [18].

1.1.4 Sensitivity of Rural Power Grids to Renewable Energy Variability and Load Fluctuations

Rural power grids are often more sensitive to small changes in both renewable energy output and electricity demand. This sensitivity presents notable challenges for grid operation. One reason for this is the physical characteristics of rural grids. These grids commonly possess weaker infrastructure and have limited access to advanced grid infrastructure. Historically, power systems were designed for a one-way flow of electricity

from large, centralized power plants to consumers [19]. Nowadays, in rural areas, there are generally fewer large, centralized generators and longer distances between energy sources and end-users. The expansion of small-scale generation, like rooftop solar panels, changes the traditional power flow. This can sometimes cause issues for distribution grids that were designed only for serving loads. These changes may require network reinforcements or upgrades. Furthermore, the nature of RES adds to grid variability. Their power output heavily depends on unpredictable weather conditions, like calm periods or heavy clouds, leading to short-term variations. This makes it more difficult to ensure a reliable and productive system, especially as renewables constitute a larger share of the grid and reduce overall system inertia. Balancing the grid becomes complex due to these unpredictable loads and weather-based generation. The intermittent nature of renewables requires a faster pace of decision-making. Managing load flow equilibrium and transient stability is particularly challenging when there are unpredictable discrepancies between demand and generation.

1.2 Emerging Renewable Energy Technologies and the Evolving Complexity of Future Power Grids

Traditional centralized energy systems struggle to reach remote areas, leaving over 1.6 billion people globally without reliable electricity access [20]. Energy poverty in rural and underserved regions presents a critical challenge to socioeconomic development, often limiting access to essential services and causing economic disadvantage. Increasing the penetration of solar energy offers a viable and scalable solution for these communities. Innovative decentralized frameworks, such as agrivoltaic systems, which combine food and energy production on the same land, can generate significant power while enhancing agricultural productivity, water management, and climate resilience [21]. Similarly, solar-powered electric vehicles (SPEVs) provide a dual benefit, offering sustainable mobility and contributing to local energy supply, particularly when integrated with charging infrastructure in public spaces. While these systems hold high potential, they introduce new complexities: intermittent energy supply from renewables like solar is uncontrollable and variable, necessitating advanced energy management. Furthermore, they involve bidirectional energy flows between prosumers and the grid, and require the integration of mobile and multifunctional assets like EVs with dynamic and unpredictable behaviors, including parking and recharging times. Traditional centralized grid architectures and control strategies are not equipped to handle such dynamic, distributed, and data-rich environments, relying on outdated unidirectional flows and often lacking the flexibility needed for intermittent sources [22]. Therefore, a new operational paradigm, such as Smart Control Energy Community (SCEC), is essential to support secure, resilient, and real-time operations for these emerging energy systems. These advanced energy systems must possess several essential capabilities:

- *Autonomous control*: Able to make operational and control decisions independently, without requiring human intervention.
- *Scalable infrastructure*: Designed to manage and coordinate operations across a vast number of devices, from local distribution networks to large-scale transmission systems.
- *Resilience*: Capable of adapting to changing conditions, including switching between grid-connected and islanded modes, with or without communication infrastructure.
- *Secure*: Equipped with mechanisms to safeguard both cyber and physical components against potential threats and intrusions.
- *Reliable and cost-effective*: Ensures consistent and economically viable energy delivery under varying system conditions.
- *Real-time capable*: Employs algorithms for control, optimization, and data analysis that function at the timescales required for real-time decision-making.

- *Supports asynchronous communication:* Capable of processing and exchanging information among components that operate on different time schedules or update rates.
- *Flexible:* Able to manage and optimize across diverse energy domains and physics, adapting to varying inputs and operating conditions.
- *Advanced predictive analytics:* Utilizing AI and ML for accurate forecasting of energy demand, supply, and system conditions to optimize operations and prevent issues.
- *Comprehensive data integration and management:* To handle large volumes of diverse data formats from various sources (e.g., sensors, smart meters, EVs) for insightful decision-making and system optimization.

Many novel RES like agrivoltaics and SPEVs are still in early development stages. These solutions can help solve energy poverty in rural areas. There is not proper SCECs designed for them. Current SCECs offer a possible solution. They can support real-time control, distributed energy resources, and mobile generation units. Most existing SCEC models are designed for urban or industrial settings. They do not address the specific needs of rural energy communities. The prosumers' interaction with each other and with the system, in ways that are not yet fully modeled or understood. Current control systems are mostly centralized. They do not handle fast dynamics, decentralized markets, or privacy concerns well. Also, many optimization methods do not support flexible, real-time decision-making for new technologies like SPEVs or agrivoltaics. SCECs should be designed to operate in these uncertain, distributed environments. However, the development of such systems is still limited in the research literature.

1.3 Learning-Based and Game-Theoretic Control for Smart Control Energy Communities

As mentioned, SCECs are a promising solution for the challenges in future energy systems. They can manage many types of energy users, technologies, and services. Decentralized and distributed SCECs are made of intelligent nodes that can work, communicate, and make decisions on their own. These networks must deal with many challenges, like changing demands and multiple stakeholders with different goals. However, the current controlling system and optimization methods are not enough. Many new devices and services are being added. There is a need for new methods that support distributed and flexible control. Game theory can help in this area [17]. It allows the modeling of systems with many independent agents. In SCECs, each node or user may have different objectives. Game-theoretic models, especially noncooperative games, can represent these competitive or self-interested behaviors. These models can be used for demand-side management, grid control, and pricing strategies [23]. DNNs can also help us. They are useful for learning complex patterns from data and making fast decisions. Together, game theory and DNNs offer strong tools for control and optimization. But most SCEC designs today do not include these tools. They often ignore the behavior of prosumers, who both produce and consume energy with unknown objectives and interests. This is a major gap, especially in rural energy communities, prosumers are very important. Their actions are hard to predict and must be modeled carefully. Without game-theoretic and data-driven models, SCECs will not be able to manage these systems effectively.

New SCEC frameworks should include:

- *Real-time operation:* Control systems must respond within seconds.
- *Asynchronous control:* Systems must handle different data and decisions happening at different times.
- *Robustness:* They must keep working during failures or attacks.
- *Scalability:* They must control many devices across large networks.

- *Behavioral modeling*: They must use game theory and DNNs to understand and guide prosumer actions.

These features are critical for future SCEC, especially in rural areas with growing renewable energy systems.

1.4 Positioning of the Thesis with Respect to Related Literature and Scientific Contributions

Smart control techniques and MPC are widely used in power market research. This is because they are strong tools for designing SCECs. However, using novel frameworks in power networks also brings many technical challenges. These must be addressed before SCECs can be fully developed and deployed.

For this reason, this thesis explores two main research directions.

1. The first direction focuses on increasing the use of RESs. The goal is to provide novel frameworks of smart parking lots compatible with the SPEVs and also dynamic AV systems. While the goal of the controller systems is to optimally control the system to reduce the dependency on the grid. This part of the research studies how to apply linear and nonlinear MPC to optimize these novel energy systems. It begins by introducing novel frameworks. Then, it develops MPC systems with robust performance.
2. The second direction looks at how to coordinate independent and self-interested agents in SCECs. The goal is to keep the grid working properly while each agent follows its own goals. This part of the work develops a data-driven framework. It helps ensure that the behavior of prosumers are modeled by DNNs when using decentralized and distributed game-theoretic models.

The thesis includes the results of four studies published in conference and journal papers by the author. It is organized into two main parts, which follow this introduction.

1.4.1 Novel Frameworks for Integrating Renewable Energy Resources in Smart Energy Systems

Rural energy communities face several challenges in adopting renewable energy resources. Access to clean energy, remains difficult in remote areas. At the same time, most land in these communities is used for agriculture, making it hard to find space for new solar installations. Installing solar panels on farmland can reduce the area available for crops, which may threaten food security. These issues show the need for new frameworks that can combine energy generation with agricultural activities, while also supporting the growing demand for clean energy in transportation. To mitigate these challenges, it is important to investigate the potential of innovative RESs and novel frameworks like dynamic AV systems and parking infrastructures compatible with SPEVs.

As a result, the first contribution of this thesis is to propose two novel frameworks for improving the integration of renewable energy resources. In Chapter 2, we introduce an innovative control framework for AV systems. AV systems allow the simultaneous use of land for both agriculture and solar energy generation, offering a promising solution to land-use conflicts. However, the shadows cast by solar panels present a significant challenge. While these shadows can protect crops from excessive heat and reduce water loss, they may also limit sunlight exposure, which can reduce crop yield. This chapter presents a method for controlling shadow placement on farmland by dynamically adjusting the azimuth and elevation angles of dual-axis solar panels. A geometric formulation is introduced to model the shadow of a rectangular panel on the ground, followed by an optimization framework that restricts the shadow to a predefined zone while ensuring minimum solar radiation within that zone throughout the day. The proposed approach balances the goals of maximizing solar energy capture and achieving precise shadow

control by using an iterative refinement method. The system is evaluated using real-world solar data from a clear day in Bari, Italy.

The electrification of transport systems is expected to increase the challenges of integrating RESs. In Chapter 3, we focus on these issues. The rapid adoption of EVs, and especially SPEVs, is changing both transportation and energy systems. However, the dynamic State of Charge (SoC) in EVs and the variable solar energy generation in SPEVs make it difficult to control and automate power flow. This is particularly challenging for Charging Pile (CP) operations because vehicles are often plugged in and out at different times. To address these challenges, we propose a novel MPC framework with a convex relaxation formulation. This approach avoids the computational complexity of traditional mixed-integer programming methods and ensures that charging and discharging do not occur at the same time. We introduce a new operational constraint to improve the safety and performance of CPs and to prevent possible damage during operation. Furthermore, we add an additional feasibility constraint to handle the dynamic nature of SoC and the prediction limitations of MPC. This constraint ensures that, even if an EV's departure time is beyond the current prediction horizon, the future optimization steps will remain feasible. The proposed controller minimizes power costs, guarantees that user-specified charge levels are reached by the time an EV disconnects, maintains feasibility in future optimization steps, and protects the CP during operation. Through numerical analysis, we show that our proposed constraints effectively prevent damage to CPs and ensure that charging and discharging never occur simultaneously. We also confirm the long-term performance of the MPC framework, demonstrating that it meets final charging requirements and maintains feasibility. In addition, we apply our framework to manage energy flow for vehicles on Lonsdale Street, Melbourne, Australia, using real-world data on vehicle arrivals, departures, solar radiation, and energy prices. Compared to previous methods, our results show a significant reduction in the power required from the grid, even when only 50% of vehicles have solar panels. Finally, we analyze prediction errors and find that the cumulative energy metric remains robust even with moderate random prediction uncertainty. This demonstrates the reliability and efficiency of the proposed MPC framework.

1.4.2 Data-Driven Modeling for Learning-Based Control of User Behavior For Noncooperative Control of Energy Communities

Rural energy communities face unique challenges when integrating renewable energy resources, not only due to technical and infrastructure limitations, but also because of the complex and often unpredictable behaviors of users. Traditional control frameworks, which rely on fixed schedules or centralized commands, may not be effective in these settings where users act independently and may not always cooperate with community goals. In such environments, the ability to predict user behavior and design control strategies that adapt to actual patterns of consumption and response is essential. Data-driven modeling and learning-based control offer promising solutions, as they can uncover hidden patterns in user actions, improve forecasts of energy demand, and adjust control signals in real-time. By considering behavioral aspects, learning-based control frameworks can encourage more efficient and sustainable energy use, even when users act in their own self-interest. Noncooperative control approaches that use learning-based response dynamics are especially valuable, as they can coordinate the actions of individual users without requiring full cooperation or perfect information. This motivates the development of novel, data-driven frameworks that can help rural energy communities achieve more reliable and efficient operation by learning from user behavior and responding adaptively to changing conditions. In Chapter 4, we introduce a new framework for the noncooperative control of energy communities using learning-based response dynamics. As more data becomes available, learning-based distributed energy management is proving to be a promising and efficient alternative to traditional model-based methods. In chapter 4, we propose a novel game-theoretic, learning-based approach for the distributed control of energy communities. Specifically, we focus on a community made up of several prosumers, each equipped

with a renewable energy source and an energy storage system. The scheduling of energy activities for all prosumers is formulated as a noncooperative game. However, instead of modeling each prosumer's behavior using an optimization problem, as is common in the literature, we use a neural network to approximate each prosumer's response strategy. We then present a distributed algorithm, based on the Banach-Picard iteration, to efficiently find an equilibrium of the game. Finally, we validate the convergence and effectiveness of our approach through numerical simulations across different realistic scenarios.

References

- [1] Liu, Y., Ma, J., Xing, X., Liu, X., and Wang, W., "A home energy management system incorporating data-driven uncertainty-aware user preference," *Applied Energy*, vol. 326, p. 119 911, 2022.
- [2] Sun, L. and You, F., "Machine learning and data-driven techniques for the control of smart power generation systems: An uncertainty handling perspective," *Engineering*, vol. 7, no. 9, pp. 1239–1247, 2021.
- [3] Strielkowski, W., Vlasov, A., Selivanov, K., Muraviev, K., and Shakhnov, V., "Prospects and challenges of the machine learning and data-driven methods for the predictive analysis of power systems: A review," *Energies*, vol. 16, no. 10, p. 4025, 2023.
- [4] Auer, J., "Eu energy policy: High time for action!" *Deutsche Bank Research, EU Monitor*, vol. 44, p. 3, 2007.
- [5] Zahid, H., Zulfiqar, A., Adnan, M., Iqbal, S., and Mohamed, S. E. G., "A review on socio-technical transition pathway to european super smart grid: Trends, challenges and way forward via enabling technologies," *Results in Engineering*, p. 104 155, 2025.
- [6] Koirala, B. P., Koliou, E., Friege, J., Hakvoort, R. A., and Herder, P. M., "Energetic communities for community energy: A review of key issues and trends shaping integrated community energy systems," *Renewable and Sustainable Energy Reviews*, vol. 56, pp. 722–744, 2016.
- [7] Shi, Z., Liang, F., and Pezzuolo, A., "Renewable energy communities in rural areas: A comprehensive overview of current development, challenges, and emerging trends," *Journal of Cleaner Production*, p. 144 336, 2024.
- [8] Lode, M. L. et al., "Energy communities in rural areas: The participatory case study of vega de valcarce, spain," *Renewable Energy*, vol. 216, p. 119 030, 2023.
- [9] Gorjian, S. et al., "Progress and challenges of crop production and electricity generation in agrivoltaic systems using semi-transparent photovoltaic technology," *Renewable and Sustainable Energy Reviews*, vol. 158, p. 112 126, 2022.
- [10] Ahmad, T., Madonski, R., Zhang, D., Huang, C., and Mujeeb, A., "Data-driven probabilistic machine learning in sustainable smart energy/smart energy systems: Key developments, challenges, and future research opportunities in the context of smart grid paradigm," *Renewable and Sustainable Energy Reviews*, vol. 160, p. 112 128, 2022.
- [11] Baek, J. and Choi, Y., "An experimental study on performance evaluation of shading matrix to select optimal parking space for solar-powered electric vehicles," *Sustainability*, vol. 14, no. 22, p. 14 922, 2022.
- [12] Meliopoulos, A. S. et al., "Smart grid technologies for autonomous operation and control," *IEEE Transactions on smart grid*, vol. 2, no. 1, pp. 1–10, 2011.
- [13] Ahmad, A. and Khan, J. Y., "Real-time load scheduling and storage management for solar powered network connected evs," *IEEE Transactions on Sustainable Energy*, vol. 11, no. 3, pp. 1220–1235, 2019.

- [14] Timpe, C., Bauknecht, D., Koch, M., and Lynch, C., “Integration of electricity from renewable energy sources into european electricity grids,” *ETC/ACC Technical Paper*, vol. 18, p. 2010, 2010.
- [15] Abidin, M., Mahyuddin, M., and Zainuri, M., “Optimal efficient energy production by pv module tilt-orientation prediction without compromising crop-light demands in agrivoltaic systems,” *IEEE Access*, 2023.
- [16] Noghani, S. A., Scarabaggio, P., Carli, R., and Dotoli, M., “Solar-powered electric vehicles into v2g-capable smart parking infrastructure for enhanced energy efficiency,” in *2024 10th International Conference on Control, Decision and Information Technologies (CoDIT)*, IEEE, 2024, pp. 575–580.
- [17] Scutari, G., Palomar, D. P., Facchinei, F., and Pang, J.-S., “Convex optimization, game theory, and variational inequality theory,” *IEEE Signal Processing Magazine*, vol. 27, no. 3, pp. 35–49, 2010.
- [18] Bünning, F. et al., “Physics-informed linear regression is competitive with two machine learning methods in residential building mpc,” *Applied Energy*, vol. 310, p. 118 491, 2022.
- [19] Paschalis, A., Bonetti, S., and Fatichi, S., “Controls of ecohydrological grassland dynamics in agrivoltaic systems,” *Earth’s Future*, vol. 13, no. 3, e2024EF005183, 2025.
- [20] Bannour, F., Souihi, S., and Mellouk, A., “Distributed sdn control: Survey, taxonomy, and challenges,” *IEEE Communications Surveys & Tutorials*, vol. 20, no. 1, pp. 333–354, 2017.
- [21] Gupta, V., Cammarano, D., and Brouder, S., “Optimizing corn agrivoltaic farming through farm-scale experimentation and modeling,” *Cell Reports Sustainability*, 2024.
- [22] Khalid, M., “Smart grids and renewable energy systems: Perspectives and grid integration challenges,” *Energy Strategy Reviews*, vol. 51, p. 101 299, 2024.
- [23] Fujiwara-Greve, T., *Non-cooperative game theory*. Springer, 2015.

Part 1

Chapter 2

Optimal Shadow-Aware Dynamic Solar Panel Orientation in Dual-Axis Agro-Voltaic Systems for Smart Energy-Agriculture Integration

Abstract

Agrioltaic systems enable the simultaneous use of land for both agriculture and solar energy generation, offering a promising solution to land-use conflicts. However, shadows cast by solar panels present a significant challenge: while they can protect crops from excessive heat and reduce water loss, they may also limit sunlight exposure, reduce crop yield, and create potential conflicts with neighboring land. This chapter presents a method for controlling shadow placement by dynamically adjusting the azimuth and elevation angles of solar panels. A geometric formulation is introduced to model the shadow of a rectangular panel on the ground, followed by an optimization framework that restricts the shadow to a predefined zone while ensuring minimum solar radiation within that zone over the course of a day. The proposed approach balances the goals of maximizing solar energy capture and achieving precise shadow control, using an iterative refinement method. The system is evaluated using real-world solar data from a clear day in Bari, Italy. Compared to an unconstrained system, the proposed method successfully confines the shadow within the desired area and satisfies global radiation constraints. The results demonstrate the system's practical potential for managing shading in real-world agrioltaic applications, preventing land-use conflicts, and enhancing overall land-use efficiency.

Contents

2.1	Introduction	10
2.2	Geometric Modeling of Solar Panel Shadowing on Farmland	12
2.3	Shadow-aware Dynamic Optimization of Solar Panel Orientation	14
2.4	Numerical Experiments and Performance Evaluation	16
2.5	Conclusions	19

2.1 Introduction

Agriculture contributes significantly to global sustainability but is also responsible for approximately 18% of global greenhouse gas emissions [1]. This dual role highlights the need for innovative and resilient agricultural solutions that enhance both environmental sustainability and operational efficiency [2]. The paradigm of Agriculture 4.0 has been recently introduced to promote sustainable farming practices by incorporating sensors, actuators, data analytics, and digitalization [3]. Within this innovative paradigm, Agrioltaic (AV) systems, which integrate PV technology into agricultural landscapes, are gaining recognition for simultaneously addressing energy sustainability and agricultural productivity challenges [4].

AV systems offer numerous advantages by generating renewable energy while providing shading that can protect crops from climatic extremes such as excessive heat and water



evaporation [5]. This dual-use of land is particularly advantageous in rural agricultural regions, which continue to experience significant energy supply challenges due to high conventional energy costs, limited electricity access, and variability inherent in renewable energy sources [6]. Historically, agriculture has been heavily reliant on fossil fuels, but the shift toward automation and smart farming necessitates a stable and efficient renewable energy infrastructure, which is often lacking in rural areas [7]. Moreover, renewable energy projects in rural settings frequently encounter social resistance, notably driven by the “Not In My Backyard” (NIMBY) phenomenon, where local communities may oppose such developments due to concerns about land use, potential reductions in property values, and impacts from renewable infrastructure installation. AV systems offer a socially acceptable solution by preserving farmland and generating renewable energy simultaneously [8].

While AV systems effectively integrate renewable energy production with agricultural land use, they inherently face challenges related to shading: as a result, the layout design and configuration of AV installations are considerably more complex than those of conventional PV plants [9]. Shadows cast by PV panels can provide beneficial microclimate conditions for crops, but simultaneously limit sunlight exposure, potentially reducing crop yields and causing conflicts with adjacent land parcels. Recent research in AV systems has explored various aspects related to shading, including ecohydrological dynamics and microclimate interactions [10], semi-transparent PV technologies for controlled light transmission [11], and advanced layout models for fixed and tracking solar arrays [5]. For example, detailed simulation-based optimization strategies have been applied to assess the trade-offs between energy production and crop yield in corn AV systems [6]. Studies have also evaluated tilt-orientation prediction methods to optimize the balance between solar irradiance and crop growth without real-time adjustments [7]. Novel approaches, such as V-shaped bifacial PV systems, have been modeled dynamically to understand shading and reflective properties more effectively [8]. Furthermore, tailored tracking strategies is developed to meet specific crop irradiance needs, such as those developed for apple orchards [12]. Reviews have broadly assessed the impact of PV panels on soil health, crop quality, and microclimates, highlighting the importance of strategic shading management in AV systems [13]. According to the state of the art, the dynamic control of AV systems and their shadows, supported by a clear geometric formulation and real-time adjustment mechanisms, remains underexplored but is essential.

This chapter aims at addressing the above-mentioned gap by introducing a novel optimization framework capable of controlling shadow placement through dynamic adjustments of a dual-axis PV panel orientation. Specifically, the objectives include:

1. Developing a geometric formulation to accurately represent the shadow cast by a dual-axis AV system and defining a practical model to express crop solar exposure requirements over farmland.
2. Establishing an optimization method that maximizes the solar tracking while restricting shadow impacts to a predefined zone and ensuring a minimum required solar exposure for crops over the course of a day.

The system is evaluated using real-world solar data from a clear day in Bari, Italy. The results demonstrate the system practical potential for effectively managing shading in real-world AV applications, thus enabling sustainable integration of energy generation and farming activities.

The proposed work differs from current literature, which predominantly relies on static configuration or simulation-based optimization methods, and does not fully leverage real-time panel orientation adjustment, leaving a significant gap in dynamic shading management. To the best of authors’ knowledge, solar tracking strategies specifically aimed at dynamic shadow control in AV systems have only been addressed in [14], [15]. In particular, [14] subsequently extended in [15] focuses on optimizing the global balance between crop light exposure and PV generation, formulating the problem as a large-scale optimization model to reduce computational complexity. However, [14], [15] do not explicitly control the spatial placement of shadows during the day, nor do they

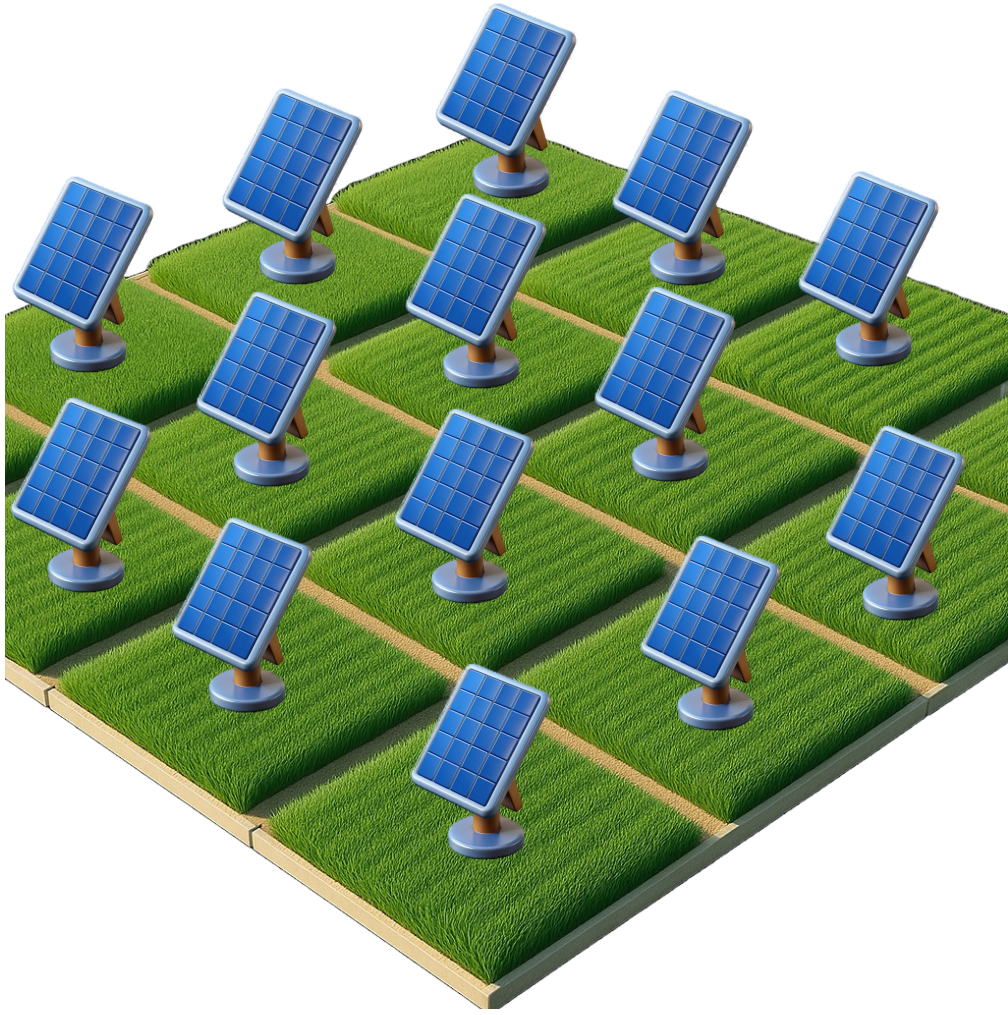


Figure 2.1: Schematic representation of the proposed dynamic AV system: the farmland is divided into rectangular cells, each hosting an individual dual-axis solar tracking unit.

dynamically adjust both azimuth and tilt angles in response to real-time solar conditions, as they deal exclusively with single-axis panel systems. Furthermore, [14], [15] assume that the exact positions of individual plants are known and model crops as discrete point targets, whereas the method proposed in this chapter considers crops as being uniformly and continuously distributed across the agricultural surface, resulting in a more practical and scalable modeling approach.

The remainder of this chapter is organized as follows. Section 2.2 represents the geometric relations and mathematical formulation used for modeling panel shadow on the ground. Section 2.3 presents the optimization framework, including the objective function and system constraints for dynamic shadow control. Section 2.4 details the numerical experiments and performance evaluation using real-world solar data. Finally, Section 2.5 concludes the chapter and outlines potential directions for future research.

2.2 Geometric Modeling of Solar Panel Shadowing on Farmland

In this section, we present the geometric modeling of the proposed system, as illustrated in Figure 2.1. The system consists of an agricultural farmland divided into multiple cells, with each cell equipped with its own PV panel. To simplify the analysis, we concentrate on the modeling of a single cell, assuming that cells are decoupled by enforcing that the shadow of each panel is restricted to the corresponding cell. We assume a flat, uniform

Table 2.1: Definition of Geometric Quantities

Symbol	Description
φ_s	Solar azimuth (clockwise from North)
α_s	Solar elevation (Sun's angle above horizon)
X_{\min}, X_{\max}	Bounds of the cell along the East–West axis
Y_{\min}, Y_{\max}	Bounds of the cell along the North–South axis
W, L	Panel width and length
H	Panel center height above ground
φ_p	Panel azimuth angle
α_p	Panel tilt angle

ground surface with negligible atmospheric scattering. These assumptions allow a purely geometric model of the shadow, independent of atmospheric diffusion or terrain variations. Finally, we assume that crops are uniformly distributed across each cell area, forming a continuous ground-level coverage.

To impose constraints related to shading, we must relate the geometry of a panel to the projected shadow. To obtain the projected shadow, we first define the panel's corner coordinates in its local reference frame, centered at the panel midpoint in the panel plane, where we consider x- and y-axes to be aligned with the panel's width and length, respectively. With half-dimensions $W/2$ and $L/2$, the corners in local coordinates are (see Figure 2.2(a)):

$$\mathbf{c}_1 = \begin{bmatrix} W/2 \\ L/2 \\ 0 \end{bmatrix}, \mathbf{c}_2 = \begin{bmatrix} W/2 \\ -L/2 \\ 0 \end{bmatrix}, \mathbf{c}_3 = \begin{bmatrix} -W/2 \\ -L/2 \\ 0 \end{bmatrix}, \mathbf{c}_4 = \begin{bmatrix} -W/2 \\ L/2 \\ 0 \end{bmatrix}$$

The global coordinate system is defined such that the panel midpoint is located at $(0, 0, H)$ and the X- and Y-axes are aligned with East and North, respectively. The transformation from local to global coordinates is given by (see Figure 2.2(b)):

$$\mathbf{C}_i(t) = \begin{bmatrix} X_i(t) \\ Y_i(t) \\ Z_i(t) \end{bmatrix} = \begin{bmatrix} 0 \\ 0 \\ H \end{bmatrix} + \mathbf{R}(\varphi_p(t), \alpha_p(t)) \mathbf{c}_i, \quad \forall i = 1, \dots, 4 \quad (2.1)$$

where the rotation matrix \mathbf{R} respects two successive rotations:

$$\mathbf{R}(\varphi_p, \alpha_p) := \mathbf{R}_z(\varphi_p) \mathbf{R}_x(\alpha_p), \quad (2.2a)$$

$$\mathbf{R}_z(\varphi_p) := \begin{bmatrix} \cos \varphi_p & -\sin \varphi_p & 0 \\ \sin \varphi_p & \cos \varphi_p & 0 \\ 0 & 0 & 1 \end{bmatrix} \quad (2.2b)$$

$$\mathbf{R}_x(\alpha_p) := \begin{bmatrix} 1 & 0 & 0 \\ 0 & \cos \alpha_p & -\sin \alpha_p \\ 0 & \sin \alpha_p & \cos \alpha_p \end{bmatrix}. \quad (2.2c)$$

The Sun's direction vector is represented by a unit vector oriented from the ground surface toward the Sun:

$$\mathbf{S}(t) ::= \begin{bmatrix} S_x \\ S_y \\ S_z \end{bmatrix} = \begin{bmatrix} \cos \alpha_s \sin \varphi_s \\ \cos \alpha_s \cos \varphi_s \\ \sin \alpha_s \end{bmatrix} \quad (2.3)$$

under the assumption that $S_z \neq 0$, i.e., the solar elevation α_s is strictly positive and the Sun is above the horizon. This ensures the projection direction is well-defined and intersects the ground plane. To compute the shadow projection of a panel corner $\mathbf{C}'_i = (X'_i, Y'_i, Z'_i)^\top$ onto the ground, we intersect the rays from the corner points in direction $-\mathbf{S}$ with the ground plane $Z = 0$. The non-negative scalar intersection parameters θ_i satisfy:

$$\forall i = 1, \dots, 4: \begin{cases} \mathbf{C}'_i = \mathbf{C}_i - \mathbf{S}\theta_i \\ Z'_i = Z_i - \theta S_z = 0 \implies \theta_i = \frac{Z_i}{S_z} \end{cases} \quad (2.4)$$

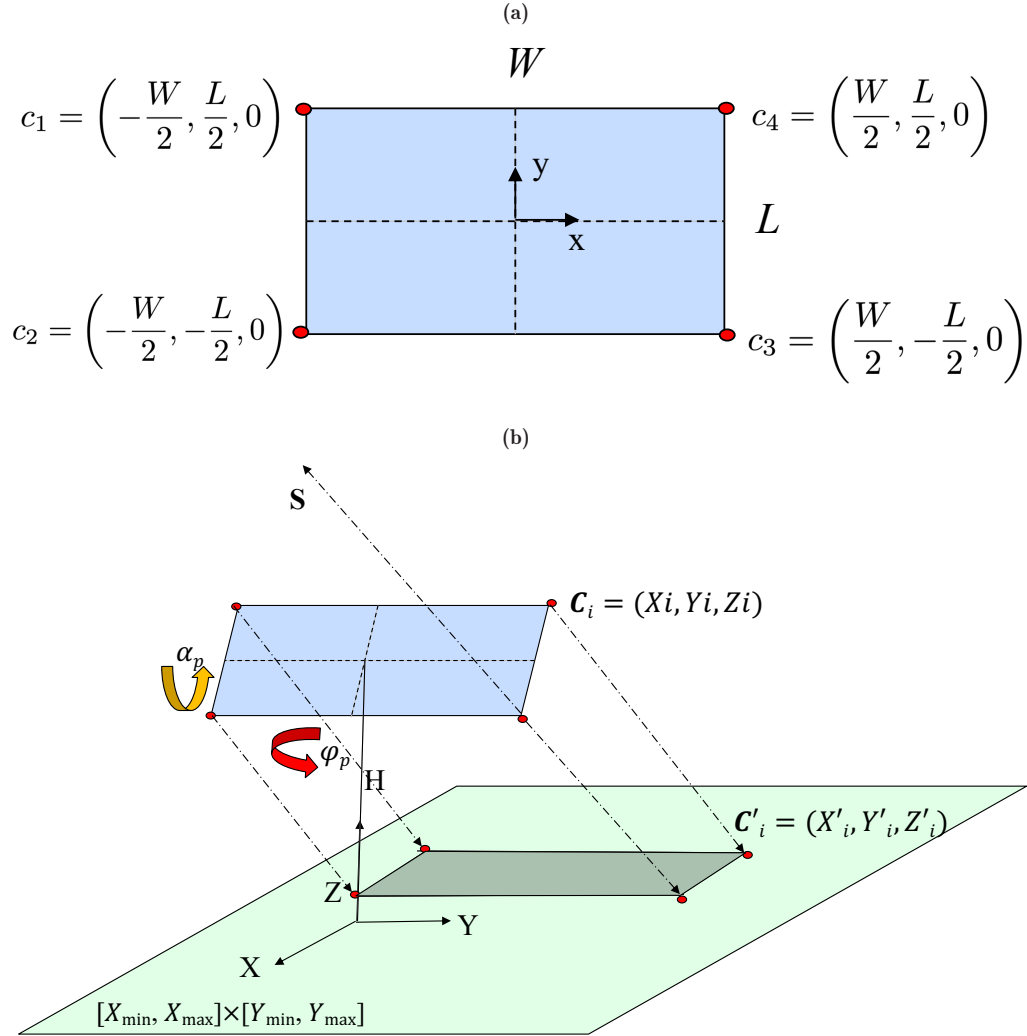


Figure 2.2: (a) Panel top view with corners' coordinates expressed in the local frame centered at the panel midpoint, where the x- and y-axes are aligned with the panel's width and length, respectively. (b) View of the panel and its shadow projected along the Sun's direction onto the ground within the corresponding cell area: the coordinates of panel corners and their shadow projections are expressed in the global frame, where the X- and Y-axes aligned with East and North, respectively.

so that the resulting shadow corners have coordinates:

$$\begin{bmatrix} X'_i \\ Y'_i \end{bmatrix} = \begin{bmatrix} X_i \\ Y_i \end{bmatrix} - \frac{Z_i}{S_z} \begin{bmatrix} S_x \\ S_y \end{bmatrix}, \quad \forall i = 1, \dots, 4. \quad (2.5)$$

where we omit the third component $Z'_i = 0$ for brevity.

2.3 Shadow-aware Dynamic Optimization of Solar Panel Orientation

We consider a PV panel system co-located with a green plant zone. The goal is to control the orientation of the solar panel over the course of a sunny day to optimally absorb radiation, subject to the following constraints:

- i)* The panel's shadow remains within the predefined plant zone bounds at every time step (pointwise constraint).
- ii)* The total solar radiation received by the plant zone over the entire day exceed a specified threshold (integral constraint).

This setup represents a trade-off between maximizing the energy production of the panel and ensuring adequate sunlight for vegetation growth. In the following, we assume that the superscript t denotes a given time slot of the day, with $t \in \{1, \dots, T\}$, where T is the total number of equal time slots in one day.

2.3.1 The Optimization Problem

The panel is modeled as a dual-axis system, allowing independent rotation about the azimuthal angle φ_p and the elevation (tilt) angle α_p , and they are decision variables at each time t , and are bounded as:

$$\varphi_p^{\min} \leq \varphi_p \leq \varphi_p^{\max}, \quad \alpha_p^{\min} \leq \alpha_p \leq \alpha_p^{\max}, \quad (2.6)$$

where these bounds for the panel's azimuth and tilt angles are introduced to reflect mechanical and manufacturing conditions.

The geometric relations established in the previous section are used to project panel shadows and compute relevant constraints. At each discrete time step t , the Sun direction vector \mathbf{S} is computed as in (2.3). The panel normal vector is expressed in the global reference frame as a function of its tilt and azimuth angles:

$$\mathbf{n}(\varphi_p, \alpha_p) = \begin{bmatrix} \sin \varphi_p \sin \alpha_p \\ \cos \varphi_p \sin \alpha_p \\ \cos \alpha_p \end{bmatrix}. \quad (2.7)$$

To ensure meaningful energy capture and prevent degenerate configurations, the optimization is only performed when the solar elevation is above a minimum threshold α_s^{\min} (e.g., 35°). If the Sun is too low, the panel defaults to a vertical configuration, and optimization is skipped, and the panel azimuth is set to face the sun horizontally ($\varphi_p = \text{atan2}(S_y, S_x)$ where atan2 is the 2-argument arctangent).

To enforce shadow containment within each farmland cell, we define a constraint enforcing any shadow corner to lie inside the rectangular cell. According to bounds shown in Figure 2.2, hence the cell imposes the following constraint on shadow's corners:

$$\forall i = 1, \dots, 4 : \begin{cases} X_{\min} \leq X'_i \leq X_{\max}, \\ Y_{\min} \leq Y'_i \leq Y_{\max} \end{cases} \quad (2.8)$$

At each time step t , the unshaded fraction of the agricultural area is computed based on the projected panel shadows. The corresponding incident solar radiation is then estimated using a simplified model of global horizontal irradiance (GHI) where it is the total solar irradiance received per unit area by a horizontal surface, and is typically expressed in watts per square meter (W/m^2).

The overall radiation reaching the entire plant area at time t is:

$$R_t = \left(1 - \frac{A_{\text{shade}}}{A_{\text{cell}}}\right) \cdot \text{GHI}_t, \quad (2.9)$$

where $A_{\text{shade}}(t)$ refers to the shaded area, and is computed by the so-called Shoelace formula as:

$$A_{\text{shade}}(t) = \frac{1}{2} \left| \sum_{i=1}^4 X'_i Y'_{i+1} - Y'_i X'_{i+1} \right|. \quad (2.10)$$

The integral constraint is expressed as a requirement that the total accumulated solar energy on the plant over the day exceeds a prescribed threshold, ensuring that the minimum daily light integral (DLI_{\min}) required for crop health is satisfied:

$$\sum_{t=1}^T R(t) \geq \text{DLI}_{\min}. \quad (2.11)$$

Let $\boldsymbol{\varphi}_p := [\phi_p(1), \dots, \phi_p(T)]^\top$ and $\boldsymbol{\alpha}_p = [\alpha_p(1), \dots, \alpha_p(T)]^\top$, so that the objective function is:

$$f(\boldsymbol{\varphi}_p, \boldsymbol{\alpha}_p) = \sum_{t=1}^T \mathbf{n}^\top(t) \mathbf{S}(t) \quad (2.12)$$

where this function sums the alignment between the panel's orientation and the Sun's direction over a time period T. Hence, maximizing this objective aligns the panel as directly as possible toward the Sun throughout the period of time T, and maximizes incident solar energy. The objective function is non-linear and non-convex due to the trigonometric relationship between the orientation angles and the panel's normal vector. It is continuous, assuming a continuous sun path and smooth trigonometric functions. Summing up, the optimization problem is formulated as follows:

$$\begin{aligned} & \text{maximize}_{\boldsymbol{\varphi}_p, \boldsymbol{\alpha}_p} f(\boldsymbol{\varphi}_p, \boldsymbol{\alpha}_p) \\ & \text{subject to (2.6), (2.8), and (2.11)} \end{aligned} \quad (2.13)$$

2.3.2 Resolution Mechanism through Iterative Panel Orientation Adjustment

The global problem in Equation (2.13) seeks to maximize cumulative solar capture while satisfying shading and energy constraints over a full time horizon. However, solving this exact problem is computationally intensive due to its non-convex, non-linear nature and the coupling across time through the integral constraint. To make the problem tractable, we instead solve a surrogate problem at each time step that aligns the panel as closely as possible with the Sun vector, using a tunable alignment target $w \in [0, 1]$. Hence, we solve the following optimization problem at each time step:

$$\begin{aligned} & \text{minimize}_{\boldsymbol{\varphi}_p, \boldsymbol{\alpha}_p} (\mathbf{n}^\top \mathbf{S} - w)^2 \\ & \text{subject to (2.6) and (2.8)} \end{aligned} \quad \begin{aligned} & (2.14) \\ & (2.15) \end{aligned}$$

where initially, $w = 1.0$ enforces ideal Sun tracking. If the cumulative radiation constraint (Equation (2.11)) is violated, w is iteratively reduced by a step size Δw , allowing more flexibility in orientation to reduce shading. This iterative panel orientation adjustment balances two competing objectives: maximizing incident irradiance and satisfying shading or exposure constraints.

2.4 Numerical Experiments and Performance Evaluation

The aim of numerical experiment is threefold: (i) to verify the ability of the system to adapt to solar conditions throughout the day, (ii) to assess the system's compliance with geometric and performance constraints, and (iii) to demonstrate that the system can meet predefined solar radiation targets through iterative refinement. This section illustrates various aspects of the method's behavior, including solar availability, panel motion over time, radiation of the ground versus alignment strictness, and physical feasibility of the resulting configurations. The simulation is implemented in Python using real solar position and GHI data provided by the `pvlib` library [16]

Algorithm 1 was implemented in Python, using the Sequential Least Squares Programming (SLSQP) solver available in the `SciPy` library [17]. In particular, the employed SLSQP method - which approximates the objective function and constraints using quadratic and linear models, respectively, and solves a sequence of quadratic subproblems to converge to an optimal solution, was configured with a tight function tolerance (`ftol=1e-9`), fine gradient step (`eps=1e-11`), and increased iteration limit (`maxiter=50000`).

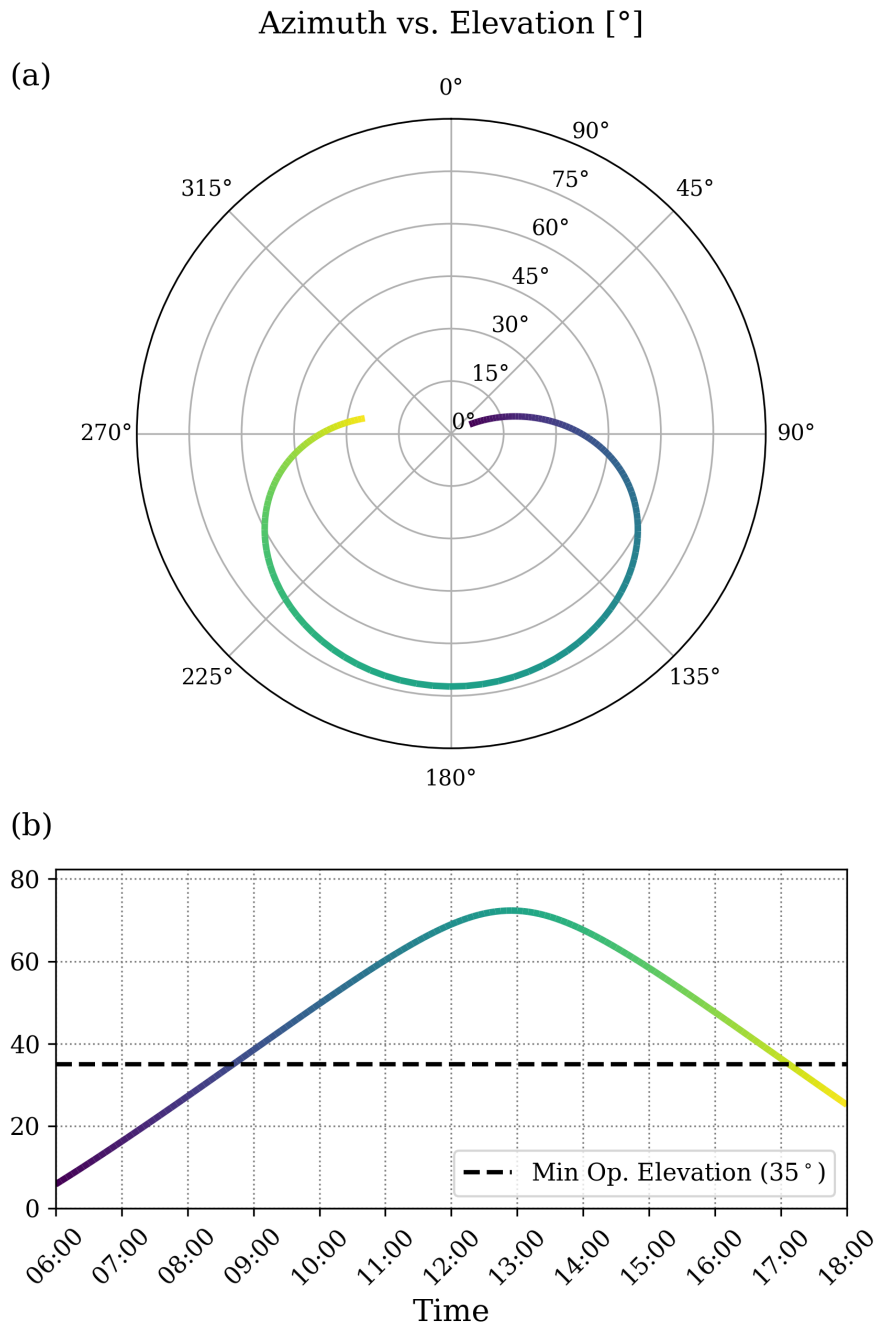


Figure 2.3: Solar path (a) and solar elevation profile (b) over the test date (June 21, 2024), as observed from the scenario location (Bari, Italy).

2.4.1 Scenario Setup

To assess the effectiveness of the proposed optimization framework for dynamic agrovoltaic systems, we performed a series of numerical simulations over a complete sunny day (June 21, 2024) in Bari, Italy (latitude: 41.1171° , longitude: 16.8719°). We consider a PV panel with a square surface of dimensions $5\text{ m} \times 5\text{ m}$, elevated at height $H = 5\text{ m}$.

Algorithm 1: Iterative Panel Orientation Adjustment

```

1:   $w \leftarrow w_{\text{init}}$ 
2:  while  $w \geq w_{\text{min}}$  do
3:    for  $t = 1$  to  $T$  do
4:      Solve: (2.14)
5:      subject to (2.8) and (2.6)
6:    end for
7:    if integral constraint (2.11) is satisfied then
8:      break
9:    else
10:      $w \leftarrow w - \Delta w$ 
11:    end if
12:  end while
13:  return Optimal  $(\varphi_p, \alpha_p), \forall i \in [1, T]$ 
    
```

The plant zone is a rectangular region on the ground defined by:

$$x \in [x_{\min}, x_{\max}] = [-3, 4.5], \quad y \in [y_{\min}, y_{\max}] = [-8, 10].$$

In this chapter, the panel's azimuth angle φ_p is bounded within $[-120^\circ, 120^\circ]$, and the tilt angle α_p is limited to $[5^\circ, 90^\circ]$. The optimization loop proceeds over discrete time steps spanning the day, with 5-minute intervals applied in this study. Here, $w \in [0, 1]$ is the target alignment between the panel and the Sun. Initially, $w = 1.0$ enforces perfect Sun tracking. If the integral energy constraint in (2.11) is not satisfied, w is reduced incrementally by Δw (here we used 0.02), relaxing the alignment in favor of reduced shading. In this study, we considered $\text{DLI}_{\min} = 7000 \text{ Wh/m}^2/\text{day}$. The iterative adjustment repeats until either the global constraint is met or a minimum acceptable w is reached as described in Algorithm 1.

2.4.2 Results Analysis and Discussion

Figure 2.3 provides spatial and temporal insight into the Sun's trajectory on the test date. The polar plot in Figure 2.3a displays the sun's position in azimuth-elevation space. The corresponding elevation-time plot in Figure 2.3b marks the operating window of the system, constrained to periods when the solar altitude exceeds 35° .

Figure 2.4 demonstrates the system's adaptation in terms of azimuth and tilt angles under pointwise shadow constraints. The upper subplot (Figure 2.4a) shows the azimuth angle evolution throughout the day. The lower subplot (Figure 2.4b) tracks the panel tilt angle. In both cases, the constrained strategy (colored gradient) is compared to an unconstrained variant (dashed gray), revealing how local feasibility considerations influence panel motion. A closer look at Fig. 4 reveals that prior to 08:35, the solar elevation is below the operational threshold (see also Figure 2.3), and the panel remains vertical (90° tilt) with its azimuth aligned horizontally to the sun. After 08:35, optimization begins. At 12:50, as the sun crosses its zenith (see also Figure 2.3) and the panel tilt approaches its minimum value, a large azimuthal rotation occurs to continue following the sun into the afternoon. After 17:05, as the sun nears sunset, the elevation drops below the threshold again.

To ensure the system meets a target cumulative radiation threshold, an iterative refinement loop reduces the alignment goal when necessary. Figure 2.5 visualizes this process, plotting total received radiation versus alignment target values. Green markers denote successful configurations, while red marker represent insufficient radiation yield. The blue line illustrates the refinement path, clearly converging toward feasibility as the alignment target is gradually relaxed.

Figure 2.6 provide a spatial validation of the optimization results using 3D visualizations of the panel and its shadow projections at two key times (09:00 and 12:00). When constraints are enforced (Figure 2.6(a) and Figure 2.6(c)), shadows remain

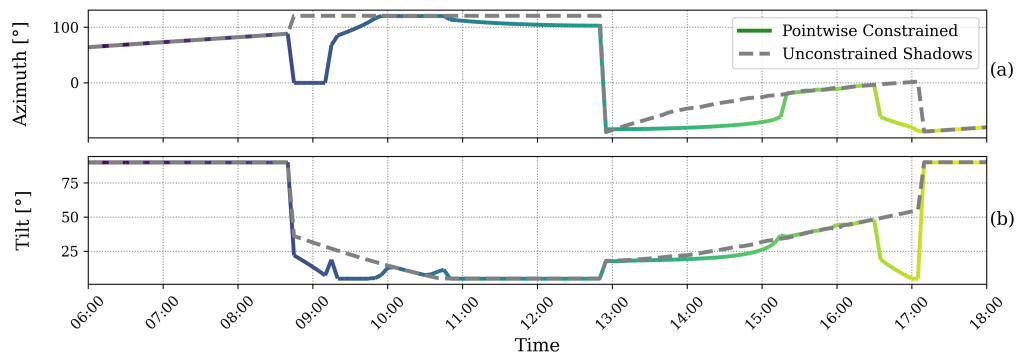


Figure 2.4: Panel azimuth (top) and tilt (bottom) angles as a function of time. Pointwise constrained results shown in color, unconstrained in dashed gray.

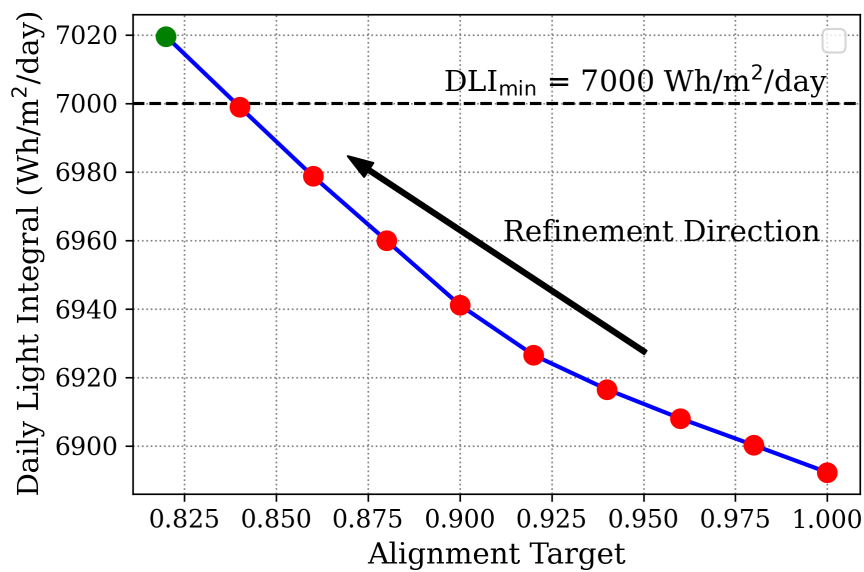


Figure 2.5: Effect of alignment target on overall radiation across the entire area . The dashed line indicates the required minimum threshold, while circle marks denote the sampled values of target alignment parameter (red: constraint not satisfied, green: constraint satisfied).

within the plant bounds, confirming feasibility. In contrast, the unconstrained cases (Figure 2.6(b) and Figure 2.6(d)) show violations, with shadows extending beyond the designated area, emphasizing the importance of constraint-aware design.

2.5 Conclusions

This chapter has proposed an optimization model for dual-axis agro-voltaic systems that maximize solar energy capture while ensuring that solar panel shadows remain within predefined farmland boundaries and the daily exposure requirements for crops are satisfied. Realistic simulation results over a full sunny day demonstrate the system's adaptability to varying solar conditions. The proposed strategy dynamically determines the optimal panel orientations by iteratively adjusting the alignment with the Sun to satisfy both energy generation objectives and agriculture-related constraints.

Future development of this work will focus on integrating machine learning techniques to enhance optimization performance, enabling coordination among neighboring cells

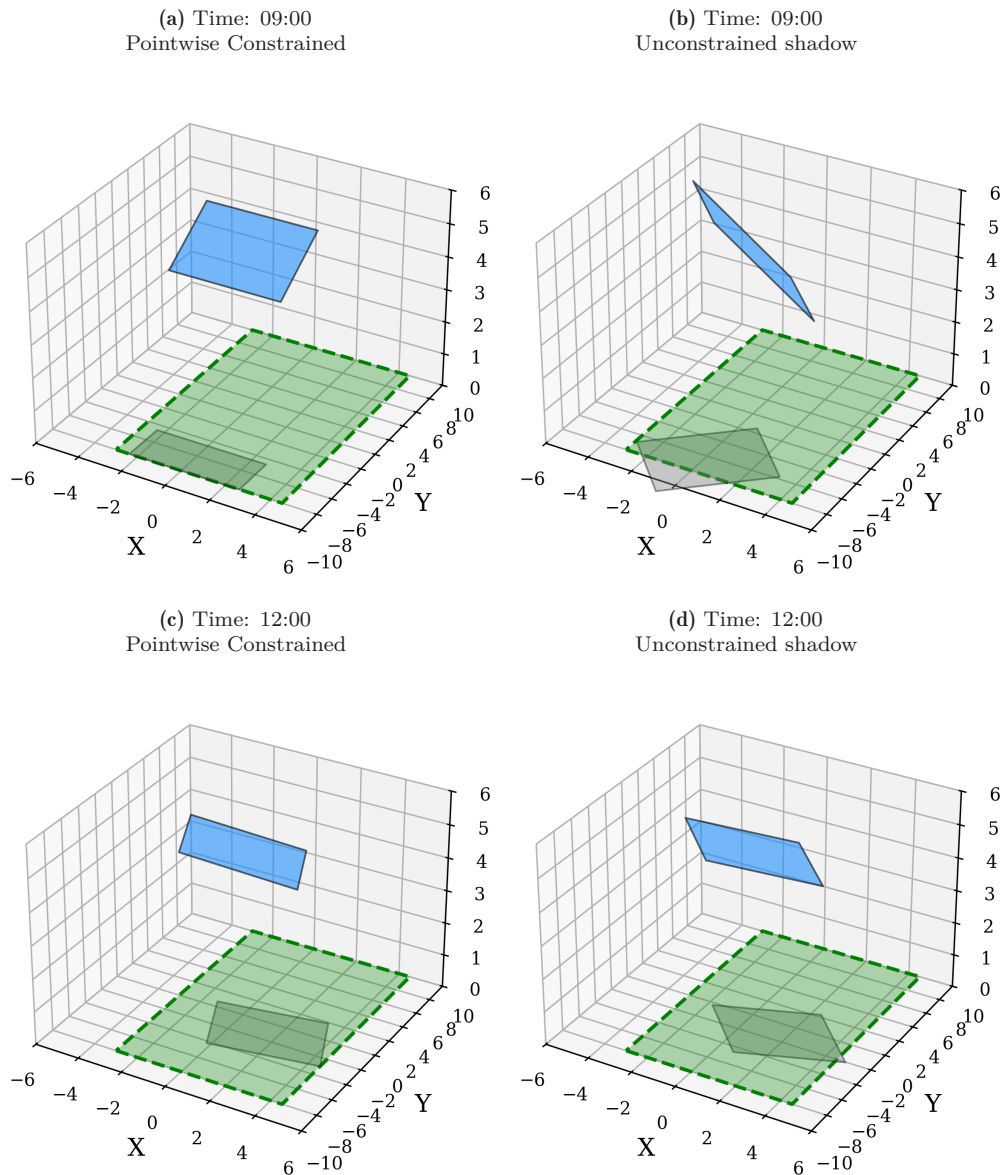


Figure 2.6: Comparison of constrained (a, c) and unconstrained (b, d) optimization results at 09:00 and 12:00. Shadow overshoot in the unconstrained cases emphasizes the need for spatial constraints.

in farmland, and extending the framework to incorporate additional energy and environmental objectives and constraints.

References

- [1] Ritchie, H. and Roser, M., “Emissions by sector,” *Our World in Data*, 2020. [Online]. Available: <https://ourworldindata.org/emissions-by-sector>.
- [2] Shahmohamadloo, R. S., Febria, C. M., Fraser, E. D., and Sibley, P. K., “The sustainable agriculture imperative: A perspective on the need for an agrosystem approach to meet the united nations sustainable development goals by 2030,” *Integrated Environmental Assessment and Management*, vol. 18, no. 5, pp. 1199–1205, 2021.

-
- [3] Soussi, A., Zero, E., Sacile, R., Trincherò, D., and Fossa, M., “Smart sensors and smart data for precision agriculture: A review,” *Sensors*, vol. 24, no. 8, p. 2647, 2024.
- [4] Gorjian, S. et al., “Progress and challenges of crop production and electricity generation in agrivoltaic systems using semi-transparent photovoltaic technology,” *Renewable and Sustainable Energy Reviews*, vol. 158, p. 112126, 2022.
- [5] Zainali, S. et al., “Direct and diffuse shading factors modelling for the most representative agrivoltaic system layouts,” *Applied Energy*, vol. 339, p. 120981, 2023.
- [6] Gupta, V. et al., “Optimizing corn agrivoltaic farming through farm-scale experimentation and modeling,” *Cell Reports Sustainability*, vol. 1, no. 7, 2024.
- [7] Abidin, M. A. Z., Mahyuddin, M. N., and Zainuri, M. A. A. M., “Optimal efficient energy production by pv module tilt-orientation prediction without compromising crop-light demands in agrivoltaic systems,” *IEEE Access*, vol. 11, pp. 71557–71572, 2023.
- [8] Guarino, S., Buscemi, A., Chiaruzzi, C., and Brano, V. L., “Modelling and analysis of v-shaped bifacial pv systems for agrivoltaic applications: A python-based approach for energy optimization,” *Applied Energy*, vol. 389, p. 125785, 2025.
- [9] Mignoni, N., Carli, R., and Dotoli, M., “Layout optimization for photovoltaic panels in solar power plants via a minlp approach,” *IEEE Transactions on Automation Science and Engineering*, 2023.
- [10] Paschalis, A., Bonetti, S., and Fatichi, S., “Controls of ecohydrological grassland dynamics in agrivoltaic systems,” *Earth’s Future*, vol. 13, no. 3, e2024EF005183, 2025.
- [11] Petrakis, T., Thomopoulos, V., and Kavga, A., “Algorithmic advancements in agrivoltaics: Modeling shading effects of semi-transparent photovoltaics,” *Smart Agricultural Technology*, vol. 9, p. 100541, 2024.
- [12] Bruno, M., Gfüllner, L. J., and Berwind, M. F., “Enhancing agrivoltaic synergies through optimized tracking strategies,” *Journal of Photonics for Energy*, vol. 15, no. 3, pp. 032703–032703, 2025.
- [13] Tan, Y. et al., “Agrivoltaics development progresses: From the perspective of photovoltaic impact on crops, soil ecology and climate,” *Environmental Research*, p. 120540, 2024.
- [14] Mignoni, N., Scarabaggio, P., Carli, R., and Dotoli, M., “Optimal Solar Tracking for Sustainable Crop Cultivation and Energy Generation in Agrivoltaics,” in *2025 9th IEEE Conference on Control Technology and Applications (CCTA)*, 2025 (submitted).
- [15] Mignoni, N., Scarabaggio, P., Carli, R., and Dotoli, M., “Controlling PV Panels Tilt Orientation for Optimal Crop Shading and Power Generation in Agrivoltaics,” *IEEE Transactions on Control Systems Technology*, 2025 (under review).
- [16] Anderson, K. S., Hansen, C. W., Holmgren, W. F., Jensen, A. R., Mikofski, M. A., and Driesse, A., “Pvlib python: 2023 project update,” *Journal of Open Source Software*, vol. 8, no. 92, p. 5994, 2023.
- [17] Virtanen, P. et al., “Scipy 1.0: Fundamental algorithms for scientific computing in python,” *Nature methods*, vol. 17, no. 3, pp. 261–272, 2020.

Chapter 3

Predictive Energy Scheduling of Smart Parking Infrastructure with Solar-powered Electric Vehicles



Abstract

This chapter presents a novel model predictive control framework for managing energy flow in smart parking infrastructures with renewable energy facilities, electric vehicles, and solar-powered electric vehicles. The proposed control framework minimizes the energy costs for the parking lot operators, ensuring the user-defined charge levels for vehicles at departure, and protecting the charging infrastructure during operation. Field validation on Lonsdale Street, Melbourne (Australia)—using real data on vehicle behavior, solar irradiance, and energy prices—shows significant grid load reduction even with partial solar production. Compared to a rule-based strategy, the MPC approach reduces operational costs by 15.32% and energy demand by 6.12%. Lastly, we show that the proposed framework is robust under forecast uncertainty, supporting its practical deployment in dynamic real-world environments.

Contents

3.1	Introduction	22
3.2	Related Works	23
3.3	The Smart Parking Infrastructure Model	25
3.4	Predictive Control of the Parking Facility	27
3.5	Numerical Experiments	29
3.6	Conclusions	38

3.1 Introduction

The electrification of transport is a key strategy to reduce greenhouse gas emissions and improve energy sustainability [1]. Among electric vehicles (EVs), solar-powered electric vehicles (SPEVs) represent a promising solution to deepen the impact of this technological revolution. SPEVs are equipped with vehicle-integrated photovoltaic systems that generate solar energy directly onboard [2]. This feature allows SPEVs to offset grid electricity consumption, potentially limiting operating costs and mitigating peak demand on power grids.

Recent technological advances and market trends suggest that integrating solar panels into electric vehicles will become increasingly common. Projections indicate that by 2030, a significant share of the global EV fleet will include solar integration [3]. By harnessing renewable energy at the point of use, SPEVs offer a novel paradigm for enhancing energy efficiency and reducing reliance on centralized infrastructure. Specifically, SPEVs can reduce the load on the central grid, lower transmission losses, and extend the driving range by utilizing self-generated energy. Moreover, they act as mobile energy producers and storage units, enabling more flexible and decentralized energy management [2], [4].

However, realizing SPEVs' full potential requires appropriate support infrastructures. As these vehicles integrate photovoltaic systems, they can not only generate energy for onboard consumption but also inject surplus electricity into the grid when conditions

allow [2]. Consequently, smart parking facilities must be equipped to manage the bidirectional and intermittent power flows characteristic of SPEVs [5]. These flows arise not only from conventional charging and discharging but also from simultaneous solar generation. This dynamic behavior complicates the charging piles (CPs) operation, especially within vehicle-to-grid (V2G) schemes that allow vehicles to feed electricity to the grid during high-demand periods [6]. In fact, SPEVs can act both as distributed energy storage and generation units. Indeed, when aggregated in a smart parking lot, EVs and SPEVs represent a unique opportunity to support grid flexibility. Nevertheless, their integration requires careful management to avoid overloading CPs or the power grid, particularly when surplus solar power from multiple vehicles occurs.

The remainder of this chapter is organized as follows. Section 3.2 reviews the related literature and presents the contribution of this work. Section 3.3 details the system model. The control framework is presented in Section 3.4. Section 3.5 provides numerical simulation results. Finally, Section 3.6 concludes the chapter and provides future outlooks.

3.2 Related Works

Integrating EVs into smart grids has motivated a wide range of studies on optimizing charging strategies to reduce costs and balance energy demand [7], [8]. Early works in this area focused on heuristic-based methods. For example, Mohamed et al. [9] proposed a real-time energy management framework for plug-in hybrid EV parks despite lacking formal optimization guarantees, potentially deviating from optimal energy allocations. In contrast, [10] introduced a two-stage optimization approach to manage large-scale EV charging under renewable energy integration. While scalable, the underlying model excludes bi-directional power flows and thus cannot support V2G applications or energy storage behavior. Game-theoretic formulations have also been applied to charging coordination. [11] presented a decentralized control strategy for plug-in hybrid EVs, though it remains limited to unidirectional charging scenarios. [12] and [13] addressed battery energy storage and degradation, respectively, with the latter embedding degradation costs within a game-theoretic V2G market design.

Several recent studies confirm the adaptability and scalability of MPC for EV charging under renewable integration. For instance, Zheng et al. [14] propose a scalable distributed MPC scheme for multi-station coordination, while Shi et al. [15] jointly optimize EV charging and power flow. Real-world data are leveraged in Dai et al. [16], where an LSTM-based forecasting model is trained on EV charging data from a major Oslo facility to support data-driven peak shaving. A block-level MPC is proposed in [17] to reduce demand charges in PV-integrated charging networks. Personalized scheduling for autonomous EVs is addressed through hierarchical MPC in [18]. Reliability in microgrids is tackled by a three-stage MPC in [19], and stochastic MPC is applied in [20] to manage HVAC and EV loads under renewable uncertainty. These studies, however, focus exclusively on conventional EVs, omitting the complexities introduced by solar generation in SPEVs.

Recent experimental studies have begun to assess SPEV-specific infrastructure. Baek and Choi [21] investigated shading matrices to optimize solar exposure for parked vehicles, illustrating the spatial sensitivity of onboard photovoltaic generation. Ahmad et al. [22] proposed a real-time load scheduling algorithm for SPEVs using Lyapunov optimization to improve PV energy sufficiency. Despite its strengths in managing user profit and local energy use, this approach lacks predictive capabilities, which limits its adaptability to system dynamics. Recently, Fakour et al. [23] conducted a comprehensive assessment of a solar photovoltaic carport canopy integrated with an EV charging station in Kaohsiung, Taiwan, demonstrating that such infrastructure can yield up to 140 MWh/year, highlighting the importance of studies on SPEV charging station infrastructures. Furthermore, the reliance on nonlinear programming impairs scalability and precludes convexity guarantees, which are critical for real-time implementation. While EV integration into energy systems has been widely explored [13], [24], [25], [26], the requirements of SPEVs remain underrepresented in the related literature. Current

infrastructure designs rarely address the dual role of SPEVs as energy generators and storage units [27].

Model predictive control (MPC) has emerged as a compelling strategy for managing such complex, time-varying energy systems [28]. MPC enables real-time optimization of energy exchanges while considering forecasted variables and system constraints. Nevertheless, several challenges persist. Unlike conventional EVs, SPEVs exhibit continuous fluctuations in their state of charge (SoC), driven by the variable output of solar panels and user driving patterns. Recent advances in MPC for V2G applications have introduced promising frameworks to manage SoC constraints. Wu et al. [29] and Diaz et al. [30] propose MPC formulations that explicitly enforce SoC targets at vehicle departure, using forecasts to guide real-time decision-making. Multi-layered MPC structures have been suggested to coordinate near-term and long-term objectives, balancing accuracy and computational load [31]. Stochastic MPC approaches introduce probabilistic constraints to accommodate uncertainty in arrival and departure times [32]. At the same time, economic incentives are employed in some studies to encourage user compliance with energy management goals [33]. Despite these developments, several limitations remain. Most MPC frameworks assume that SoC constraints are only relevant when the departure time falls within the prediction horizon, neglecting long-term feasibility. Additionally, few models explicitly address the risks of dual charging or consider CP operational safety under uncertain, solar-driven power flows. Moreover, real-world validations of MPC for SPEVs remain scarce, and the effect of prediction errors on cumulative energy performance is mainly unexplored.

To address the above-discussed challenges, in this chapter, we introduce a novel control and optimization framework for energy management in smart parking lots that serve both EVs and SPEVs. Specifically, the contributions of this chapter are reported below.

- We develop a novel convex MPC framework tailored for SPEVs charging infrastructure that considers the stochastic nature of vehicle arrivals, departures, and solar generation. A convex model is applied to prevent simultaneous charging and discharging, eliminating the need for mixed-integer formulations and limiting computational overhead.
- To enhance system robustness, we introduce an operational constraint to protect CPs, particularly in scenarios involving unexpected solar surges or abrupt user behavior. A dynamic constraint is integrated to ensure inter-temporal consistency across control horizons.

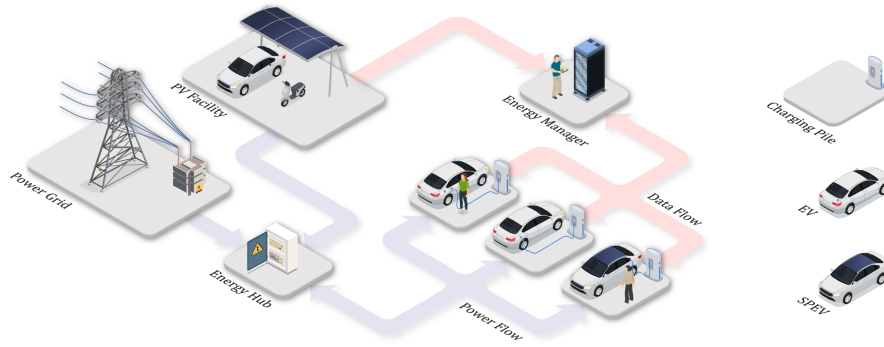
The proposed framework is validated using real-world data from the central business district of Melbourne, Australia. A brief comparison between our work and the most related studies is listed in Table 3.1.

Notation: Let \mathbb{R} , $\mathbb{R}_{>0}$, and $\mathbb{R}_{\geq 0}$ denote the sets of real, strictly positive real, and non-negative real numbers, respectively. Known parameters are represented by uppercase letters (e.g., A), while decision variables are denoted by lowercase letters (e.g., a). Given a finite set $\mathcal{S} \subset \mathbb{N}$, we denote by $\inf(\mathcal{S})$ and $\sup(\mathcal{S})$ its infimum and supremum. In this chapter, we adopt the standard notation used in MPC. Let x represent a generic variable, and $x(t | k)$ denotes the predicted value of x at a future time slot t , based on the information available at time k . The prediction horizon is defined as $\mathcal{H}_k := \{k, \dots, t, \dots, k + H\}$, where H represents its length and Δt is the step size. Additionally, we assume that the control horizon is equal to the prediction horizon¹.

¹In MPC, the prediction horizon determines how far into the future the system anticipates from its current state, while the control horizon, often shorter, specifies the duration for which control strategies are calculated. A longer prediction horizon generally results in smoother, less aggressive control inputs, facilitating a gradual transition toward the desired state. Conversely, a shorter prediction horizon leads to more aggressive control actions. Thus, the lengths of these horizons play a key role in ensuring the stability and effectiveness of the MPC framework [34], [35]

Table 3.1: Comparative Review of EV Charging Control Literature

Study	Methodology	Scope	Strengths	Limitations / Gaps Addressed
Mohamed et al. [9]	Heuristic real-time energy management (fuzzy control)	Grid-connected PHEV charging parks with PV	Adaptive to uncertainty in SoC and arrival times	No formal optimization guarantees or robustness; lacks battery safety logic, No SPEV
Wang et al. [10]	MILP + Lagrangian duality in VANET-enhanced grid	Fast-charging routing under mobility	Location-aware, scalable, cost-optimal navigation	Assumes perfect VANET communication and data fidelity, No SPEV
Zheng et al. [14]	Distributed MPC with convexified OPF	Multi-station EV networks in grid	Grid-aware, scalable, privacy-preserving	Assumes full EV data and participation; no PV dynamics
Wu et al. [29]	MDP + BRTDP for PV-assisted EVCS with V2G, under uncertain user behavior and dynamic pricing	Energy management for PV-assisted EV charging stations	Realistic modeling + efficient algorithm + real data validation	Assumes full V2G participation, No SPEV, No real-world implementation
Shi et al. [15]	Centralized MPC	Multi-CS distribution grid coordination	Accurate load forecasting, cost-aware	No PV modeling or SoC dynamic constraints, No SPEV
Yang et al. [17]	Block Model Predictive Control	uncertain demand forecasts in a distribution grid setting	Economic realism + real-time control + innovative MPC design	No integration with renewables/V2G, not tested on real-world datasets, No SPEV
Fakour et al. [23]	Empirical solar performance study	Standalone PV-EV station	Real-world power yield (140 MWh/year), inverter test	No control, no optimization, no SoC modeling
Present Study	Convex MPC + Dynamic constraints	SPEVs in smart parking lots with case study	Real-time, SoC-aware, solar-adaptive; avoids MIP overhead	First to ensure inter-horizon, SoC safety, CP protection, and scalable real-world SPEV validation


Figure 3.1: Schematic of the smart parking infrastructure supporting both EVs and SPEVs. Pink arrows indicate data flow, while purple arrows denote power flow.

3.3 The Smart Parking Infrastructure Model

This section presents the novel model for smart parking infrastructure designed to support both EVs and SPEVs while integrating renewable power generation. The system architecture is illustrated in Fig. 3.1. The infrastructure includes an on-site photovoltaic (PV) system, multiple CPs, an energy hub that routes all power flows, and an energy manager (EM). The EM manages all data and information flows, enabling the real-time optimization of power flows within the facility and with the main power grid. Each vehicle, whether an EV or an SPEV connects to a CP. While EVs contribute energy solely via their onboard batteries, SPEVs additionally generate electricity through vehicle-integrated PV panels. These panels are mounted directly on the vehicle rooftops, supplementing the solar power harvested by the parking infrastructure itself.

Assumption 3.3.1

The inherent variability of solar irradiance makes it difficult to accurately forecast the power output of the parking facility's PV system and the rooftop-mounted PV arrays of SPEVs over long horizons. Nevertheless, forecasts of PV power production

with reasonable accuracy are available for up to three days in advance [4]. Since the prediction horizons considered in this study are well within this forecast window, solar generation is here treated as a deterministic input. This modeling choice is further justified by the use of a predictive control framework, which updates forecasts at each control step and thus inherently mitigates the effect of prediction errors. \square

Assumption 3.3.2

The EM has full authority over the power flows within the facility, including control of PV generation, grid imports, and vehicle-specific charge/discharge operations at each CP. \square

More specifically, let us consider a parking facility consisting of a set of CPs, denoted as $\mathcal{N} := \{1, \dots, i, \dots, N\} \subset \mathbb{N}$, where N represents the total number of CPs. The solar power generation of the PV infrastructure at the parking facility at each time step t is denoted by $R(t) \in \mathbb{R}_{\geq 0}$. In accordance with Assumption 3.3.1, this quantity is treated as a deterministic input, dependent on parameters such as solar irradiance, PV panel area, and system efficiency.

Following Assumption 3.3.2, the EM governs both data and power flows throughout the facility over the prediction horizon \mathcal{H}_k , as illustrated by the bi-directional arrows in Fig. 3.1. Unlike traditional approaches that rely on individual vehicle-based models, the proposed framework adopts a more practical system-level view. Rather than tracking individual vehicle models, the EM supervises the CPs, which dynamically interact with vehicles as they connect and disconnect. Thus, lower-level control tasks are delegated to CPs. Consequently, from this point onward, the power generation capacity and storage dynamics of a vehicle connected to $i \in \mathcal{N}$ are abstracted as the generation and storage behavior of the CP itself. For each $i \in \mathcal{N}$, we define a set of vehicle arrival times, $\mathcal{A}_i \subset \mathbb{N}$. The initial SoC of a vehicle arriving at $i \in \mathcal{N}$ at time $t \in \mathcal{A}_i$ is represented by $\text{SoC}_{\text{in},i}(t) \in \mathbb{R}_{\geq 0}$. Similarly, we define a set of vehicle departure times, $\mathcal{D}_i \subset \mathbb{N}$, and denote the charging requirement of a vehicle leaving $i \in \mathcal{N}$ at time $t \in \mathcal{D}_i$ as $\text{SoC}_{\text{en},i}(t) \in \mathbb{R}_{\geq 0}$. The solar power generation for $i \in \mathcal{N}$ is represented as $R_i(t) \in \mathbb{R}_{\geq 0}$.

At any time step t , the EM can either charge $c_i(t)$ or discharge $d_i(t)$ the storage capacity associated with $i \in \mathcal{N}$. Accordingly, the discrete-time storage dynamics governing the evolution of the SoC for each $i \in \mathcal{N}$, denoted as $s_i(t)$, is given by:

$$s_i(t) = \delta_i(t) (s_i(t-1) + \eta_c c_i(t-1)\Delta t - \eta_d d_i(t-1)\Delta t), \quad \forall i \in \mathcal{N}, \forall t \in \mathcal{H}_k, \quad (3.1)$$

where parameter $\delta_i(t) \in 0, 1$ is a time-dependent parameter derived from the known arrival and departure times of the vehicle, and is equal to one if a vehicle is connected to CP i at time t , i.e., $\delta_i(t) = 1$, and zero otherwise. The SoC at t denoted by $s_i(t)$ is a state variable. Parameters η_c and η_d are the known charging and discharging efficiencies, with $0 < \eta_c < \eta_d$.

To represent the physical limitations of the storage device, we introduce the following constraints:

$$s_i(t) \geq \delta_i(t) \text{SoC}_{\text{min}}(t), \quad \forall i \in \mathcal{N}, \forall t \in \mathcal{H}_k, \quad (3.2)$$

$$s_i(t) \leq \delta_i(t) \text{SoC}_{\text{max}}(t), \quad \forall i \in \mathcal{N}, \forall t \in \mathcal{H}_k, \quad (3.3)$$

$$0 \leq c_i(t) \leq \delta_i(t) C_{\text{max}}(t), \quad \forall i \in \mathcal{N}, \forall t \in \mathcal{H}_k, \quad (3.4)$$

$$0 \leq d_i(t) \leq \delta_i(t) D_{\text{max}}(t), \quad \forall i \in \mathcal{N}, \forall t \in \mathcal{H}_k, \quad (3.5)$$

where $\text{SoC}_{\text{max}}(t)$ and $\text{SoC}_{\text{min}}(t)$ denote the maximum and minimum energy storage levels, respectively. The parameters $C_{\text{max}}(t)$ and $D_{\text{max}}(t)$ define the upper bounds for charging and discharging, taking into account physical limitations imposed by the inverter and the storage device. All these parameters are time-varying, as different vehicles may be connected to each $i \in \mathcal{N}$ through the horizon \mathcal{H}_k .

The initial SoC at $t \in \mathcal{A}_i$ is known. Thus, we impose:

$$s_i(t) = \text{SoC}_{\text{in},i}(t), \quad \forall i \in \mathcal{N}, \forall t \in \mathcal{A}_i \cap \mathcal{H}_k, \quad (3.6)$$

while to guarantee that each vehicle meets its final SoC requirement upon departure, we impose that:

$$s_i(t) \geq \text{SoC}_{\text{en},i}(t), \quad \forall i \in \mathcal{N}, \quad \forall t \in \mathcal{D}_i \cap \mathcal{H}_k. \quad (3.7)$$

A critical challenge arises when a vehicle's departure time lies outside the horizon \mathcal{H}_k . In such cases, the EM may allocate insufficient energy within the current horizon \mathcal{H}_k , potentially leading to future infeasibility since the remaining time and power constraints may be inadequate to meet the required terminal SoC in (3.7). A naive approach would be to assume that all vehicles depart within the current control horizon. While this guarantees feasibility, it undermines the advantages of a predictive framework. To address this challenge, we propose the dynamic constraint:

$$s_i(t) \geq \delta_i(t) \text{SoC}_{\text{en},i}(l_i(t)) - \sum_{j=t}^{l_i-1} \delta_i(t) \eta_c C_{\text{max}}(j) \Delta t, \quad \forall i \in \mathcal{N}, \quad \forall t \in \mathcal{H}_k, \quad (3.8)$$

where l_i is the earliest departure time following the latest arrival within the prediction horizon, defined as $l_i(t) = \inf(\{t' \in \mathcal{D}_i \mid t' \geq t\})$. Constraint (3.8) ensures that, at each time t , the current SoC is sufficient to reach the desired final SoC by the vehicle's departure time, even when the actual departure lies outside the current control horizon.

The following technical constraints are also imposed to represent the physical bounds on solar power flows:

$$0 \leq v(t) \leq R(t), \quad \forall i \in \mathcal{N}, \quad \forall t \in \mathcal{H}_k, \quad (3.9)$$

$$0 \leq v_i(t) \leq R_i(t), \quad \forall i \in \mathcal{N}, \quad \forall t \in \mathcal{H}_k, \quad (3.10)$$

where $v(t)$ represents the curtailed power from the PV parking facility and $v_i(t)$ denotes the curtailed portion of solar power from $i \in \mathcal{N}$.

To ensure the safe operation of the CPs, we define the following constraint on the net power exchanged with a connected vehicle:

$$d_i(t) - c_i(t) + R_i(t) - v_i(t) \leq P_{\text{max}}, \quad \forall i \in \mathcal{N}, \quad \forall t \in \mathcal{H}_k, \quad (3.11)$$

where P_{max} denotes the maximum allowable power for the CP interface.

Finally, when local generation is insufficient to satisfy the demand, the EM may exchange power with the main grid, denoted by $g(t)$, at each time step t . We assume that grid power is only drawn, i.e.,

$$g(t) \geq 0, \quad \forall t \in \mathcal{H}_k. \quad (3.12)$$

Under this assumption, the power balance within the system over the control horizon \mathcal{H}_k is enforced by the following equation:

$$\sum_{i \in \mathcal{N}} (-R_i(t) + v_i(t) - d_i(t) + c_i(t)) = R(t) - v(t) + g(t), \quad \forall t \in \mathcal{H}_k. \quad (3.13)$$

3.4 Predictive Control of the Parking Facility

The EM aims at coordinating all power flows within the parking lot while fulfilling the charging requirements of all connected vehicles. Specifically, the EM seeks to minimize the total cost of energy drawn from the main grid, reduce the degradation of both EVs and SPEV storage devices, and promote efficient resource utilization, treating all vehicles uniformly. This is achieved through an MPC framework that optimizes energy usage over a finite prediction horizon. Adopting an MPC strategy allows the system to adapt to real-time variations in vehicle arrivals, solar generation forecasts, and electricity prices, mitigating the impact of forecast uncertainties by continuously re-solving the optimization problem over a receding horizon. Specifically, the EM aims at minimizing the cost of

Algorithm 3.1 MPC Energy Scheduling

```

1: for  $k = 0, 1, 2, \dots$  do
2:   Get  $\lambda(t|k), \forall t \in \mathcal{H}_k$ 
3:   Get  $R(t|k), \forall t \in \mathcal{H}_k$ 
4:   for  $i \in \mathcal{N}$  do
5:     Update  $\mathcal{A}_i, \mathcal{D}_i, \forall i \in \mathcal{N}$ 
6:     Get  $R_i(t|k), \forall t \in \mathcal{H}_k$ 
7:     Get  $\text{SoC}_{\text{in}}(j), \forall j \in \mathcal{A}_i \cap \mathcal{H}_k$ 
8:     Get  $\text{SoC}_{\text{en}}(j), \forall j \in \mathcal{D}_i \cap \mathcal{H}_k$ 
9:   end for
10:  Solve (3.14)
11:  Apply  $g(k+1|k), v(k+1|k)$ 
12:  Apply  $c_i(k+1|k), d_i(k+1|k), v_i(k+1|k), \forall i \in \mathcal{N}$ 
13:  Update  $s_i(k+1|k)$  using (3.1)
14: end for
    
```

energy drawn from the main grid, where the unit energy price at time t is denoted by $\lambda(t)$ and is assumed to be known over the control horizon \mathcal{H}_k .

To mitigate the impact of frequent charge and discharge cycles on the battery's lifespan, we consider two given cost coefficients, $\alpha \geq 0$ and $\beta \geq 0$, with $\alpha + \beta > 0$, representing the penalties associated with battery charging and discharging operations, respectively.

The resulting optimal energy scheduling problem over the control horizon \mathcal{H}_k involves $(3N + 2)H$ optimization variables and is formulated as follows:

$$\begin{aligned}
 & \underset{\substack{g(t), v(t) \\ c_i(t), d_i(t), v_i(t)}}{\text{minimize}} && \sum_{t \in \mathcal{H}_k} \Delta t \left(\lambda(t)g(t) + \sum_{i \in \mathcal{N}} (\alpha c_i(t) + \beta d_i(t)) \right) && (3.14) \\
 & \text{subject to} && (3.1) - (3.13).
 \end{aligned}$$

Notably, both the objective function and the constraint set of (3.14) are convex. This ensures that the solution space avoids local minima and supports the efficient computation of globally optimal solutions [28].

Remark 3.4.1

The storage model defined by equations (3.1)–(3.8) does not inherently prevent simultaneous charging and discharging. That is, both $c_i(t)$ and $d_i(t)$ can take strictly positive values during the same time slot t . To avoid this undesired behavior without introducing binary variables—and thus preserving convexity, a set of sufficient convexity conditions can be imposed, as described in [28]. These include: $0 < \eta_c < \eta_d$, $\alpha, \beta > 0$, $(\alpha + \beta) > 0$, and non-negative electricity prices $\lambda(t) \geq 0$ for all $t \in \mathcal{H}_k$. Under these conditions, any control policy that results in simultaneous charging and discharging is strictly suboptimal with respect to the convex cost function. Hence, any convex gradient-based solver avoids such solutions, maintaining physical consistency without requiring mixed-integer programming [28], [36]. \square

The proposed MPC framework for parking energy scheduling is outlined in Algorithm 1. At each time step k , the following sequence of operations is performed (lines 2–13 of Algorithm 1). First, the EM system receives the updated energy price coefficients $\lambda(t)$ from the main grid (line 2) and generates PV power production forecasts for the parking infrastructure PV facility using solar radiation data (line 3). Next, for each charging pile (line 4), vehicle-specific information such as arrival and departure times (line 5), PV power forecasts (line 6), and the initial and required final states of charge (line 7-8) are collected. Subsequently, the EM solves the online optimal control problem (3.14) (line 10). The resulting actions for the current step are then applied in closed-loop form (line 11-13).

3.5 Numerical Experiments

This section evaluates the proposed framework across three scenarios, designed to test its effectiveness under varying conditions from controlled simulations to real-world integration. All simulations are performed using MATLAB R2023a on a machine equipped with an Apple M2 8-core CPU and 8GB of RAM.

Vehicles are modeled with a nominal storage capacity of 50 kWh. To preserve vehicle battery health, the SoC is constrained within the range [15%, 85%] of the nominal capacity, in accordance with established best practices [37]. The initial SoC values are uniformly distributed within the range [15%, 55%], while the required SoC levels at departure fall within [55%, 85%] of the nominal capacity. Charging and discharging efficiencies are set to $\eta_c = 0.95$ and $\eta_d = 1/\eta_c$, respectively. The maximum allowable power exchanged between a CP and a vehicle during a time slot P_{\max} is set to 5 kWh.

To evaluate the influence of the prediction horizon in the various scenarios, we define the cumulative energy purchased from the grid over the simulation period as:

$$E_g = \sum_{k=0}^K g(k)\Delta t, \quad (3.15)$$

where K is the length of the simulation period.

3.5.1 Scenario 1

The first scenario evaluates two core aspects of the proposed framework: (i) whether the convex formulation prevents simultaneous charging and discharging and (ii) the role of SPEVs in reducing dependency on the main grid.

The first scenario considers a simulation of $K = 24$ hours with $\Delta t = 1$ hour, during which all vehicle arrivals and departures occur within the prediction horizon. The optimization is implemented using a 1-hour time step (i.e., $\Delta t = 1$ and $H = 24$). The facility includes a rooftop PV array covering 20, m², mounted at a 30-degree tilt with an efficiency of 16%. Solar irradiance forecasts are sourced from the U.S. Climate Reference Network [38] while power prices follow the pricing scheme reported in Table 3.2.

We consider a parking lot consisting of $N = 10$ CPs, each managing multiple vehicles. In this setting, 50% of the vehicles are assumed to be SPEVs, with the remaining 50% being conventional EVs. Vehicle behavior, arrival, departure, and SoC trajectories is kept consistent across both cases to ensure a fair comparison. Two infrastructure configurations are examined:

- **PL1:** Roofed parking lot with both EVs and SPEVs.
- **PL2:** Unroofed parking lot with both EVs and SPEVs.

It should be noted that, although PL1 includes both EVs and SPEVs, the presence of a rooftop structure prevents the system from harnessing the SPEVs' generation capabilities.

Figure 3.2 presents the results for PL1. Figure 3.2(a) shows the 24-hour profiles of grid power exchange, power generated by the parking lot's PV system, and parking lot's curtailed solar power. Charging pile #3 is selected as a representative example, and as shown in Fig. 3.2(b), charging and discharging operations occur at distinct time intervals, confirming the effectiveness of the convex relaxation strategy embedded in the control framework. The corresponding SoC profile is illustrated in Fig.3.2(c), demonstrating that CP #3 successfully meets the charging demands of four vehicles over the day.

The results for PL2 are shown in Fig. 3.3. Figure 3.3(a) displays the 24-hour profiles for grid power exchange, power generated by the parking lot's PV system, and curtailed solar power. The charging and discharging patterns for CP #3 are reported in Fig. 3.3(b), while Fig. 3.3(c) shows the corresponding SoC profile. Initial SoC values are identical to those in PL1 to ensure comparable conditions. Figure 3.3(d) highlights the power generated by vehicle-mounted PV panels and the associated curtailed power.

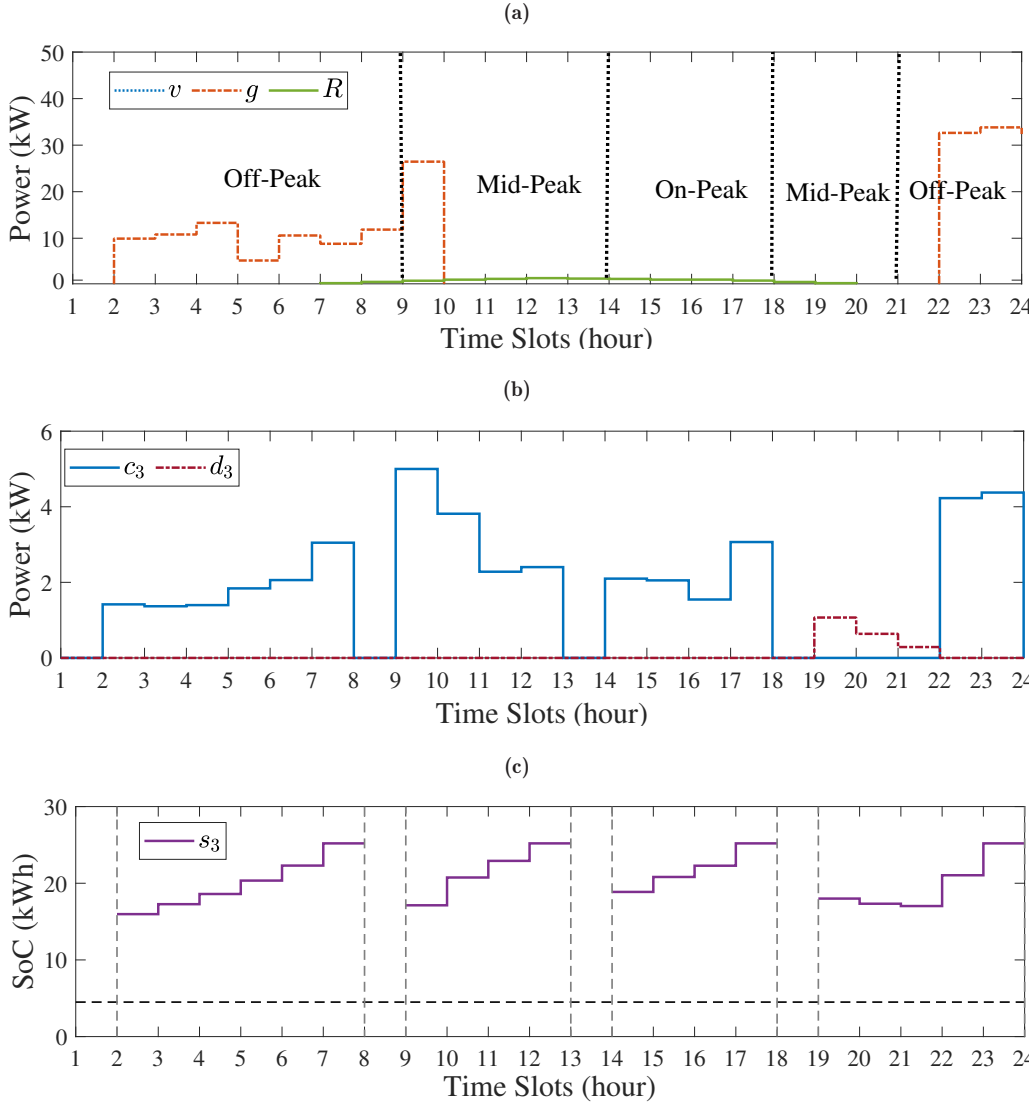


Figure 3.2: Scenario 1. Simulation results of configuration PL1: (a) grid power exchange g , PV power generation R , and curtailed PV power v ; (b) charging and discharging profiles of vehicles at CP #3; (c) SoC profiles for vehicles at CP #3.

Table 3.2: Pricing scheme for Scenario 1 and 2.

Time	Pricing Period	Power Price $\lambda(t)$
9 PM to 9 AM	Off-Peak	\$0.08/kWh
9 AM to 2 PM	Mid-Peak	\$0.13/kWh
2 PM to 6 PM	On-Peak	\$0.18/kWh
6 PM to 9 PM	Mid-Peak	\$0.13/kWh

Finally, the difference between the grid power exchange in PL1 and PL2 is presented in Fig. 3.4. The results show a lower grid power demand in PL2, confirming the enhanced independency enabled by SPEV integration and highlighting the practical advantages of the proposed architecture.

3.5.2 Scenario 2

To investigate the distinctive characteristics of SPEVs within the context of a V2G-capable system, we conducted a comparative analysis between PL2 and PL3. PL2 pertains to the second case, where we have an unroofed or partially uncovered parking lot, providing an opportunity for SPEVs to harness solar energy through their PV panels. We studied

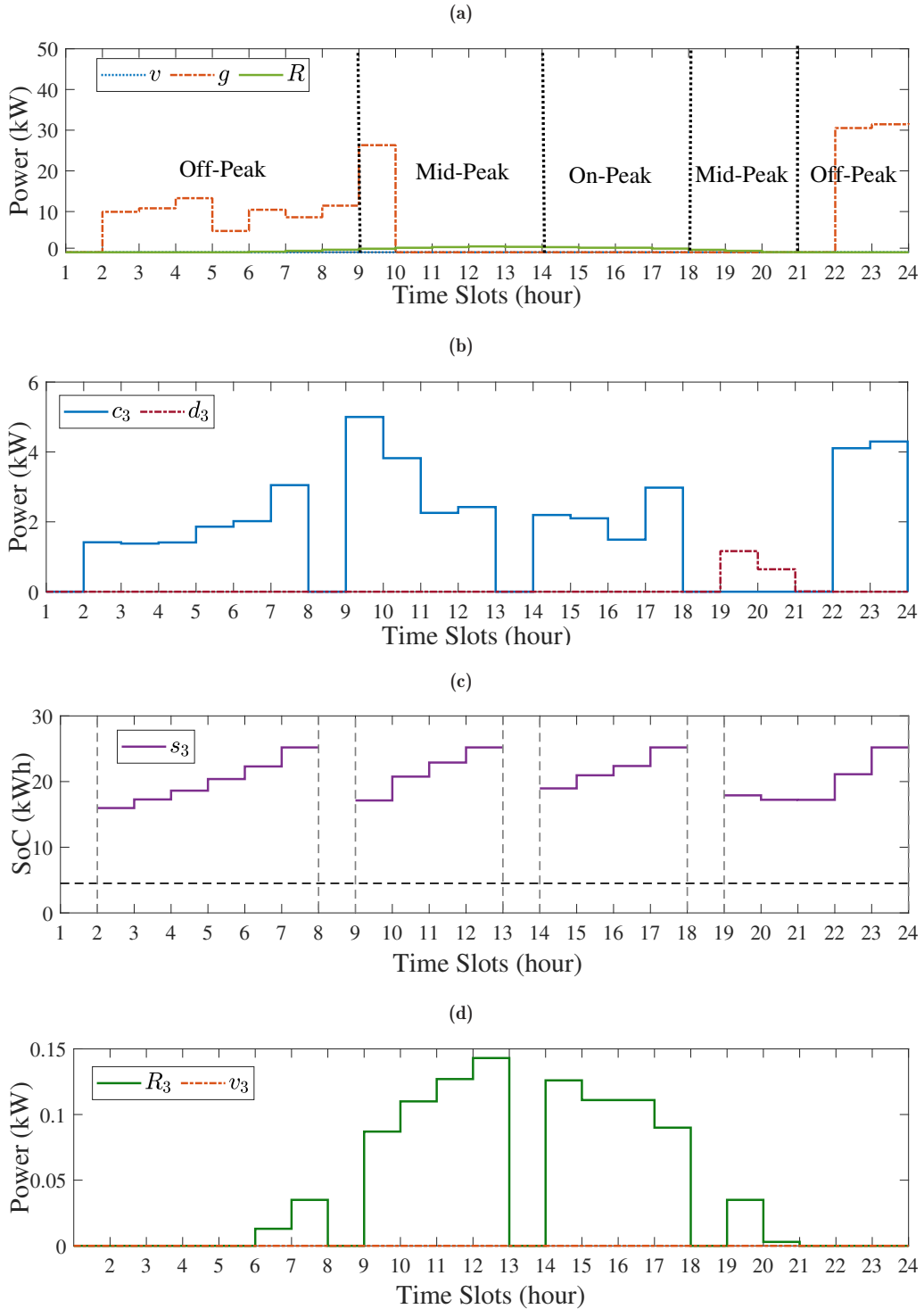


Figure 3.3: Scenario 1. Simulation results of configuration PL2: (a) grid power consumption g , PV power generation R , and curtailed PV power v ; (b) Charging and discharging profiles of vehicles at CP #3; (c) SoC profiles for vehicles at CP #3; (d) PV generation and curtailed power from SPEVs at CP #3.

this case in various scenarios, and in certain time horizons, observed situations where an SPEV experienced extreme solar penetration, generating surplus energy. Concurrently, the energy management system required substantial energy, leading to high discharging from the Energy Storage System (ESS). The results of this analysis for a specific SPEV are depicted in Fig. 3.7. In addition, we performed a similar analysis for the third case

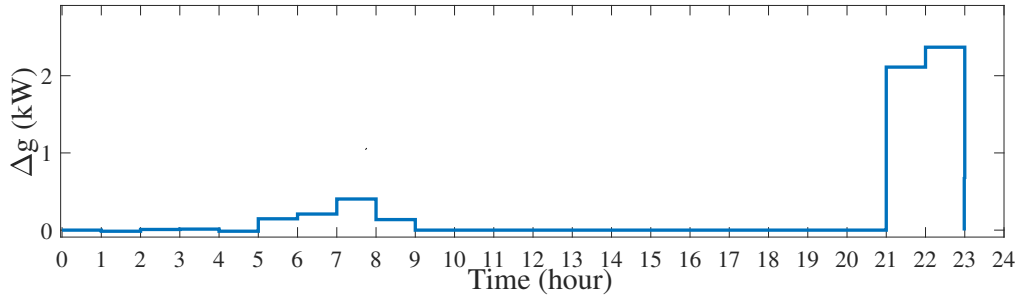
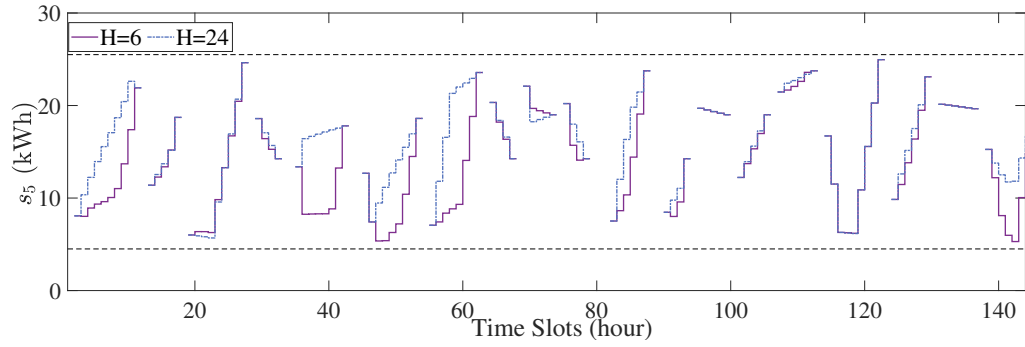


Figure 3.4: Scenario 1. Difference in power exchanged with the main grid between configurations PL1 (roofed parking lot) and PL2 (unroofed parking).

(a)



(b)

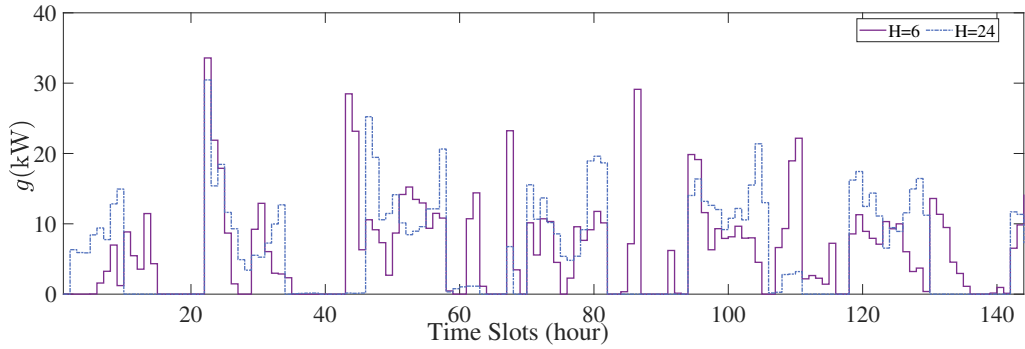


Figure 3.5: Scenario 2. Simulation results for two prediction horizons ($H = 6$ and $H = 24$). (a) SoC profiles for vehicles at CP #5 and (b) power exchanged with the main grid over the simulation period.

(PL3), where we implemented our proposed MPC model.

As previously elucidated, PL2 represents an unroofed V2G parking lot incompatible with SPEVs, while PL3 embodies an integrated V2G System catering to both EVs and SPEVs. In the comprehensive overview of the daily profiles for PL2, Fig. 3.7(a) illustrates the variations in v , g , and R . It is imperative to note that the quantity of R is consistent across PL1, PL2, and PL3. For this illustration, CP2 is selected as a representative charging pile. In Fig. 3.7(b), the charging and discharging dynamics for CP2 within PL2 are depicted. Notably, Fig. 3.7(c) reveals that CP2 serves a single vehicle throughout the 24 hours in PL2. In Fig. 3.7(d), the illustration demonstrates a critical observation: in PL2, which lacks compatibility with SPEVs, the amount of Power Delivered to the Vehicle from the Charging Pile ($P_{PDC} = d - c + R - v$) exceeds the designated maximum power capacity (P_{max}). This discrepancy poses a potential risk of damage to the charging infrastructure. Conversely, highlighting the contrast observed in PL3, compatibility with SPEVs ensures that P_{PDC} remains within the prescribed limits of P_{max} , as depicted in

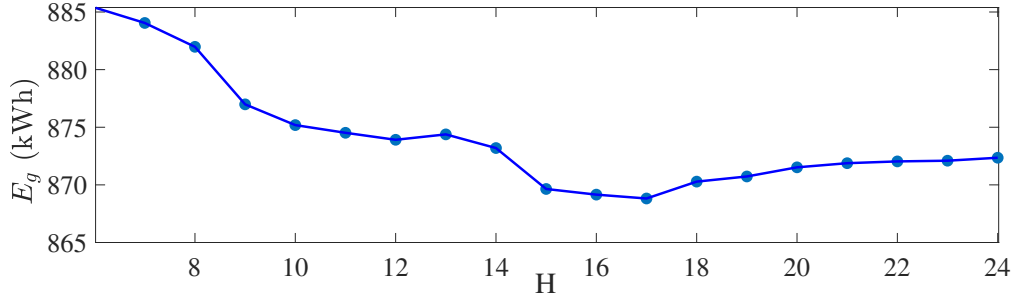


Figure 3.6: Scenario 2. Cumulative energy exchanged with the main grid under different prediction horizons.

Fig. 3.8. This distinction underscores the advantageous impact of SPEV integration in PL3, mitigating the risk of damage and optimizing the performance of the V2G system.

3.5.3 Scenario 3

The second scenario investigates how the prediction horizon length influences the feasibility and performance of the proposed MPC framework. Nineteen horizons, with $H \in [6, 24]$, are evaluated over a fixed simulation of $K = 168$ time steps with $\Delta t = 1$ hour. The parking infrastructure includes $N = 10$ CPs, of which five are dedicated to SPEVs. Energy prices follow the time-of-use scheme detailed in Table 3.2.

This analysis considers cases where vehicle departure times may fall outside the current prediction horizon, which can pose challenges for ensuring constraint satisfaction. Figure 3.5(a) shows the SoC trajectories for vehicles connected to CP #5 under two horizons of $H = 6$ and $H = 24$. Although constraints are satisfied in both cases—even when departure times lie outside the prediction window—the resulting control policies differ, leading to distinct SoC trajectories. As shown in Fig. 3.5(b), this also affects grid power usage, with the longer horizon ($H = 24$) yielding a 1.47% reduction in cumulative consumption over the full simulation period.

To better assess the impact of the prediction horizon, Fig. 3.6 depicts the cumulative power purchased from the grid over the simulation period for different horizon values $H \in [6, 24]$. As shown in Fig. 3.6, increasing the prediction horizon allows the system to make better decisions, resulting in a reduced cumulative E_g until a plateau is reached around $H = 16$.

3.5.4 Scenario 4

The third scenario applies the proposed framework to real-world data to assess its practical relevance. The simulation considers the parking spots at Lonsdale Street in Melbourne, Australia (Fig. 3.9). We assume all the parking spots are equipped with a CP. We use a 15-minute duration ($\Delta t = 0.25$ hour) time slot with a simulation length of 1 year. Vehicle arrival and departure patterns are derived from on-street parking sensors installed along Lonsdale Street, using datasets from 2015 and 2016 [39], [40]. Fig. 3.10(a) illustrates the number of vehicles recorded at both daily and 15-minute intervals over the course of the entire year.

Since radiation and price data for 2015–2016 were unavailable, the corresponding values from 2023–2024 were used for the same calendar period. Solar radiation data are sourced from the City of Ballarat, Victoria, Australia, using measurements collected in Ballarat at regular 15-minute intervals [41]. Figure 3.10(b) shows the processed radiation profile used for PV power generation forecasts. Electricity price data are obtained from the Australian Energy Market Operator (AEMO) [42], which provides 5-minute interval pricing. For consistency with the simulation resolution, the data are aggregated to 15-minute intervals by averaging. Outliers are removed using a Z-score approach [43], while

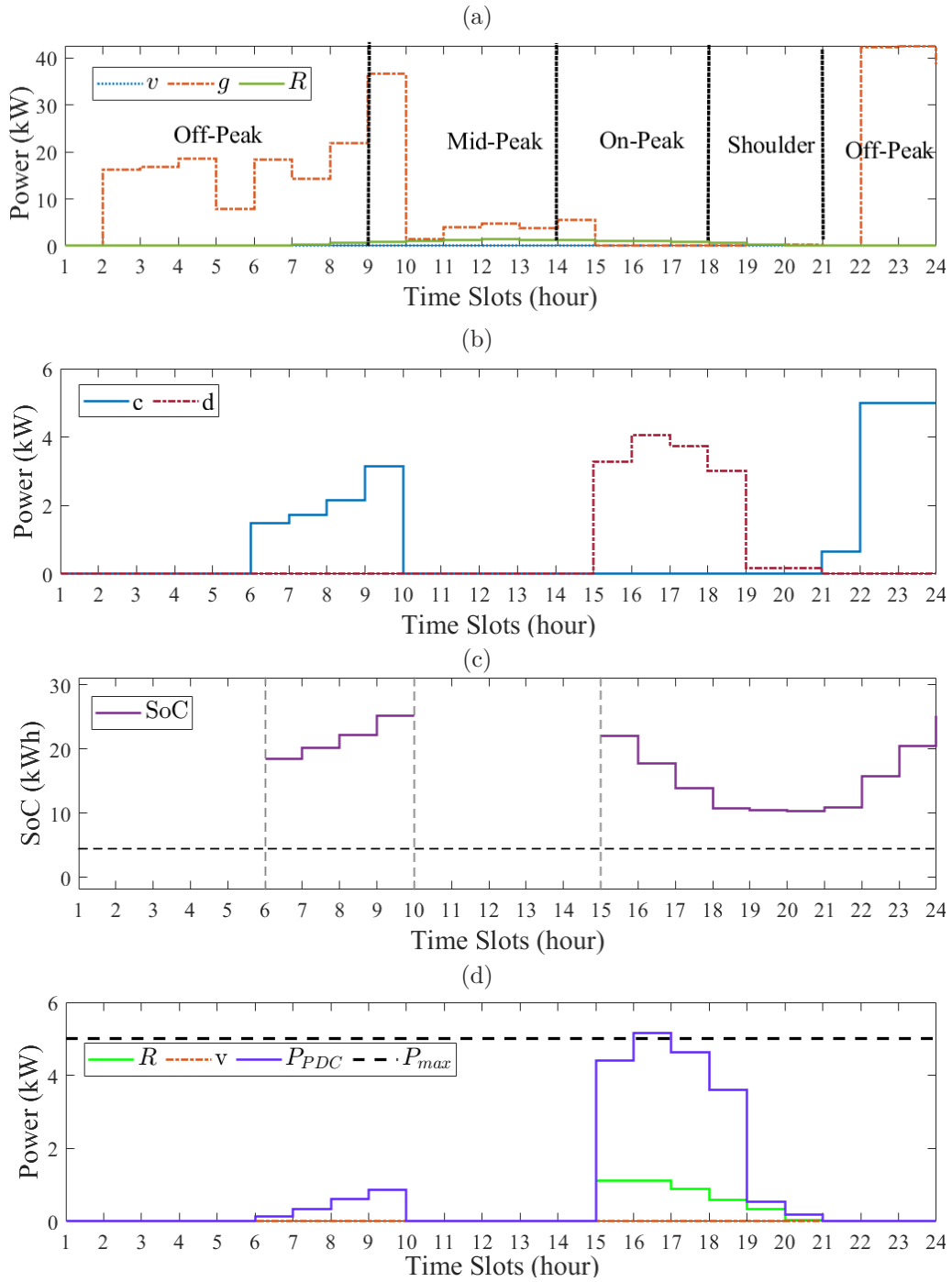


Figure 3.7: Simulation results of the unroofed V2G parking lot incompatible with SPEVs (PL 2) under scenario # 2: (a) Power profile obtained through the MPC implementation, (b) ESS charging and discharging behavior of vehicle connected to charging pile # 2, (c) ESS state of charge related to SPEV in charging pile # 2, (d) P_{PDC} , PV power profile and the related curtailed power of SPEV in charging pile # 2.

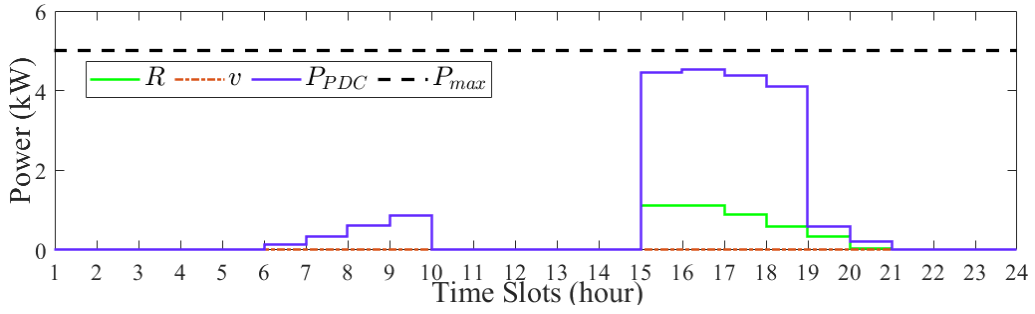


Figure 3.8: Simulation results of integrated V2G system for EVs and SPEVs (PL 3) under scenario # 2: P_{PDC} , PV power profile, and the related curtailed power of SPEV in charging pile # 2.

(a)

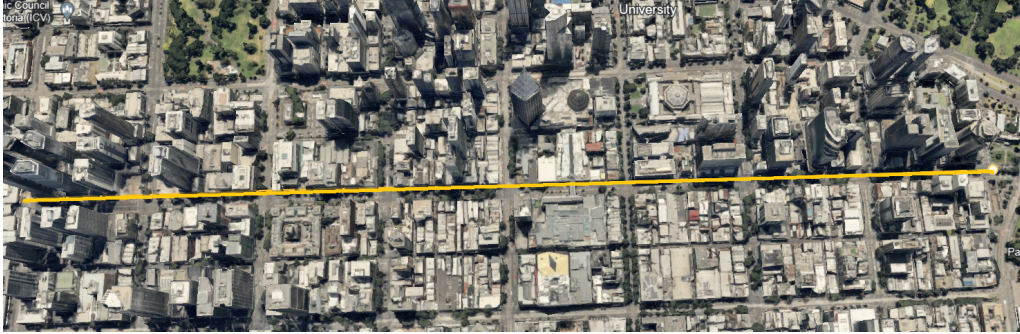


Figure 3.9: Overview of Lonsdale Street, Melbourne, Australia: aerial perspective from Google Earth, providing a broader context of the street within the cityscape.

all power price values are shifted such that the smallest value is set to zero in line with convex relaxation constraints [28]. The resulting price profile is depicted in Fig. 3.10(c).

We assess the impact of SPEV integration by varying their share from 0% to 100% across the 74 CPs. As shown in Fig.3.13, the total energy exchanged with the grid decreases consistently with higher SPEV penetration—from 145.7 MWh at 0% to 55.2 MWh at 100%, corresponding to a 62.1% reduction. Figure 3.11 illustrates this trend for the two extreme cases. When no SPEVs are present, as reported in Fig.3.11(a), the parking system fully depends on external energy. In contrast, full SPEV integration reported in Fig.3.11(b), results in the lowest grid power usage throughout the year. The corresponding charging and discharging profiles of CP #3 are shown in Fig.3.12. As expected, grid dependency is the highest when no SPEVs are present due to the absence of onboard solar generation. These findings highlight the benefits of incorporating SPEVs into the parking infrastructure. By leveraging onboard solar generation, the system reduces its grid dependency, improves energy self-sufficiency, and contributes to more sustainable and cost-effective operations.

To evaluate the performance of the proposed MPC-based control strategy, we consider a rule-based benchmark policy that operates without any forecast information. At each time step k , the EM measures the current electricity price $\lambda(k)$ and the total available solar generation $R_{tot}(k)$, which includes both central and rooftop PV from the parking facility and SPEVs. For each vehicle, the EM computes the maximum feasible charging rate, based on technical constraints and residual energy demand and the average charging rate required to reach the energy target by the departure time.

The control logic depends on a comparison between $\lambda(k)$ and a fixed price threshold λ_{th} , and between $R_{tot}(k)$ and the aggregate charging demand. Specifically: i) if the price is low or solar generation is abundant, all vehicles are charged at their maximum feasible rate, using grid energy only if renewables are insufficient; ii) if the price is high but solar generation suffices to meet the average demand, solar power is shared proportionally among the vehicles; iii) if both the price is high and solar is insufficient, each vehicle is

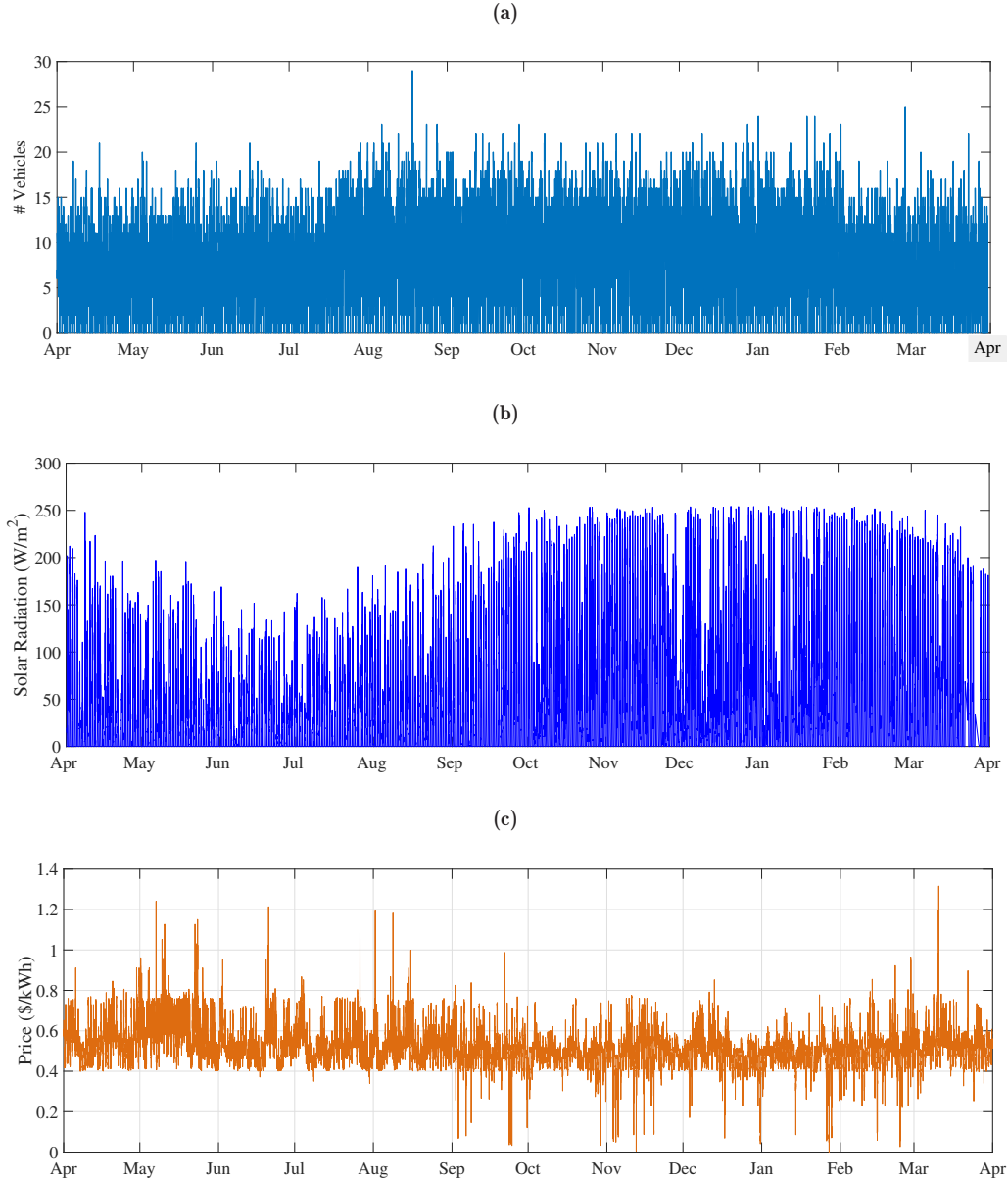


Figure 3.10: Scenario 3. (a) On-street parking occupancy; (b) Solar radiation measurements on a 15-minute interval scale; (c) Energy prices.

charged at its average required rate, with the grid compensating any residual shortfall.

We compare both strategies in a scenario where 50% of the vehicles are SPEVs. The rule-based policy results in an energy consumption of $E_g = 6.72 \times 10^4$ kWh, which is 6.12% higher than that of the MPC approach, indicating comparable energy efficiency. However, the MPC achieves a significantly lower operational cost: it yields a total cost of $\$3.8057 \times 10^4$, compared to $\$4.3887 \times 10^4$ for the rule-based policy at $\lambda_{th} = 0.5$ \$, corresponding to a 15.32% cost reduction.

Finally, we evaluated the impact of prediction errors on the cumulative energy exchange with the main grid over the simulation period, as shown in Fig.3.14. A constant bias of -5% , 0% , and $+5\%$ was applied to the forecasted data, along with two levels of additive white noise 5% and 10%. These error levels are consistent with typical forecasting uncertainties reported in the literature [44], [45]. The results show that the cumulative energy exchange remains relatively stable across all cases, confirming the robustness of the proposed framework under moderate levels of prediction uncertainty.

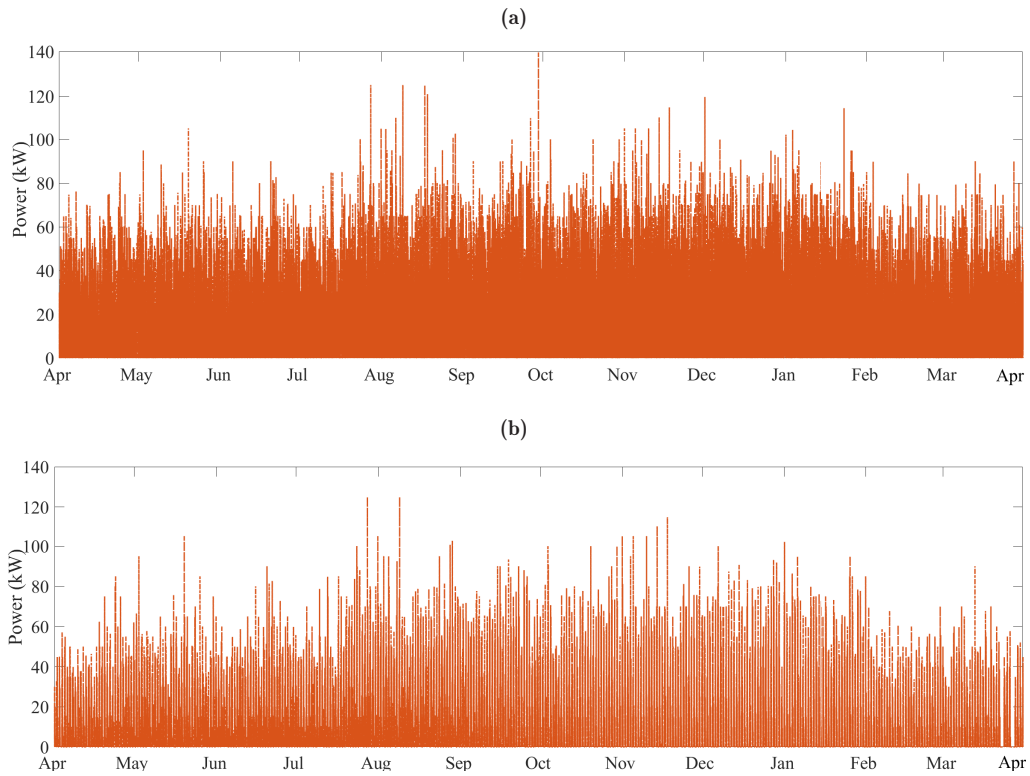


Figure 3.11: Scenario 3. Power exchanged with the main grid for (a) 0% SPEV and (b) 100% SPEV integration.

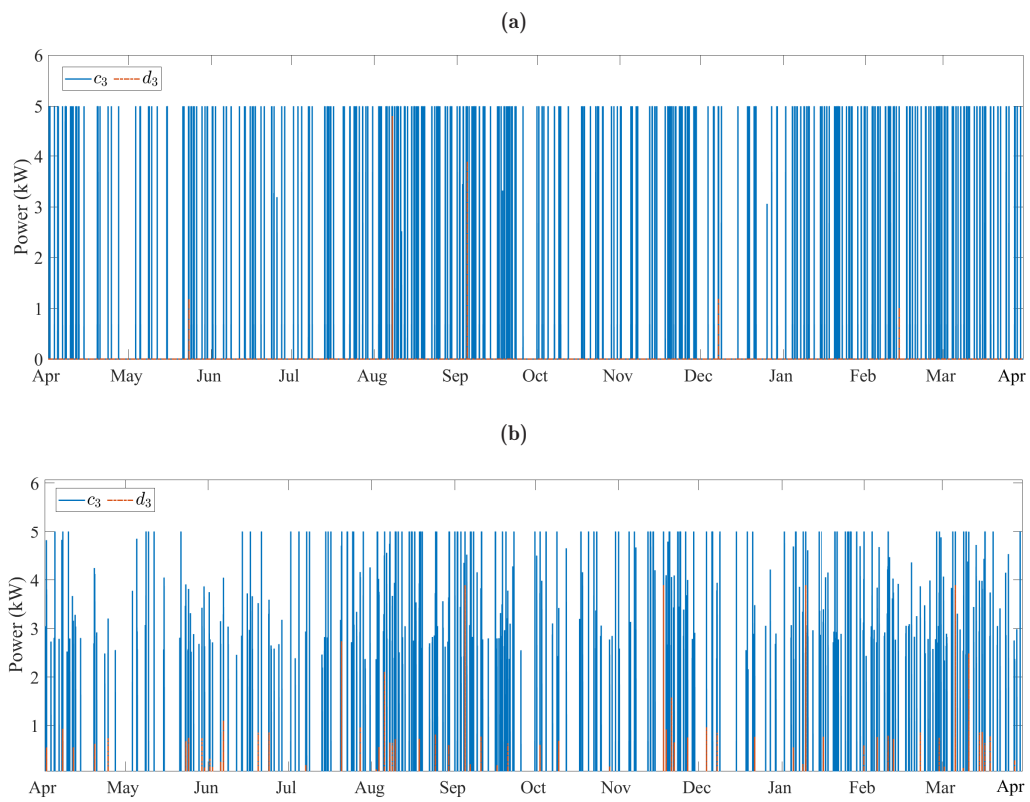


Figure 3.12: Scenario 3. Charging and discharging profiles for CP #3 with (a) 0% SPEV and (b) 100% SPEV integration.

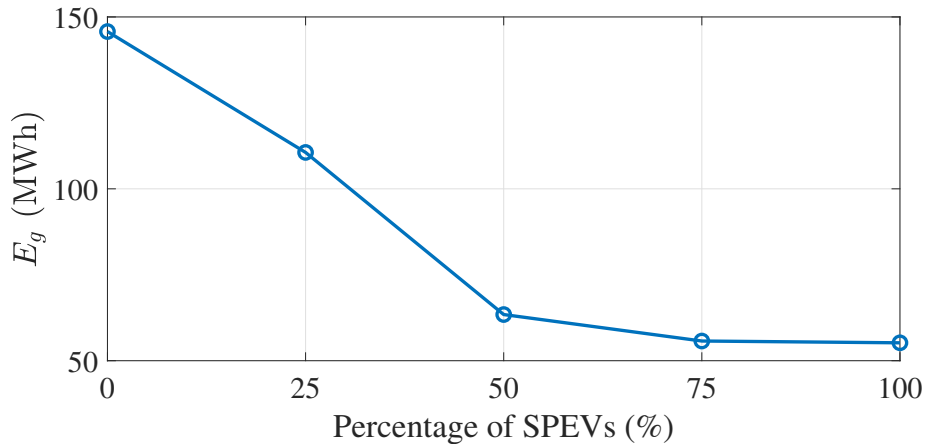


Figure 3.13: Scenario 3. Cumulative energy exchanged with the main grid as a function of the percentage of SPEVs.

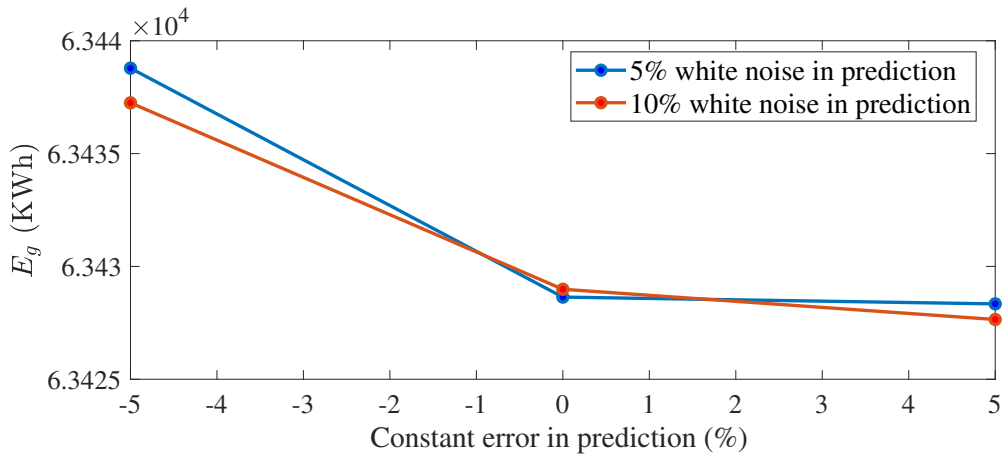


Figure 3.14: Scenario 3. Cumulative energy exchanged with the main grid under different prediction errors.

3.6 Conclusions

This chapter presented a model predictive control framework for smart charging infrastructures compatible with conventional and solar-powered electric vehicles.

The framework was validated through extensive simulations using real-world data, including electricity prices, solar irradiance profiles, and vehicle activity logs from a parking facility in Melbourne, Australia. Results show that the approach reduces grid energy usage by up to 27% and prevents simultaneous charging and discharging events.

Robustness was assessed via a sensitivity analysis accounting for forecast uncertainty in solar generation and vehicle availability. The framework remained effective under such variability, with only minor impacts on cost and constraint satisfaction, demonstrating its suitability for real-world deployment.

Future research directions include extending the proposed framework incorporating dynamic pricing and market mechanisms, and exploring decentralized or game-theoretic formulations for distributed energy management.

References

- [1] Valderrama, D. F., Ferro, G., Parodi, L., and Robba, M., “A bilevel optimization approach for Balancing Markets with electric vehicle aggregators and smart charging,” *IFAC Journal of Systems and Control*, p. 100 296, 2025.
- [2] Commault, B., Duigou, T., Maneval, V., Gaume, J., Chabuel, F., and Voroshazi, E., “Overview and perspectives for vehicle-integrated photovoltaics,” *Applied Sciences*, vol. 11, no. 24, p. 11 598, 2021.
- [3] Yamaguchi, M. et al., “Development of high-efficiency and low-cost solar cells for pv-powered vehicles application,” *Progress in Photovoltaics: Research and Applications*, vol. 29, no. 7, pp. 684–693, 2021.
- [4] Singla, P., Duhan, M., and Saroha, S., “A comprehensive review and analysis of solar forecasting techniques,” *Frontiers in Energy*, pp. 1–37, 2021.
- [5] Pochont, N. R. et al., “Recent trends in photovoltaic technologies for sustainable transportation in passenger vehicles—A review,” *Renewable and Sustainable Energy Reviews*, vol. 181, p. 113 317, 2023.
- [6] Tang, X., Sun, C., Bi, S., Wang, S., and Zhang, A. Y., “A holistic review on advanced bi-directional EV charging control algorithms,” *ACM SIGEnergy Energy Informatics Review*, vol. 1, no. 1, pp. 78–88, 2021.
- [7] Deng, Y., Gupta, A., and Shroff, N. B., “Fleet sizing and charger allocation in electric vehicle sharing systems,” *IFAC Journal of Systems and Control*, vol. 22, p. 100 210, 2022.
- [8] Manikandan, S., “Investigation on the stability of networked-control integrated energy systems for frequency regulations,” *IFAC Journal of Systems and Control*, vol. 25, p. 100 219, 2023.
- [9] Mohamed, A., Salehi, V., Ma, T., and Mohammed, O., “Real-time energy management algorithm for plug-in hybrid electric vehicle charging parks involving sustainable energy,” *IEEE Transactions on Sustainable Energy*, vol. 5, no. 2, pp. 577–586, 2013.
- [10] Wang, M., Liang, H., Zhang, R., Deng, R., and Shen, X., “Mobility-aware coordinated charging for electric vehicles in vanet-enhanced smart grid,” *IEEE Journal on Selected Areas in Communications*, vol. 32, no. 7, pp. 1344–1360, 2014.
- [11] Liu, Y., Deng, R., and Liang, H., “Game-theoretic control of phev charging with power flow analysis,” *AIMS Energy*, vol. 4, no. 2, pp. 379–396, 2016.
- [12] Li, X. et al., “Modeling and control strategy of battery energy storage system for primary frequency regulation,” in *2014 International Conference on Power System Technology*, IEEE, 2014, pp. 543–549.
- [13] Scarabaggio, P., Carli, R., Parisio, A., and Dotoli, M., “On controlling battery degradation in vehicle-to-grid energy markets,” in *2022 IEEE 18th International Conference on Automation Science and Engineering (CASE)*, IEEE, 2022, pp. 1206–1211.
- [14] Zheng, Y., Song, Y., Hill, D. J., and Meng, K., “Online distributed mpc-based optimal scheduling for ev charging stations in distribution systems,” *IEEE transactions on industrial informatics*, vol. 15, no. 2, pp. 638–649, 2018.
- [15] Shi, Y., Tuan, H. D., Savkin, A. V., and Duong, T. Q., “Model predictive control for smart grids with multiple electric-vehicle charging stations,” *IEEE Transactions on Smart Grid*, vol. 9, no. 4, pp. 2642–2653, 2018. DOI: [10.1109/TSG.2017.2725424](https://doi.org/10.1109/TSG.2017.2725424).
- [16] Dai, X. et al., “Data-driven ev charging load forecasting and smart charging,” *Transportation Research Procedia*, vol. 72, pp. 2832–2839, 2023.

-
- [17] Yang, L., Geng, X., Guan, X., and Tong, L., “Ev charging scheduling under demand charge: A block model predictive control approach,” *IEEE Transactions on Automation Science and Engineering*, vol. 21, no. 2, pp. 2125–2138, 2023.
- [18] Saatloo, A. M., Mehrabi, A., Marzband, M., and Aslam, N., “Hierarchical user-driven trajectory planning and charging scheduling of autonomous electric vehicles,” *IEEE Transactions on Transportation Electrification*, vol. 9, no. 1, pp. 1736–1749, 2022.
- [19] Jiao, F., Zou, Y., Zhang, X., and Zhang, B., “A three-stage multitimescale framework for online dispatch in a microgrid with evs and renewable energy,” *IEEE Transactions on Transportation Electrification*, vol. 8, no. 1, pp. 442–454, 2021.
- [20] Zhou, F., Li, Y., Wang, W., and Pan, C., “Integrated energy management of a smart community with electric vehicle charging using scenario-based stochastic mpc,” *Energy and Buildings*, vol. 259, p. 111 884, 2022. DOI: [10.1016/j.enbuild.2022.111884](https://doi.org/10.1016/j.enbuild.2022.111884).
- [21] Baek, J. and Choi, Y., “An experimental study on performance evaluation of shading matrix to select optimal parking space for solar-powered electric vehicles,” *Sustainability*, vol. 14, no. 22, p. 14 922, 2022.
- [22] Ahmad, A. and Khan, J. Y., “Real-time load scheduling and storage management for solar powered network connected evs,” *IEEE Transactions on Sustainable Energy*, vol. 11, no. 3, pp. 1220–1235, 2019.
- [23] Fakour, H. et al., “Evaluation of solar photovoltaic carport canopy with electric vehicle charging potential,” *Scientific Reports*, vol. 13, no. 1, p. 2136, 2023.
- [24] Mignoni, N., Carli, R., and Dotoli, M., “Distributed noncooperative mpc for energy scheduling of charging and trading electric vehicles in energy communities,” *IEEE Transactions on Control Systems Technology*, 2023.
- [25] Mignoni, N., Carli, R., and Dotoli, M., “A Noncooperative Stochastic Rolling Horizon Control Framework for V1G and V2B Scheduling in Energy Communities,” in *2023 European Control Conference (ECC)*, IEEE, 2023, pp. 1–6.
- [26] Hosseini, S. M., Carli, R., and Dotoli, M., “Robust optimal energy management of a residential microgrid under uncertainties on demand and renewable power generation,” *IEEE Transactions on Automation Science and Engineering*, vol. 18, no. 2, pp. 618–637, 2021.
- [27] Noghani, S. A., Scarabaggio, P., Carli, R., and Dotoli, M., “Solar-powered electric vehicles into v2g-capable smart parking infrastructure for enhanced energy efficiency,” in *2024 10th International Conference on Control, Decision and Information Technologies (CoDIT)*, IEEE, 2024, pp. 575–580.
- [28] Garifi, K., Baker, K., Christensen, D., and Touri, B., “Convex relaxation of grid-connected energy storage system models with complementarity constraints in dc opf,” *IEEE Transactions on Smart Grid*, vol. 11, no. 5, pp. 4070–4079, 2020.
- [29] Wu, Y., Zhang, J., Ravey, A., Chrenko, D., and Miraoui, A., “Real-time energy management of photovoltaic-assisted electric vehicle charging station by markov decision process,” *Journal of Power Sources*, vol. 472, p. 228 356, 2020. DOI: [10.1016/j.jpowsour.2020.228356](https://doi.org/10.1016/j.jpowsour.2020.228356).
- [30] Diaz-Londono, C., Orfanoudakis, S., and Vergara, P. P., “A simulation tool for v2g enabled demand response based on model predictive control,” *arXiv Preprint*, vol. arXiv:2405.11963, 2024, Link to article: <https://arxiv.org/abs/2405.11963>.
- [31] Nawaz, A., Wu, J., Ye, J., Dong, Y., and Long, C., “Distributed mpc-based energy scheduling for islanded multi-microgrid considering battery degradation and cyclic life deterioration,” *Applied Energy*, vol. 333, p. 120 312, 2023. DOI: [10.1016/j.apenergy.2023.120312](https://doi.org/10.1016/j.apenergy.2023.120312).

- [32] Wang, B., Dehghanian, P., and Zhao, D., “Chance-constrained energy management system for power grids with high proliferation of renewables and electric vehicles,” *IEEE Transactions on Smart Grid*, vol. 10, no. 3, pp. 2656–2668, 2019. DOI: [10.1109/TSG.2018.2889561](https://doi.org/10.1109/TSG.2018.2889561).
- [33] Wang, R., Li, Y., Wang, P., and Niyato, D., “Design of a v2g aggregator to optimize phev charging and frequency regulation control,” in *2013 IEEE International Conference on Smart Grid Communications (SmartGridComm)*, 2013, pp. 7–12. DOI: [10.1109/SmartGridComm.2013.6687932](https://doi.org/10.1109/SmartGridComm.2013.6687932).
- [34] Müller, M. A. and Worthmann, K., “Quadratic costs do not always work in mpc,” *Automatica*, vol. 82, pp. 269–277, 2017.
- [35] Li, P., Kang, Y., Zhao, Y.-B., and Wang, T., “Networked dual-mode adaptive horizon mpc for constrained nonlinear systems,” *IEEE Transactions on Systems, Man, and Cybernetics: Systems*, vol. 51, no. 12, pp. 7435–7449, 2020.
- [36] Garifi, K., Baker, K., Christensen, D., and Touri, B., “Control of energy storage in home energy management systems: Non-simultaneous charging and discharging guarantees,” *arXiv preprint arXiv:1805.00100*, 2018.
- [37] Jin, X., Baker, K., Christensen, D., and Isley, S., “Foresee: A user-centric home energy management system for energy efficiency and demand response,” *Applied Energy*, vol. 205, pp. 1583–1595, 2017.
- [38] Diamond, H. J. et al., “Us climate reference network after one decade of operations: Status and assessment,” *Bulletin of the American Meteorological Society*, vol. 94, no. 4, pp. 485–498, 2013.
- [39] Melbourne, C. of, *On-street car parking sensor data 2015*, <https://discover.data.vic.gov.au/dataset/on-street-car-parking-sensor-data-2015>, Data includes parking event details such as vehicle arrivals, departures, and adherence to restrictions, collected via in-ground sensors in Melbourne CBD., 2017.
- [40] Melbourne, C. of, *On-street car parking sensor data 2016*, <https://discover.data.vic.gov.au/dataset/on-street-car-parking-sensor-data-2016/resource/2caa3442-5423-40f9-9076-477f66c7d282>, Detailed parking event data including arrivals, departures, and adherence to restrictions recorded via in-ground sensors in Melbourne CBD for the year 2016., 2024.
- [41] Data.Vic, *Solar radiation observations dataset*, Accessed: December 29, 2024, 2024. [Online]. Available: <https://discover.data.vic.gov.au/dataset/solar-radiation-observations>.
- [42] (AEMO), A. E. M. O., *Aggregated price and demand data - national electricity market (nem)*, Accessed: December 29, 2024, 2024. [Online]. Available: <https://www.aemo.com.au/energy-systems/electricity/national-electricity-market-nem/data-nem/aggregated-data>.
- [43] Yaro, A. S., Maly, F., Prazak, P., and Maly, K., “Outlier detection performance of a modified z-score method in time-series rss observation with hybrid scale estimators,” *IEEE Access*, 2024.
- [44] Fathima, T., Nedumpozhimana, V., Lee, Y. H., Winkler, S., and Dev, S., “Predicting solar irradiance in Singapore,” in *2019 Photonics & Electromagnetics Research Symposium-Fall (PIERS-Fall)*, IEEE, 2019, pp. 3164–3167.
- [45] Bai, M., Zhou, Z., Chen, Y., Liu, J., and Yu, D., “Accurate four-hour-ahead probabilistic forecast of photovoltaic power generation based on multiple meteorological variables-aided intelligent optimization of numeric weather prediction data,” *Earth Science Informatics*, vol. 16, no. 3, pp. 2741–2766, 2023.

Part 2

Chapter 4

Noncooperative Control of Energy Communities through Learning-based Response Dynamics

Abstract

With the growing availability of data, learning-based distributed energy management is emerging as a viable and efficient alternative to traditional model-based schemes. In this context, we propose a novel game-theoretic learning-based method for the distributed control of energy communities. In particular, we consider a community that includes several prosumers equipped with a renewable energy source and an energy storage system. The scheduling of energy activities of all prosumers is formulated as a noncooperative game. Nevertheless, unlike the state-of-the-art, where an optimization problem is typically defined to model the behavior of each prosumer, we approximate each prosumer response strategy using a neural network. We propose a distributed algorithm based on the well-known Banach-Picard iteration to efficiently seek for an equilibrium of the game. Lastly, the convergence and effectiveness of the proposed approach are validated through numerical simulations under different realistic scenarios.

Contents

4.1	Introduction	43
4.2	Related Works	44
4.3	The Energy Community Model	45
4.4	The Learning-Based Game Model	47
4.5	Numerical Experiments	49
4.6	Conclusions	51

4.1 Introduction

Among the various innovative solutions recently introduced to address climate change concerns [1], [2], energy communities (ECs) are regarded as one of the enablers for achieving a sustainable energy transition[3]. ECs are indeed collectives of private, public, or mixed users who actively collaborate to establish smart energy systems, with the main goal of facilitating the optimal use of renewable energy sources (RESs) and extensive use of energy storage systems (ESSs) [4].

The effective management of energy flows within the EC is essential for achieving sustainability and economic feasibility. This task is commonly carried out through centralized methods, which can be straightforwardly implemented due to their simplicity. Nevertheless, these approaches are limited by (i) scalability and single-point failure issues [5] and (ii) the unwillingness of ECs users to yield their autonomy to a centralized entity. In fact, for most users, the main reason to join an EC is the possibility of increasing selfishness and energy independence [6].

In light of the above issues, game theory is the ideal candidate framework for controlling ECs in a distributed setting, as it can be used to model interacting decision-makers, the so-called players [7], [8] Specifically, noncooperative game-theoretic approaches are

particularly suitable for controlling selfish players with individual dynamics and constraints aimed only at maximizing their welfare, possibly in competition with each other [9]. In this context, one of the most important concepts is the *Nash equilibrium* (NE) [10], which represents an approach to define the solution of a noncooperative game in many applications.

In traditional game settings, players' behaviors are characterized by cost functions, numerically quantifying the outcome of their decisions [11]. Therefore, the applicability of game-theoretical models is limited by the possibility of finding suitable functions that can realistically model players' preferences. Indeed, the standing assumption of most game theoretical models for ECs requires cost functions representing users' expenses. Nevertheless, this requirement goes against the fact that EC users are humans, and thus, they have complex behaviors transcending merely economic considerations.

In recent years, with the increasing availability of data, there has been a growing interest in exploring machine learning (ML) approaches to adapt model and control techniques to dynamic energy scenarios [12]. These learning techniques offer promising solutions to address various challenges in classical mathematical problems. Among these approaches, Neural Networks (NNs) have demonstrated their effectiveness in numerous prediction tasks, especially in predicting human behavior decisions [13]. Therefore, NNs are ideal candidates for approximating the behavior of ECs' users.

In this work, we aim to merge the effectiveness of game theoretic frameworks to model ECs in a noncooperative and realistic fashion with the capacity of NNs to approximate the behaviors of users participating in a community. Therefore, unlike other approaches that typically define an optimization problem to represent each user's behavior, we employ an NN to learn and represent the optimal energy allocation strategy for each prosumer in the EC. Specifically, we present a novel game-theoretic framework for ECs in which an NN approximates the user's response dynamics in response to other users' actions. To seek this equilibrium, we propose a novel distributed algorithm based on the well-known Banach-Picard iteration. Lastly, the convergence and effectiveness of the proposed approach are validated through numerical simulations under different realistic scenarios.

The remainder of the chapter is organized as follows. Section 4.2 provides a review of the related literature. Section 4.3 describes the model of the EC. Section 4.4 discusses the learning-based game theoretical control method. Section 4.5 illustrates the results of numerical simulations. Finally, conclusions and possible future works are drawn in Section 4.6.

4.1.1 Basic Notation

\mathbb{R}^n , $\mathbb{R}_{>0}^n$, and $\mathbb{R}_{\geq 0}^n$ represent the sets of real, positive real, and non-negative real n -dimensional vectors, respectively. A^\top denotes the transpose of matrix A , while $\|A\|$ denotes the square norm of A . $\mathbf{0}_n$ and $\mathbf{1}_n$ indicate the column vectors with n entries all equal to 0 and to 1, i.e., $\mathbf{0}_n := (0, \dots, 0)^\top \in \mathbb{R}^n$ and $\mathbf{1}_n := (1, \dots, 1)^\top \in \mathbb{R}^n$, respectively. The n -dimensional identity matrix is defined as \mathbf{I}_n . Moreover, $\mathbf{x} := \text{col}(\mathbf{x}_1, \dots, \mathbf{x}_n)$ is equal to $\mathbf{x} := (\mathbf{x}_1^\top, \dots, \mathbf{x}_n^\top)^\top$. We introduce the mapping $\Pi_X : \mathbb{R}^n \rightarrow X$ as the projection onto the closed nonempty set $X \subseteq \mathbb{R}^n$, defined as $\Pi_X(y) = \arg \min_{x \in X} \|x - y\|$.

4.2 Related Works

The integration of game theory, ML, and control theory has emerged as a promising approach for optimizing the operation of energy systems. Indeed, in recent years, several research efforts have been directed toward developing advanced control strategies that leverage these interdisciplinary techniques to enhance energy efficiency and reliability across various sectors.

One notable trend in the literature is the use of optimization techniques for building energy control [14]. Several studies work on integrating ML methods with control strategies

to enhance performance and adaptability [15] and [13]. For example, [16] and [17] explore the use of ML techniques to optimize energy storage control in home energy management systems, ensuring efficient utilization while guaranteeing non-simultaneous charging and discharging. Moreover, [18] compares the competitive performance of physics-informed regression methods in residential buildings to conventional ML approaches. Validation and experimental studies are crucial in assessing the effectiveness and feasibility of the proposed control methodologies. Works such as [19] provide valuable insights by presenting experimental results demonstrating the efficacy of ML-based control strategies in real-world building environments. These studies contribute to bridging the gap between theoretical developments and practical implementation, facilitating the adoption of innovative control techniques in building automation systems. In parallel, works [20] and [21] contribute significantly to this field by introducing novel control strategies for ECs. These works employ game-theoretic approaches and distributed control frameworks to optimize the operation of energy systems.

Despite significant progress, several challenges remain to be addressed in the control of ECs. Leveraging the current growth of learning-based methods, particularly in NNs, presents a promising avenue for enhancing the efficiency of game-theoretic-based control methods. By employing learning techniques to develop the best response mapping tools, systems can effectively predict the optimal responses of distributed energy systems [21]. This approach enables energy management systems to dynamically adjust their strategies based on real-time data and evolving system conditions, thereby improving the overall system efficiency and stability. Integrating learning-based tools into game-theoretic control methods facilitates prompt and adaptive decision-making with low computation costs. For instance, the implementation of NNs as a best response mapping tool holds significant potential for advancing the field of energy management and optimizing the performance of complex energy systems. Additionally, exploring novel approaches for distributed optimization, multi-agent coordination, and peer-to-peer energy trading presents promising avenues for future research.

4.3 The Energy Community Model

This work considers an EC model, whose scheme is shown in Fig. 4.1. The EC comprises an *EC Manager* and a set of users, which in the rest of this work will be referred to as (energy) *prosumers*¹.

4.3.1 The Energy Community Manager

The EC Manager coordinates the energy flows within the community, facilitating transactions of energy among prosumers. Specifically, the manager broadcasts an energy price profile for the horizon $\mathcal{H} := \{1, \dots, h, \dots, H\}$ of H time steps, where $h \in \mathcal{H}$ denotes the generic time slot. Consequently, prosumers can buy or sell energy to the manager based on the provided energy price profile.

For the sake of simplicity, we will assume that the EC Manager can offset any surplus or deficit of energy within the community, resulting from the energy exchange between prosumers, by sourcing energy externally, such as from the utility grid. Note that we will not model the relation between the EC manager and the utility grid, as this falls outside the scope of our study.

4.3.2 The Prosumer Model

Let us consider a set \mathcal{N} of N prosumers, indexed by $n \in \mathcal{N} := \{1, \dots, N\} \subseteq \mathbb{N}$, participating in the EC. Besides their energy consumption, each prosumer $n \in \mathcal{N}$ might have one or more RESs and/or an ESS. The energy production and consumption for prosumer $n \in \mathcal{N}$

¹The term is a portmanteau of the words producer and consumer, indicating a blurred distinction between the production and consumption activities of users.

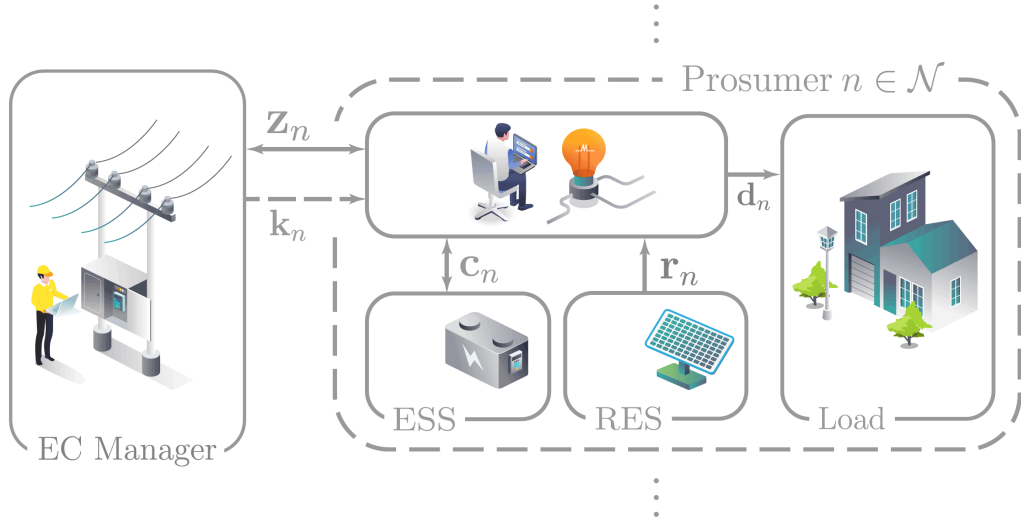


Figure 4.1: Scheme of the proposed energy community with a specific focus on a single prosumer $n \in \mathcal{N}$.

in the generic time step $h \in \mathcal{H}$ are defined as $r_n(h)$ and $d_n(h)$, respectively. Thus, the corresponding profiles over the horizon \mathcal{H} are defined as $\mathbf{r}_n := (r_n(h))_{h \in \mathcal{H}}^\top \in \mathbb{R}_{\geq 0}^H$ and $\mathbf{d}_n := (d_n(h))_{h \in \mathcal{H}}^\top \in \mathbb{R}_{\geq 0}^H$.

The ESS dynamics for each prosumer $n \in \mathcal{N}$ is modeled as a first-order discrete-time system:

$$SoC_n(h) = SoC_n(h-1) + \eta_n^\top c_n(h), \forall h \in \mathcal{H}, \forall n \in \mathcal{N}, \quad (4.1)$$

where the state parameter $SoC_n(h)$ denotes the state of charge, $c_n(h) := (c_n^+(h), c_n^-(h))^\top$ collects the charging $c_n^+(h)$ and discharging $c_n^-(h)$, while $\eta_n := (\eta_n^+, -\eta_n^-)^\top$ collects the corresponding efficiencies. Storage efficiencies are influenced by various factors, such as temperature and operating conditions; however, for the sake of simplicity, let us consider them as constant [22]. Let us also define vectors $\mathbf{c}_n := \text{col}(\mathbf{c}_n^+, \mathbf{c}_n^-) \in \mathbb{R}_{\geq 0}^{2H}$, $\mathbf{c}_n^+ := (c_n^+(h))_{h \in \mathcal{H}} \in \mathbb{R}_{\geq 0}^H$, $\mathbf{c}_n^- := (c_n^-(h))_{h \in \mathcal{H}} \in \mathbb{R}_{\geq 0}^H$ and $\mathbf{SoC}_n := (SoC_n(h))_{h \in \mathcal{H}} \in \mathbb{R}_{\geq 0}^H$.

For each prosumer $n \in \mathcal{N}$ the maximum storage capacity SoC_n^{\max} should be considered:

$$\mathbf{SoC}_{n \in \mathcal{N}} \leq \mathbf{1}_H SoC_n^{\max}, \quad \forall n \in \mathcal{N}, \quad (4.2)$$

while to take into account the limitations of inverters, we introduce the following technical constraints:

$$\mathbf{c}_n \leq \mathbf{1}_{2H} c_n^{\max}, \quad \forall n \in \mathcal{N}, \quad (4.3)$$

where c_n^{\max} is the maximum rate of charging/discharging.

Prosumers can buy/sell energy from/to the EC Manager. Therefore, let us define $z_n^+(h)$ and $z_n^-(h)$ as the energy's purchase/sale from/to the EC Manager at time $h \in \mathcal{H}$, respectively. Further, we define vectors $\mathbf{z}_n := \text{col}(\mathbf{z}_n^+, \mathbf{z}_n^-) \in \mathbb{R}_{\geq 0}^{2H}$, $\mathbf{z}_n^+ := (z_n^+(h))_{h \in \mathcal{H}} \in \mathbb{R}_{\geq 0}^H$, and $\mathbf{z}_n^- := (z_n^-(h))_{h \in \mathcal{H}} \in \mathbb{R}_{\geq 0}^H$.

We impose that for each prosumer $n \in \mathcal{N}$, the energy flow balance must be respected at the individual level:

$$\mathbf{d}_n - \mathbf{r}_n + \Lambda \mathbf{c}_n = \Lambda \mathbf{z}_n, \quad \forall n \in \mathcal{N}, \quad (4.4)$$

where $\Lambda := (\mathbf{I}_H, -\mathbf{I}_H)$.

Let us collect for each prosumer its decision variables as:

$$\mathbf{x}_n := \text{col}(\mathbf{c}_n, \mathbf{z}_n), \quad \forall n \in \mathcal{N}, \quad (4.5)$$

and therefore, define a set of local constraints as:

$$\Omega_n := \{ \mathbf{x}_n \in \mathbb{R}_{\geq 0}^{4H} \mid (1) - (4) \text{ hold} \}, \quad \forall n \in \mathcal{N}. \quad (4.6)$$

4.3.3 Energy Cost

ECs are usually created to allow the sharing of resources between prosumers and to increase the integration of renewable sources. This is often achieved through dynamic pricing schemes aimed at minimizing the imbalance between the prosumers' aggregate consumption and their RES production. Thus, let us assume that prosumers in the EC are subjected to a dynamic pricing scheme, such as the overall purchase of energy reduced by any profit (due to the sale of energy), which can be formally defined as:

$$\mathbf{k}_n^\top \Lambda \mathbf{z}_n, \quad \forall n \in \mathcal{N}, \quad (4.7)$$

where $\mathbf{k}_n = (k_n(h))_{h \in \mathcal{H}}$ is a vector collecting the time-varying energy price broadcasted by the EC manager to the prosumer $n \in \mathcal{N}$. We assume that this price is equal for both the purchase and sale of energy. Note that this formulation allows for a generalized and realistic scheme for ECs, as different participants in the energy community may sign different contracts and thus be subjected to different pricing schemes.

Lastly, monetary loss due to degradation of ESS can also be taken into account with a simple relation as:

$$\gamma_n \mathbf{1}_{2H}^\top \mathbf{c}_n, \quad \forall n \in \mathcal{N}, \quad (4.8)$$

where γ_n represents ESS's degradation coefficients.

4.4 The Learning-Based Game Model

Requiring the minimization of the imbalance between the prosumers' aggregate consumption and production imposes the dynamic pricing scheme in (4.7) to be dependent on prosumers' strategies. A natural framework to capture such a competitive scenario relies on game theory.

Let us define the vector \mathbf{x} collecting all decision variables of prosumers in the EC as follows:

$$\mathbf{x} := (\mathbf{x}_1, \dots, \mathbf{x}_N) \in \mathbb{R}_{\geq 0}^{4HN}, \quad (4.9)$$

and the vector \mathbf{x}_{-n} collecting all prosumers' decision variables except that of prosumers n as:

$$\mathbf{x}_{-n} := (\mathbf{x}_1, \dots, \mathbf{x}_{n-1}, \mathbf{x}_{n+1}, \dots, \mathbf{x}_N) \in \mathbb{R}_{\geq 0}^{4H(N-1)}. \quad (4.10)$$

Thus, let us define the energy cost vector as:

$$\mathbf{k}_n(\mathbf{x}_{-n}) := q_n \mathbf{W}_{-n}^\top \mathbf{x}_{-n} \quad (4.11)$$

where matrix \mathbf{W}_{-n} is defined as:

$$\mathbf{W} := ((\mathbf{0}_{H \times 2H}, w_j \Lambda)^\top)_{j \in \mathcal{N} \setminus n} \in \mathbb{R}^{4H(N-1) \times H} \quad (4.12)$$

and where values w_n indicate the influence of prosumer $n \in \mathcal{N}$ on the energy cost of other prosumers while q_n is the energy cost coefficients, different for each prosumer $n \in \mathcal{N}$. In such formulation, each prosumer has a limited view of the other prosumers' strategies via an aggregative function $\mathbf{k}_n(\cdot)$. Note that this formulation aligns our work with the well-known class of aggregative games [23]

In this chapter, for the sake of brevity, we define the two following scenarios:

- **Pricing model 1:** $w_n \neq w_m, q_n = q_m, \forall n, m \in \mathcal{N}$
- **Pricing model 2:** $w_n = w_m, q_n \neq q_m, \forall n, m \in \mathcal{N}$.

and therefore, we can define the overall cost for each prosumer as follows:

$$J_n(\mathbf{x}_n, \mathbf{x}_{-n}) = \mathbf{k}_n(\mathbf{x}_{-n})^\top \Lambda \mathbf{z}_n + \gamma_n \mathbf{1}_{2H}^\top \mathbf{c}_n, \quad \forall n \in \mathcal{N}. \quad (4.13)$$

In the game, prosumer $n \in \mathcal{N}$ aims at minimizing its cost function (equivalently, maximizing its payoff) by selecting a strategy $\mathbf{x}_n \in \Omega_n$, taking into account the strategies chosen by the other prosumers (\mathbf{x}_{-n}), as follows:

$$\forall n \in \mathcal{N} : \begin{cases} \min_{\mathbf{x}_n} & J_n(\mathbf{x}_n, \mathbf{x}_{-n}) \\ \text{s.t.} & \mathbf{x}_n \in \Omega_n. \end{cases} \quad (4.14)$$

The above problem N-interdependent problems are the so-called NE problem (NEP), whose solution is a NE, formally defined as follows.

Definition 4.4.1 (Nash equilibrium)

A NE is a collective strategy such that:

$$\forall n \in \mathcal{N} : J_n(\mathbf{x}_n^*, \mathbf{x}_{-n}^*) \leq \inf \{ J_n(\mathbf{x}_n, \mathbf{x}_{-n}^*) \mid \mathbf{x}_n \in \Omega_n \}.$$

□

Informally speaking, a NE is a collective strategy profile that secures that no individual prosumer can achieve an advantage by deviating independently from their respective \mathbf{x}_n^* , assuming all other prosumer adhere to it.

Various approaches exist for computing a NE for (4.4.1), with the best response iteration being one of the most used [8]. However, computing the exact best responses is intractable for most games yet it becomes feasible when cost functions are differentiable in their argument and admit continuous and smooth derivatives. When cost functions are convex and local sets convex and compact a NE for (4.4.1) not only exists but also proves to be unique and can be computed through the best response iteration.

Nevertheless, the significance of this equilibrium concept diminishes when prosumers deviate from their actions based on the minimization of cost function (4.13), which ideally represents the most rational behavior of prosumers, i.e., the behavior that is based merely on economic considerations. Indeed, such an assumption does not encompass scenarios in which prosumers, who are ultimately humans, may have extremely complex –and irrational– behavior.

In light of this, despite efforts to realistically approximate prosumers' preferences through functions, in several scenarios, it is more convenient to measure prosumers' behavior by evaluating their responses to other prosumers' decisions. Thus, an alternative to defining functions representing prosumers' behavior is to utilize approaches capable of collecting past actions of prosumers with respect to others' strategies and predicting future responses to forthcoming actions. In this context, employing learning-based approaches proves advantageous because they can leverage extensive datasets and discern complex patterns and relationships within the data [12], [13].

Therefore, in our work, we operate under the assumption of lacking prior knowledge of the cost function in (4.13). Instead, we employ NNs to approximate the responses of prosumers based on historical observations of their actions.

Specifically, let us consider that for a generic prosumer $n \in \mathcal{N}$ a set of previous data regarding its behavior, denoted as \mathcal{S}_n , is available. For each sample $s \in \mathcal{S}_n$, we observe the strategy selected by player $n \in \mathcal{N}$ defined as $\mathbf{x}_n^s \in \mathbb{R}_{\geq 0}^H$, given the environment defined by the energy cost $\mathbf{k}_n^s \in \mathbb{R}_{\geq 0}^H$, RES production $\mathbf{r}_n^s \in \mathbb{R}_{\geq 0}^H$ and energy demand $\mathbf{d}_n^s \in \mathbb{R}_{\geq 0}^H$. Note that the energy cost is a function of other prosumers' decisions $\mathbf{x}_{-n}^s \in \mathbb{R}_{\geq 0}^{(N-1)H}$.

By leveraging this dataset, we can train a NN to approximate prosumers' behavior as:

$$\forall n \in \mathcal{N} : \quad \tilde{\mathbf{x}}_n = \Phi_n(\mathbf{k}_n, \mathbf{r}_n, \mathbf{d}_n) \quad (4.15)$$

where $\tilde{\mathbf{x}}_n$ is the response of prosumer $n \in \mathcal{N}$ yielded by a NN. Note that, as the strategy returned by (4.15) may yield infeasible as is provided by a NN, i.e., $\tilde{\mathbf{x}}_n \notin \Omega_n$. Thus, let us project into the feasible set Ω_n the NN output as:

$$\forall n \in \mathcal{N} : \quad \mathbf{x}_n = \text{proj}_{\Omega_n} \Phi_n(\mathbf{k}_n, \mathbf{r}_n, \mathbf{d}_n). \quad (4.16)$$

Algorithm 4.1 Picard-Banach Distributed Scheme

- 1: Set $\mathbf{r}_n, \mathbf{d}_n, \mathbf{x}_n^0 \in \Omega_n, \forall n \in \mathcal{N}$
 - 2: **while** $\|\mathbf{x}^{k+1} - \mathbf{x}^k\| < \varepsilon$ **do**
 - 3: EC Manager updates $\mathbf{k}_n^k(\mathbf{x}_{-n}^k), \forall n \in \mathcal{N}$
 - 4: Prosumers update:
 $\mathbf{x}_n^{k+1} \leftarrow \text{proj}_{\Omega_n}(\mathbf{k}_n^k, \mathbf{r}_n, \mathbf{d}_n), \forall n \in \mathcal{N}$
 - 5: $k \leftarrow k + 1$
 - 6: **end while**
-

Remark 4.4.1

Intuitively, (4.16) represents an approximated, thus not optimal, version of the so-called best response of player $n \in \mathcal{N}$ when its behavior is approximated with a NN. Thus, once trained, (4.16) is an alternative approach for approximating $\mathbf{x}_n = \text{argmin}_{\mathbf{x}_n \in \Omega_n} J_n(\mathbf{x}_n, \mathbf{x}_{-n})$ of (4.14). \square

Let us now propose an algorithm to seek an equilibrium, that, as shown in Algorithm 4.1, is based on the well-known Picard-Banach response iteration. The algorithm is repeated iteratively.

At each iteration k , the EC Manager updates the energy cost vector \mathbf{k}_n^k for each prosumer $n \in \mathcal{N}$, based on the strategies chosen by other prosumers \mathbf{x}_{-n}^k . Consequently, each prosumer $n \in \mathcal{N}$ updates its strategy \mathbf{x}_n^{k+1} . This update is based on the current energy cost vector \mathbf{k}_n^k , renewable energy production \mathbf{r}_n , and energy demand \mathbf{d}_n . The projected strategy onto the feasible set Ω_n ensures that the updated strategy remains feasible.

These steps are repeated until the difference between consecutive iterations $\|\mathbf{x}^{k+1} - \mathbf{x}^k\|$ of prosumer strategies is below a predefined tolerance ε . If the condition is met, the algorithm terminates, indicating convergence. Otherwise, it proceeds to the next iteration.

Notably, this algorithm assumes that prosumers are myopic in the sense that they are essentially making their move in response to their opponents' strategies based on the results of a learning-based approach, which can be suboptimal for their real behavior.

4.5 Numerical Experiments

In this section, we show the performance of the proposed algorithm through different numerical experiments. For the sake of brevity, the tests are conducted on an EC composed of $N = 100$ prosumers. However, the framework has the ability to be applied on larger scales.

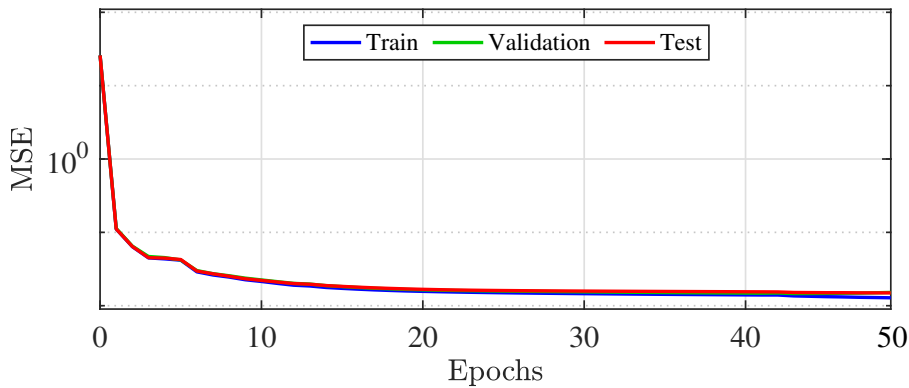


Figure 4.2: Learning process: MSE evolution over epochs.

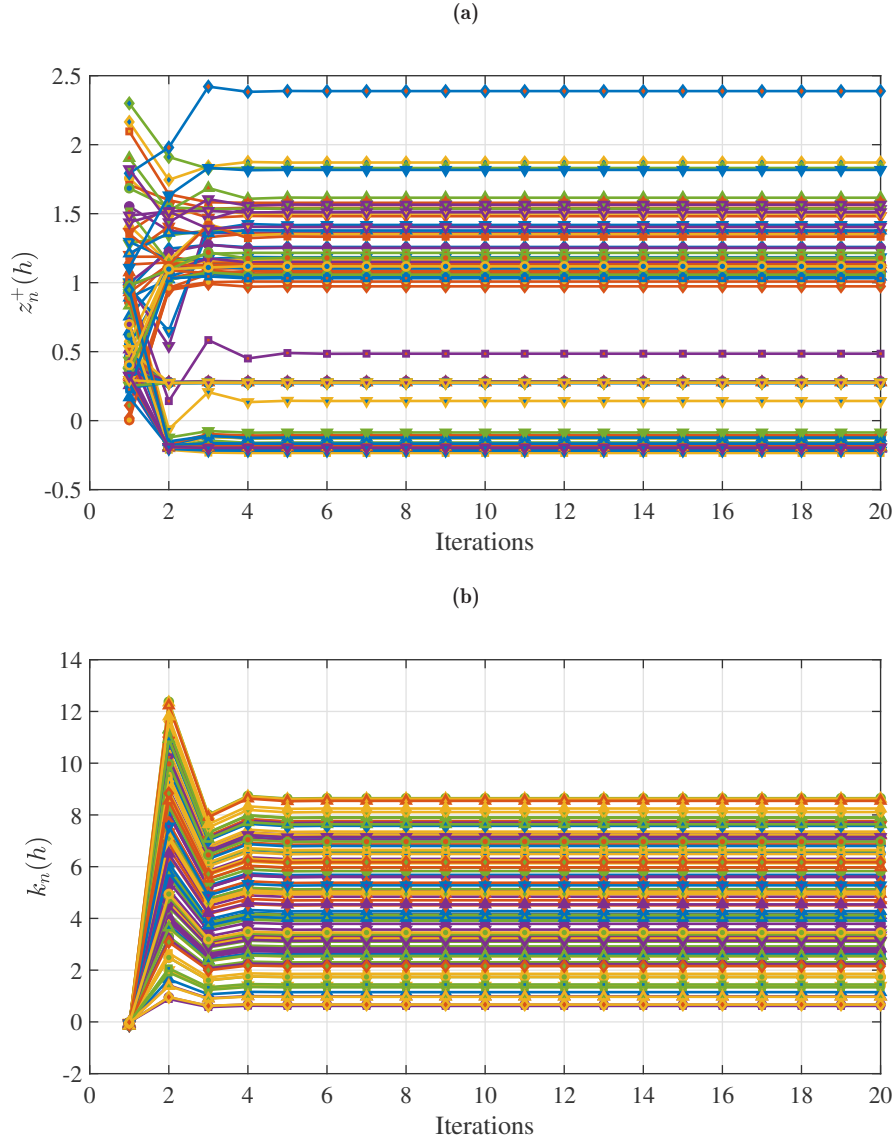


Figure 4.3: Equilibrium among the prosumers through the proposed algorithm in Scenario 1: (a) EC Manager power convergence (b) convergence of the price.

The scheduling horizon corresponds to $H = 10$ time slots each of which is one-hour. Each active prosumer has its own ESS and RES. In particular, we implemented the proposed control approach in MATLAB 2023a on a laptop with an M2 8-core CPU and 8GB of memory. To assess the proposed framework with two pricing models, we accomplished a comparison between two different scenarios, described as follows:

- Scenario 1: The system uses the **pricing model 1**.
- Scenario 2: The system uses the **pricing model 2**.

For training the NNs, we collect data from past optimization runs, where input features include the energy demand of each prosumer considering the photovoltaic generation ($\mathbf{d}_n - \mathbf{r}_n$), \mathbf{SoC}_n , and energy prices (\mathbf{k}_n) over the time horizon. The corresponding optimal energy allocations obtained from the optimization process serve as the target labels for training the NN. The total number of examples is 100,000, where the term “example” is a particular instance of data obtained through the previous experience of the prosumer. We should mention that in this work we use offline results to train our NN to assess our proposed framework, however, the applicability of the present work is not

restricted to this kind of implementation. That is, in real-world applications, there have been many implemented ECs, where they are obtaining their optimal solutions through online optimization, while their best responses can be saved to use as training data in similar communities with a very low implementation cost.

We design a relatively NN architecture to be able to capture the complex relationships between input features and optimal energy allocations. The NN takes the features as input, hence the input dimension is $3H$, and the output dimension is 1, where it is the predicted optimal energy allocations for each prosumer or entity in the EC. The architecture of the NN comprises 10 hidden layers, each with a hidden dimension of 20 neurons. Here, the learning rate is specified as 0.01, and the training dataset is divided into a ratio of 0.8 for training. It should be noted that the whole training process is conducted over 100 epochs. The selection of hyperparameters is the result of an iterative trial-and-error process aimed at optimizing NN performance with the Mean Squared Error (MSE) serving as the optimization metric for tuning the hyperparameters. The learning process is depicted in Fig. 4.2, illustrating the MSE for test data across 100 epochs.

In scenario 1, convergence among the prosumers is demonstrated in Fig. 4.3. Specifically, Fig. 4.3(a) illustrates that prosumers with varying demands reach equilibrium within a low number of iterations. Additionally, Fig. 4.3(b) depicts the convergent prices for each prosumer. It can be seen that $k_n(h)$ varies across different prosumers in Scenario 1.

Equilibrium among the prosumers in scenario 2 is illustrated in Fig. 4.4. Particularly, in Fig. 4.4(a), each prosumer exhibits a distinct demand, and after 20 iterations, each one attains its intended demand. It can also be seen in Fig. 4.4(b) that all prosumers have the same $k_n(h)$ and achieve equilibrium.

4.6 Conclusions

This work introduces a novel game-theoretic learning-based approach for managing energy communities (ECs) in a distributed fashion. The addressed system comprises diverse prosumers, each with independent energy demands, equipped with renewable energy sources and storage systems. Our methodology models prosumers using neural networks to derive their response strategies. We propose a distributed algorithm to converge towards an equilibrium. Lastly, we validate the convergence of our method through two distinct scenarios that show the effectiveness of our proposed approach.

Future research will address extending the proposed approach to different control goals (e.g., introducing a new pricing mechanism). Additionally, exploring advanced neural network architectures can enhance accuracy in modeling prosumers' behavior, facilitating more precise response strategies for individual prosumers.

References

- [1] Zahmoun, S., Ouammi, A., Sacile, R., Benchrifa, R., and Zero, E., "Optimal operation scheduling of a combined wind-hydro system for peak load shaving," *IEEE Transactions on Automation Science and Engineering*, 2024.
- [2] Vitti, M., Facchini, F., and Mummolo, G., "Assessing the decarbonisation potential of waste-to-hydrogen routes in the energy transition phase: An environmental analytical model," *Journal of Cleaner Production*, vol. 457, p. 142 345, 2024.
- [3] Gjorgievski, V. Z., Cundeva, S., and Georghiou, G. E., "Social arrangements, technical designs and impacts of energy communities: A review," *Renewable Energy*, 2021.
- [4] Wang, H., Xie, Z., Pu, L., Ren, Z., Zhang, Y., and Tan, Z., "Energy management strategy of hybrid energy storage based on pareto optimality," *Applied Energy*, vol. 327, p. 120 095, 2022.

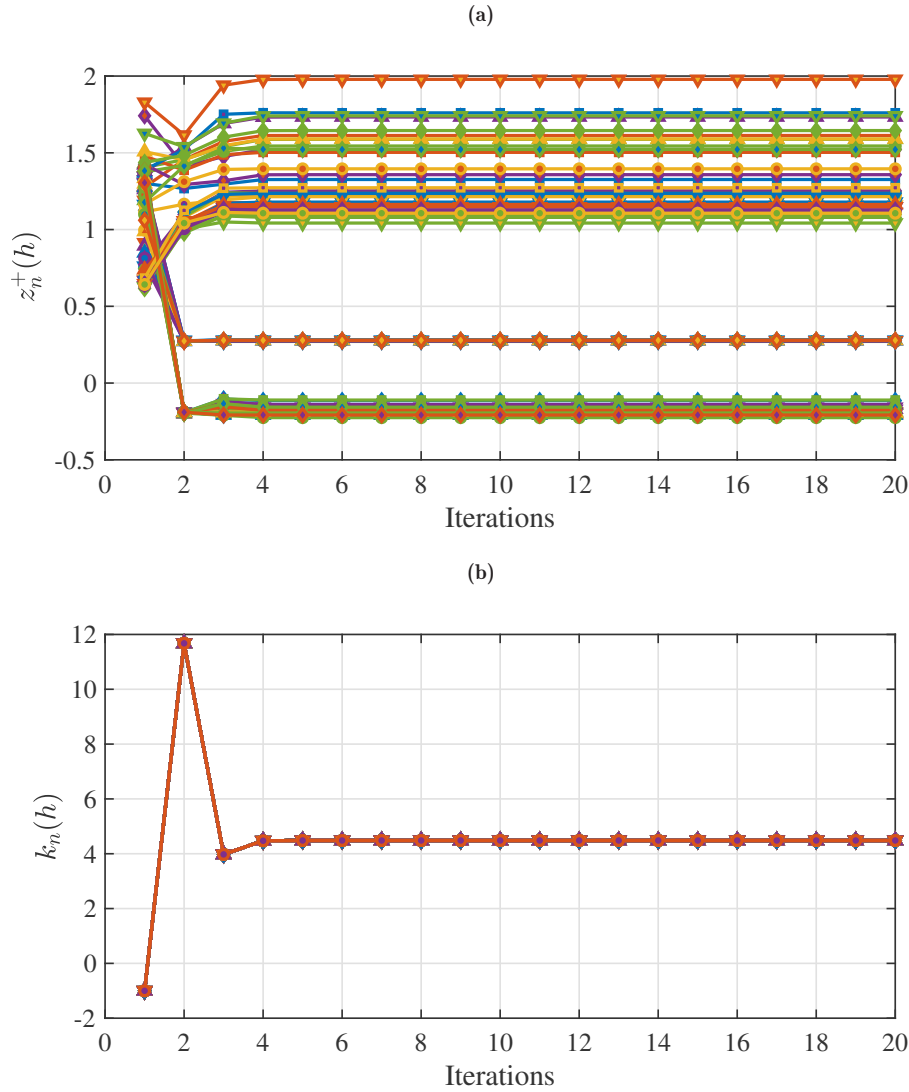


Figure 4.4: Equilibrium among the prosumers through the proposed algorithm in Scenario 2; (a) EC Manager power convergence, (b) convergence of the price.

- [5] Bannour, F., Souihi, S., and Mellouk, A., “Distributed sdn control: Survey, taxonomy, and challenges,” *IEEE Communications Surveys & Tutorials*, vol. 20, no. 1, pp. 333–354, 2017.
- [6] Khalid, M., “Smart grids and renewable energy systems: Perspectives and grid integration challenges,” *Energy Strategy Reviews*, vol. 51, p. 101 299, 2024.
- [7] Mignoni, N., Scarabaggio, P., Carli, R., and Dotoli, M., “Control frameworks for transactive energy storage services in energy communities,” *Control Engineering Practice*, vol. 130, p. 105 364, 2023.
- [8] Scutari, G., Palomar, D. P., Facchinei, F., and Pang, J.-S., “Convex optimization, game theory, and variational inequality theory,” *IEEE Signal Processing Magazine*, vol. 27, no. 3, pp. 35–49, 2010.
- [9] Fujiwara-Greve, T., *Non-cooperative game theory*. Springer, 2015.
- [10] Myerson, R. B., “Nash equilibrium and the history of economic theory,” *Journal of Economic Literature*, vol. 37, no. 3, pp. 1067–1082, 1999.

-
- [11] Scarabaggio, P., Grammatico, S., Carli, R., and Dotoli, M., “Distributed demand side management with stochastic wind power forecasting,” *IEEE Transactions on Control Systems Technology*, vol. 30, no. 1, pp. 97–112, 2021.
 - [12] Brunke, L. et al., “Safe learning in robotics: From learning-based control to safe reinforcement learning,” *Annual Review of Control, Robotics, and Autonomous Systems*, vol. 5, pp. 411–444, 2022.
 - [13] Drgoňa, J., Picard, D., Kvasnica, M., and Helsen, L., “Approximate model predictive building control via machine learning,” *Applied Energy*, vol. 218, pp. 199–216, 2018.
 - [14] Ma, Y., Kelman, A., Daly, A., and Borrelli, F., “Predictive control for energy efficient buildings with thermal storage: Modeling, stimulation, and experiments,” *IEEE control systems magazine*, vol. 32, no. 1, pp. 44–64, 2012.
 - [15] Yang, S., Wan, M. P., Chen, W., Ng, B. F., and Dubey, S., “Model predictive control with adaptive machine-learning-based model for building energy efficiency and comfort optimization,” *Applied Energy*, vol. 271, p. 115 147, 2020.
 - [16] Garifi, K., Baker, K., Touri, B., and Christensen, D., “Stochastic model predictive control for demand response in a home energy management system,” in *2018 IEEE power & energy society general meeting (PESGM)*, IEEE, 2018, pp. 1–5.
 - [17] Hertneck, M., Köhler, J., Trimpe, S., and Allgöwer, F., “Learning an approximate model predictive controller with guarantees,” *IEEE Control Systems Letters*, vol. 2, no. 3, pp. 543–548, 2018.
 - [18] Bünning, F. et al., “Physics-informed linear regression is competitive with two machine learning methods in residential building mpc,” *Applied Energy*, vol. 310, p. 118 491, 2022.
 - [19] Zhang, H., Seal, S., Wu, D., Bouffard, F., and Boulet, B., “Building energy management with reinforcement learning and model predictive control: A survey,” *IEEE Access*, vol. 10, pp. 27 853–27 862, 2022.
 - [20] Scarabaggio, P., Carli, R., and Dotoli, M., “Noncooperative equilibrium-seeking in distributed energy systems under ac power flow nonlinear constraints,” *IEEE Transactions on Control of Network Systems*, vol. 9, no. 4, pp. 1731–1742, 2022.
 - [21] Mignoni, N., Carli, R., and Dotoli, M., “Distributed noncooperative mpc for energy scheduling of charging and trading electric vehicles in energy communities,” *IEEE Transactions on Control Systems Technology*, vol. 31, no. 5, pp. 2159–2172, 2023.
 - [22] Garifi, K., Baker, K., Christensen, D., and Touri, B., “Convex relaxation of grid-connected energy storage system models with complementarity constraints in dc opf,” *IEEE Transactions on Smart Grid*, vol. 11, no. 5, pp. 4070–4079, 2020.
 - [23] Parise, F. and Ozdaglar, A., “Sensitivity analysis for network aggregative games,” in *2017 IEEE 56th Annual Conference on Decision and Control (CDC)*, IEEE, 2017, pp. 3200–3205.

Chapter 5

Summery & Conclusions

This thesis has investigated the control of future rural energy communities, focusing on the challenges of integrating renewable energy sources and coordinating the actions of diverse participants. The research has advanced along two complementary directions. On the one hand, it has developed new operational frameworks for innovative infrastructures, such as agrivoltaic fields and parking facilities with solar-powered electric vehicles. On the other hand, it has proposed learning-based, game-theoretic approaches to coordinate decentralized and self-interested agents, which led to scalable and autonomous solutions for energy communities.

This thesis set out to explore how we can increase renewable energy penetration in rural energy communities while ensuring reliable and sustainable operation. First, we explored which innovative frameworks could enable such an increase. In response, two complementary solutions were developed: a dynamic agrivoltaic system capable of balancing energy capture with agricultural needs, and a smart parking infrastructure designed to integrate both conventional and SPEV. In the second step, we considered how these frameworks could be operated effectively under real conditions. The thesis demonstrated that shadow-aware orientation strategies in agrivoltaics and a convex model predictive control in parking systems allow renewables to be properly utilized without violating agricultural, technical, or safety constraints. Finally, the third concern addressed how decentralized and self-interested actors in energy communities could be coordinated without centralized control. Here, a game-theoretic learning-based framework was proposed, enabling prosumers to adapt their strategies and reach equilibrium in a distributed manner.

The specific contributions and key findings of each chapter are reported hereafter:

- The agrivoltaic study contributes a geometric model and a constrained tracking strategy. It regulates azimuth and tilt to confine shadows within each cell while satisfying a minimum daily light integral. An iterative relaxation of the tracking target balances energy maximization with crop exposure. Day-long simulations for Bari, Italy demonstrate feasibility and precise shadow placement.
- The parking-lot study proposes a tractable MPC that avoids mixed-integer burdens. It enforces no simultaneous charge/discharge, protects charging piles, and preserves feasibility when departures lie beyond the prediction horizon. Using real prices, irradiance, and activity logs from Melbourne, the controller reduces grid energy up to 27% and outperforms a rule-based baseline by 15.32% in cost when SPEVs are 50%. Robustness analyses show minor sensitivity to forecast errors.
- The energy-community study replaces explicit best-response optimization with learned responses. Prosumers update strategies using neural networks trained on historical optimal actions. A distributed algorithm then reaches equilibrium in few iterations across pricing scenarios, suggesting a scalable path to autonomy and privacy.

From a theoretical and methodological perspective, the thesis has introduced three original contributions. The first is a dynamic, shadow-aware control formulation for dual-axis agrivoltaic systems, which simultaneously enforces spatial shadow containment and daily light requirements for crops through an iterative alignment mechanism. The second is a convex model predictive control architecture from the perspective of CPs for smart parking infrastructures compatible with SPEVs, which guarantees the safety of CPs, prevents simultaneous charging and discharging, and ensures feasibility across multiple horizons. The third is a learning-based, noncooperative control framework for

energy communities, where the behavior of prosumers is modeled using neural networks and equilibria are computed through a distributed fixed-point algorithm.

On the empirical and practical side, we have validated these contributions under realistic conditions. The agrivoltaic control was tested on real solar data from Bari, Italy, over a complete day. The parking framework was assessed using a year-long dataset from Melbourne, Australia, which included real energy prices, solar irradiance, and vehicle activities. Finally, the community control scheme was shown to achieve equilibrium in multi-prosumer settings under different pricing models.

To advance this line of research, it is essential to acknowledge the conditions within which the present findings were obtained. The agrivoltaic study was developed under the assumptions of flat terrain, decoupled cells, and uniform crop distribution, and it relied on a simplified irradiance model and a clear-sky day. The parking framework was validated through simulations with deterministic forecasts. The community control approach was demonstrated in stylized scenarios based on historical data, without yet addressing equilibrium efficiency under model mismatch or communication delays.

Building on these results, future work could extend agrivoltaic models to more complex terrains and variable crop distributions, validate smart parking control through experimental pilots with real hardware, and enhance the energy community framework with richer behavioral models and robustness to communication and privacy constraints.

